Comparative Evaluation of Advanced Coal-Based Power Plants

von
Yanzi Chen Bernero, M.S.
aus Fuzhou, V.R. China

Von der Fakultät
für Prozesswissenschaften
der Technischen Universität Berlin
zur Erlangung des akademischen Grades
Doktor der Ingenieurwissenschaften
genehmigte Dissertation

Promotionsausschuß:

Vorsitzender: Prof. Dr.-Ing. G. Wozny
Gutachter: Prof. Dr.-Ing. G. Tsatsaronis
Prof. Dr.-Ing. H. Auracher

Tag der wissenschaftlichen Aussprache: 14 November 2001

Berlin 2002

D 83

Zusammenfassung

Das Ziel dieser Studie ist es, vier fortschrittliche kohlebefeuerte Kraftwerkskonzepte hinsichtlich des Wirkungsgrades, der Stromgestehungskosten und der Emissionen unter vergleichbaren wirtschaftlichen und technischen Bedingungen zu bewerten. Betrachtet werden ein überkritisches Dampfkraftwerk SC 580°C, ein extern befeuertes Kombikraftwerk (HIPPS), ein Kombikraftwerk mit zirkulierender Druckwirbelschichtfeuerung mit vorgeschalteter Teilvergasung (PFBC) und ein Kombikraftwerk mit integrierter Kohlevergasung (IGCC). Ein konventionelles kohlenstaubbefeuertes Dampfkraftwerk (PCC) dient als Bezugsanlage, die den gegenwärtigen Stand der Technik von Kohlekraftwerken darstellt.

Für jeden Kraftwerkstyp wurden sowohl eine Exergieanalyse als auch eine Wirtschaftsanalyse durchgeführt und der Einfluss wichtiger wirtschaftlicher und technischer Annahmen auf das Ergebnis dieser Analysen untersucht. Dadurch können der Ort, der Betrag, und die Ursachen der realen thermodynamischen Verluste bestimmt werden. Mögliche Maßnahmen zur Wirkungsgradesteigerung und Verminderung der Stromgestehungskosten werden aufgezeigt.

Das extern kohlebefeuerte Kombikraftwerk erscheint aus sowohl thermodynamischer als auch wirtschaftlicher Sicht vorteilhaft. Das HIPPS-Kraftwerk weist einen exergetischen Wirkungsgrad von 48,5% auf und hat Stromgestehungskosten (LCE), die um 3,7% höher liegen als beim PCC. Wird das HIPPS ausschließlich mit Kohle befeuert, nimmt der Wirkungsgrad um 3,7% ab, ohne bemerkbare Änderungen der LCE. Das PFBC zeigt den zweithöchsten Wirkungsgrad (5,8% niedriger als beim HIPPS), und die niedrigsten LCE. Beim IGCC, dessen exergetischen Wirkungsgrad um 11,0% niedriger als der des HIPPS liegt, sind die höchsten LCE zu erwarten. Für das SC 580°C Kraftwerk ist der Wirkungsgrad um 19,3% niedriger als für HIPPS, dennoch um 9,4% höher als für das PCC. Die LCE dieses Kraftprozesses liegen zwischen denen vom HIPPS und vom IGCC. Mit einer Erhöhung der Dampfparameter auf 700°C und 365 bar kann ein weiterer Gewinn von 7,5% am Wirkungsgrad erzielt werden, ohne spürbare Einbusse an den LCE.

Das HIPPS ergibt sich als die vielversprechendste langfristige Alternative für Stromerzeugung auf Kohlebasis. Während die SC-Technologie zur Deckung des kurzfristigen Strombedarfs im Vordergrund steht, stellen die PFBC und IGCC eine mögliche Lösung für den mittelfristigen Bedarf und für den Einsatz niederwertiger Brennstoffe dar.

Abstract

The purpose of this study is to comparatively evaluate four types of advanced conceptual power plants based on coal. With efficiency, cost-of-electricity, and emissions as main criteria, the evaluation was made under consistent design conditions and economic assumptions. The plants considered are a supercritical steam power plant (SC 580°C), an indirectly coal-fired power system (HIPPS), an advanced pressurized fluidized-bed combustion power plant (PFBC), and an integrated gasification-combined-cycle power plant (IGCC). Reflecting the technology standard of the current coal power plants, a conventional steam power plant (PCC) was chosen for comparison. Exergetic and economic analyses have been performed for each type of the plants, together with parametric studies. The main sources of thermodynamic inefficiencies as well as the dominating contributors to the cost of electricity are identified. Potential improvements of both the performance and the cost effectiveness are discussed, and the environmental impact of each plant is briefly presented.

The HIPPS appears to be the thermodynamically and economically most viable option, capable of achieving a 48.5% overall exergetic efficiency while allowing a levelized cost of electricity (LCE) by merely 3.7% higher than that of the PCC power plant. If the HIPPS is fueled only with coal, the system efficiency is expected to decrease by 3.7% and the LCE remains basically unchanged. The PFBC has the second highest plant efficiency, 5.8% lower than that of the HIPPS, and the lowest LCE among the four. The IGCC power plant possesses an exergetic efficiency 11.0% lower than that of the HIPPS and the highest LCE. The SC 580°C yields the lowest overall exergetic efficiency among all the plants, 19.3% lower than that of the HIPPS. Still, it is 9.4% higher than that of the conventional PCC plant. The LCE of this plant lies between that of the HIPPS and that of the IGCC. Further elevating the steam parameters to 700°C and 365 bar promises an increase of 7.5% in efficiency, without a necessary rise in the LCE.

As a conclusion, among the four technologies, the HIPPS is the best option for the power generation based on coal in the far future. While SC power plants can be the choice to meet the short-term needs of new capacity, PFBC and IGCC plants could provide solutions for both middle-term power generation and use of low-rank fuel feedstock.

Acknowledgement

I thank sincerely my advisor, Prof. Dr.-Ing. George Tsatsaronis, who gave me the opportunity of being a Ph.D. candidate and introduced me to the world of Exergoeconomics. A scholar of great wisdom and learning, he cared for, guided and supported me throughout the time I stayed with him. Thanks also goes to my graduate advisory committee members Prof. Dr.-Ing. G.Wozny of the Institute of Process Engineering, Technical University of Berlin and Prof. Dr.-Ing. H. Auracher of the Institute of Energy Engineering, Technical University of Berlin for their pertinent comments and suggestions.

The graduate students in Room 411 of the Mechanical Engineering Department of Tennessee Technical University and my colleagues of Institute of Energy Engineering, Technical University Berlin provided me with unreserved help and input to this work. Hereby I express my deep gratitude to them, especially to Andreas Krause and Moungho Park.

I am greatly indebted to the Center for Electric Power, Tennessee Technical University and to the Technical University of Berlin for the financial support and the excellent study and working environment.

I appreciate from my very heart the boundless love, understanding, tolerance, and self-sacrifice my families ensured to me over the years when I was involved in this work. In particular, my husband Stefano has always stood by me, cheering me up when I felt low and encouraging me when I was about to give up. Without him, I might have not been able to finish this work.

Contents

List of symbols

Symbols

C	coefficient for correcting cooling effects on turbine efficiency
C	cost of an equipment item [thousand-dollar]
$\dot{E}$	exergy flow rate associated with a material stream [MW]
$\dot{H}$	enthalpy flow rate [MW]
$\dot{m}$	mass flow rate [kg/s]
p	pressure [bar]
$\dot{Q}$	heat transfer [MW]
r	air compressor pressure ratio
$\dot{S}$	entropy flow rate [kW/kg·K]
T	temperature [°C]
$\dot{W}$	work rate [MW]
x	mole fraction of a chemical constituent of a mixture
y_D	exergy destruction ratio

Greek letters

α	scaling exponent for the current cost of an equipment item
Δ	turbine efficiency adjusting factor induced by blade cooling
ϵ	exergetic efficiency
η	turbine isentropic efficiency

Subscripts

0	environmental state
D	exergy destruction
F	fuel exergy
$GTIT$	gas turbine inlet temperature
k	the kth component of a power plant
L	exergy losses
LP	low pressure
HP	high pressure
net	net power output

P	product exergy
PE	purchased-equipment
$poly$	polytropic efficiency
tot	referring to the entire power plant
W	at design capacity
Y	at current capacity

List of abbreviations

AFUDC	Allowance for funds used during construction
AGR	Acid gas removal
ASU	Air separation unit
CC	Carrying charges
CCR	Carbon conversion ratio
CD	Condenser
CGCU	Cold gas cleanup
DOE	Department of Energy (USA)
EPRI	Electric Power Research Institute (USA)
ESP	Electrostatic precipitator
EU	European Union
FGD	Flue gas desulfurization
FWH	Feedwater heater/heating
GT	Gas turbine
HGCU	Hot gas cleanup
HIPPS	High-performance power system
HIPPSC	High-performance power system based only on coal
HHV	Higher heating value
HP	High pressure
HRSG	Heat-recovery steam generator
HTF	High-temperature furnace
IGCC	Integrated gasification-combined-cycle
IP	Intermediate pressure
ISO	International Standards Organization
LCE	Levelized cost of electricity
LHV	Lower heating value
LP	Low pressure
O&M	Operating and maintenance
PC	Pulverized coal
PCC	Pulverized coal combustion
PCF	Plant capacity factor
PEC	Purchased-equipment costs
PFBC	Pressurized fluidized-bed combustion/combustor
PPCC	Pressurized pulverized coal combustion
PTD	Pinch temperature difference
RH	Reheating or reheater

SC	Supercritical
SCC	Spencer, Cotton, and Cannon (method)
SG	Steam generator
ST	Steam turbine
TCR	Total capital requirement
TCI	Total capital investment
TDC	Total direct costs
TIC	Total indirect costs
TPC	Total plant costs
TRR	Total revenue requirement
TTD	Terminal temperature difference
TUB	Technische Universität Berlin
VHP	Very high pressure

1. Introduction

The availability of affordable electricity is essential to the economic strength of a nation. Electricity generation has therefore gained remarkable attention over the last few decades.

Among the existing technologies, coal-fired power plants dominate nowadays the electricity generation worldwide. The most plentiful fossil fuel available, especially in the large electric power producing countries like the United States and China, coal has assumed its key role in electric power generation after the Arab oil embargo in October 1973 and the subsequent oil price increases in 1974 and 1979. Great efforts have been made in many countries since then to search for advanced technologies for power generation with coal, and to lessen the dependence on imported oil supplies (Engi & Icerman (1995)).

In the 21st century, the electric power generation with coal is expected to face new challenges. The electric industry is reluctant to risk long-term investments in electricity generation facilities that are associated with advanced technologies as the power industry deregulates and becomes a market-driven one. It is therefore extremely urgent to investigate new concepts for electricity production at capital costs as low as possible.

The biggest challenge is, nevertheless, the concern over the global climate change. A portion of reduction of greenhouse gases, especially CO_2 from fossil fuel use, might be achieved through options such as emission trading and credits for investing in emission reduction projects. However, substantial reductions in emissions can only be achieved by advanced technologies when electricity is generated using coal. The general goal of ongoing energy R&D activities is to ensure a more efficient, environmentally cleaner, more economic, and more flexible use of coal.

In this chapter, the close relation between coal and electricity genera-

tion is shortly examined. It is followed by a brief review of the R&D activities in the field of advanced technologies for electricity generation using coal. At end of the chapter, the motivation and the aim of this study are stated.

1.1 Coal and electricity generation

The global electricity demand has been increasing continuously. Based on information provided by the International Energy Agency (IEA), it is estimated that, over the time period 1971-1995, the world average annual growth of power generation demand was 3.8%, higher than the 3.2% average annual growth rate of global economy in the same time period (Birol & Argiri (1999)). In the next 20 years, the world electricity demand is projected to grow at approximately 3.0% per year, provided that the world economy will grow, in the same period, at a rate of 3.1% per year.

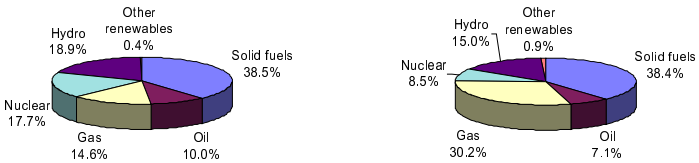

Figure 1.1: Overview of the world electricity generation by fuel source. Left: for year 1995; Right: for year 2020 (Birol & Argiri (1999)).

Coal takes a decisive position in the field of electricity generation worldwide. The overall coal production throughout the world was about 3,656 million tons in 1998. Approximately 60% of current global electricity generation relies on fossil fuels. Solid fuels (mainly coal) alone contribute to about 38% of the total electricity generation, and this percentage is expected to remain essentially unchanged up to year 2020, see Figure 1.1. It is anticipated that the total international demand for electricity will grow from 2,921 GW in 1995 to 5,091 GW in

2015, resulting in an increase of the total world use of coal for power generation by over 50% (DOE (1999b)).

In the United States, which consume a quarter of the world energy demand, fossil fuels provide 68% of the overall national need in the electricity generation sector. Coal accounts for 55% of the electricity need and is expected to continue to fuel the majority of electric power production (DOE (1999b)). The national electricity generation capacity was estimated as 722 GW at end of 1995 and is expected to be 915 GW by the year 2015.

In 1996, coal accounted for 15% of the total energy consumption in the European Union.

As the second largest electricity producer in the world, China's installed capacity reached 250 GW by the end of 1997, with an annual electricity generation of 1132 TWh. Out of the 250 GW capacity, 75.8% used fossil fuels, while 81.9% of the 1132 TWh was provided by coal-fired power plants (World Bank (2000)). China accounted for 29% of the world's total coal consumption in 1996.

Coal will continue to be an important factor in the world electricity generation and in the economy development as well. Wherever natural gas is unavailable or costly, or inexpensive, coal is accessible, coal would be the favored fuel for electricity generation. As technologies such as integrated gasification-combined-cycle power plants, advanced gas turbine systems, and fuel cells are to come to maturity, coal will remain in some regions of the world the most economical long-term fuel for electricity production thanks to its low cost and the resulting favorable cost of electricity. The main obstacle for using coal as fuel in electricity generation for the future would be then the related emissions, CO_2 above all.

The efficiency of a coal-fired power plant is of significant importance for the environmental impact associated with the use of coal. A coal-fired power plant with an efficiency of 50% would emit 40% less CO_2 than a plant using today's technologies. With high-efficiency coal technologies, the global CO_2 emissions could be maintained at about 15,000 million tons per year by 2075, in spite of the fast growth of world coal use (DOE (2000a)). From the environmental view point it is very important to adopt advanced, more efficient power plants that use coal in a cleaner and more economic way.

1.2 Technological background

Motivated by the urgent need of advanced technologies for electricity generation using coal as fuel, projects related with clean coal technologies for power generation are undertaken worldwide, particularly in the United States, in Europe, and in Asia.

Addressing the energy situation in Europe that suffers from insecurity, regional disparity, and unsolved environmental concerns (THERMIE (1996)), developing and exploiting new energy technologies has been recognized as one of the key solutions. Some energy demonstration activities have been intensely held over the last years within the scope of the European Union (EU). The primary goal is, through a successful demonstration of new technologies for electricity generation, to encourage the widespread adoption of the demonstrated technology wherever appropriate within the Community.

In general, the following advanced coal power plant technologies have been investigated in various studies supported by the EU:

- Pulverized coal combustion with ultra supercritical steam conditions (SC)
- Circulating fluidized-bed combustion (CFBC)
- Pressurized fluidized-bed combustion (PFBC)
- Integrated gasification-combined-cycle (IGCC)
- Pressurized pulverized coal combustion (PPCC)

Except for the PPCC, all the above mentioned technologies are being applied in first commercial power plants for electricity production (Zehner (1998)). It must be emphasized that the clean coal technologies can only be adopted if they are competitive with technologies using other fossil fuels.

In the case of the United States, the national energy supply relies heavily on fossil fuels. About 84% of the country's energy needs nowadays is covered by fossil fuels. This percentage might be as high as 90% in year 2020 (DOE (1999b)). The Department of Energy (DOE), USA has sponsored a program called the Coal and Power Systems (C&PS) (DOE (1999b)), in partnership with industry and state governments. One of its key elements, namely the Near- and Mid-Term Development and Demonstration, consists of two parts:

- Clean Coal Technology demonstrations
- High-efficiency, ultra-clean coal- and natural-gas-power systems

To be concluded by 2005, the eleven projects concerning Advanced Electric Power Generation in the Clean Coal Technology demonstrations cover following technologies:

- Fluidized-bed combustion system
- Integrated gasification-combined-cycle system
- Integrated gasification-fuel-cell system
- Coal-fired diesel engine
- Advanced slagging combustor

The second part, the high-efficiency, ultra-clean coal- and natural-gas-power systems, consists of strategies including:

- Utility-scaled advanced turbine systems (ATS)
- Low-emission boiler system (LEBS)
- Indirectly coal-fired power system (HIPPS)
- Pressurized fluidized-bed combustion (PFBC) system with hot gas filter
- Integrated gasification-combined-cycle (IGCC) system producing market-based fuel and chemical products

The indirectly coal-fired power system is also called high-performance power system (HIPPS). In this power system, the hot gases from coal combustion are kept from contacting a gas turbine. Rather, the gases heat a working fluid (such as air) that drives the gas turbine. A reengineering of conventional pulverized-coal boiler, the low-emission boiler system includes advanced combustion and innovative flue gas cleaning systems to achieve higher efficiencies, lower emissions, and lower costs.

While the Advanced Electric Power Generation projects in the Clean Coal Technology demonstration program are to provide environmentally sound, more efficient, and less costly electric power to cover the near- and mid-term needs, the high-efficiency, ultra-clean coal- and natural-gas-power systems will foster ultra-high-efficient, environmentally superior, and cost-competitive systems for long-term electric power generation (DOE (1999a) and DOE (1999b)).

Clean Coal Technologies are under development also in Asia. In China, for example, the options include supercritical technology, atmospheric fluidized-bed combustion, and coal gasification (World Bank (2000)).

1.3 Motivation and aim of the work

Improvements of electric power plants can only be achieved through a variety of efforts. Aspects such as adoption of advanced power systems, further developments in material technology, innovative techniques in power plant design, manufacturing, construction, and operation are commonly considered of potential for a higher efficiency, better plant availability, and lower electricity cost.

As indicated in Section 1.2, there are many advanced coal-based electric power generation technologies capable of meeting the challenge of the future power market. Among them are:

- Pulverized-coal power plant with ultra supercritical (SC) steam conditions
- Indirectly coal-fired power system (HIPPS)
- Advanced pressurized fluidized-bed combustion (PFBC) power plant
- Integrated gasification-combined-cycle (IGCC) power plant

Even if none of these technologies will be able to fully achieve the efficiency, environmental, and cost goals that are needed in the next decades, they embody the basic advanced technologies for the power plants in the farther future.

However, power plants using advanced technologies have to be competitive against the conventional ones in terms of economy, ecology, and availability. It is commonly required that the cost of efficiency enhancement associated with advanced power plants be lower than the saving on fuels over the entire plant life time. Thermodynamic assessments and cost estimations of these advanced power plants are therefore essential.

Most of the research projects on the advanced power plants are carried out by different government organizations and industry groups, individually, under strong competition and with different methodologies. As a consequence, the results from such projects might be affected by these factors and might not always provide objective results. It is necessary to compare these power plants in an objective and neutral way.

In addition, there always exists a contradiction: On one hand, an individual power plant usually operates under particular conditions

and is subject to its inherent limitations. On the other hand, it is desired that the assessment and comparison of potential options be based on design specifications and cost assumptions as consistent as possible. An organic combination of these two sides will have a positive influence upon the soundness of the the assessment and comparison. It should be emphasized that the relative characteristics of performance and cost effectiveness among the power plants are more important than the absolute estimation of each one in the sense of power plant planning and policy making.

Motivated by the above thoughts, the author conducts a comparative evaluation of the above mentioned four types of advanced coal-fired power plants, with system efficiency, cost-of-electricity, and emissions as main criteria, under consistent design conditions and economic assumptions. The aim of this work is, through an evaluation of these four types of advanced electric power generation plants, to disclose the practical limits to the overall efficiency, to reveal the relative potential of the economic effectiveness, to display the emission reduction capability, and to identify – above all – the strength and the weakness of each technology. The present study should give a basic idea on how competitive these four types of plants would be in the power generation market of the future.

Chapter 2 presents an overview of the state-of-the-art of the four types of power plants and describes shortly some important ongoing research activities in these areas. The methodology followed throughout this study is briefly described in Chapter 3. The tools for thermodynamic simulation of the power plants as well as the basic assumptions are presented also in the same chapter.

Thorough exergetic analyses, together with some parametric studies, have been carried out for the four types of power plants and for a conventional PCC steam power plant. The latter represents an average standard of today's power generation based on coal. The true ineffectiveness of each power plant is thus quantified and the key factors affecting the overall efficiency are defined. By means of the economic analyses the levelized cost of electricity is calculated for each plant type. All these results are presented in Chapter 4.

The central task of Chapter 5 is the *comparative* evaluation of the four types of power plant. It contains three parts: The exergetic evaluation, the economic evaluation, and the emission evaluation. After a com-

parison of the overall efficiencies of the power plants, the possibilities of improving the efficiencies are discussed, based on the results provided in Chapter 4. The economic evaluation is based on the levelized cost of electricity. Factors that have significant effects on this cost are discussed and the potential influence of parameters such as fuel price and plant capacity factor is predicted. The issue of emissions and of plant operation are briefly addressed at end of this chapter.

Chapter 6 gives a summary of the conclusions reached in this study, as well as an outlook for the four advanced technologies for power generation.

2. State-of-the-art in electricity generation using coal

The chemical energy of coal can be converted directly through combustion (e.g., pulverized coal combustion, cyclone combustion, stroke combustion, and fluidized bed combustion) or indirectly (e.g., first through gasification or liquefaction, then through combustion or electrochemical reactors). A gas turbine and/or a fuel cell system might be thereinto involved. It should be mentioned that the latest advances in gas turbine technologies have helped bring the overall efficiency of a coal-fueled power plant to 45% (LHV) or higher, such as the case with the integrated gasification-combined-cycle power plants and the advanced fluidized-bed combustion power plants. This is partly because gas turbines exploit coal energy in a more rational manner than steam turbines that are conventionally involved in coal-fueled power plants.

In this chapter, a presentation of the state-of-the-art of the four types of coal-based power plant studied in this work is given first, followed by a brief overview of other competing electric power generation technologies using gas turbine systems, nuclear power plants, and renewable energy.

2.1 Pulverized coal combustion

One of the oldest technologies still dominating electricity generation is the pulverized coal combustion (PCC). Most of the world's coal-fired power plants and over 80% of power plants in the USA utilize this technology (Ruth (1999)). The world market for new coal-based

power plants from now to 2010 is worth about 700 billion dollars, among it 80% based on pulverized fuel technology with the remainder being gasification and fluidized-bed systems (EU (1999)).

First employed in the 1920s, PCC technology has proven to be simple, reliable, adaptable to most types of coal, and suitable for large electric power plants. The fine coal powder (50 microns or smaller) ensures pulverized coal firing an equivalent combustion rate to that of oil or gas. With modern burners, pulverized coal combustion can yield efficiency and low emissions. Thanks to its potential for further improvement, the PCC technology is the preeminent one for the near future.

Over the time period from the 1980s to the 1990s, commercially supplied conventional (subcritical) PCC power plants with flue gas desulfurization (FGD) with nominal capacities of 500 MWe were priced in the mid 1300$/kWe (in 1995 dollars). Now, due to the technology and economic advancement, the total plant costs for this type of power plants would be further lowered (DOE (1999e)).

Newer PCC power plants adopt supercritical steam conditions. The first supercritical steam power plants were built in the 1950s. Worldwide, more than 400 supercritical steam plants are in operation, with plant efficiencies approaching 45% (LHV) (World Bank (2000)). Among them is the world's largest lignite-fired steam power plant Schwarze Pumpe in Germany. Equipped with two 800 MW steam turbine generators, it runs under steam conditions 250 bar/544°C/562°C. The plant efficiency is about 41% (LHV). Table A.1 lists some supercritical steam power plants worldwide. It is very likely that the new pulverized coal plants built in EU countries will use supercritical steam conditions (EU (1999)). In China, four units of this type of power plant are in operation, with a total capacity of 2200 MW. Power plants amounting 7500 MW are under construction or planned (World Bank (2000)).

As pointed out in Chapter 1, the decisive issue for the promotion of pulverized coal technology is its environmental impact. This can be addressed by enhancing the system efficiency and by using more effective emissions control technologies. Driven by these two strategies, current development in design of power plants based on pulverized-coal technology focuses on higher steam parameters, incorporating gas turbines, low-emission burners, and better system integration.

The progresses made to date in material technology have been pushing

the fresh steam state to as high as 290 bar and 600°C, as indicated by Table A.1. As expected, these parameters will further increase. In addition, elevated boiler feedwater preheating temperatures, reduced boiler cold flue gas recirculation, and improved steam turbine efficiency benefit from advances in material technology.

Although all well-known ferritic and ferritic/martensitic steels have been in use, the advanced steam parameters impose a general change to improved steels in most areas of the boiler, steam piping, and turbine. The gains in efficiency through the use of higher steam parameters depend strongly on the metallurgical development, which ensures the reliability of the advanced steam power plants.

The problematic sections of supercritical steam boilers are the water walls, superheaters and thick-walled outlet headers/steam lines. The use of a material at elevated temperatures is mainly limited by its creep strength and resistance to degradation, in the form of embrittlement or softening. Superheaters are additionally vulnerable to high temperature corrosion. The general requirements for the materials used at elevated temperatures are the following (Scarlin (1997)):

- High creep strength at high temperature
- High toughness and resistance to embrittlement during long-term use at high temperature
- Resistance to steam oxidation and/or fireside corrosion
- Ease of fabrication for large forged and cast components, including weldability.

Nowadays, steam conditions up to 300 bar/600°C/620°C are achievable using steels with 12% chromium content. Up to 315 bar/620°C /620°C austenite is needed. Nickel-based alloys, e.g. Inconel, would permit 350 bar/700°C/720°C, yielding efficiencies possibly up to 48% (Paul (2000)).

New nickel-based superalloys will feature the new plants conceived by the "700°C" project. Superalloys for the hottest areas of the steam path will be developed targeting (a) creep strength in the range of 100 N/mm^2 at 750°C, and (b) minimum production costs. Simultaneously, development programs of austenites and ferrites have also been set up (Vanstone et al. (1998)) to reduce the use of nickel-based superalloys to the minimum.

In the following, three projects are briefly depicted. They reflect the

latest efforts in pulverized coal technology for electricity generation.

2.1.1 The "700°C" Project

Due to the fact that more advanced technologies - associated with material and manufacturing - will be attainable in about one decade, steam conditions higher than those in practice are proposed to further boost the steam power plant efficiency. A joint European group of manufacturers, utilities and institutes launched a project named "Advanced (700°C) PCC Power Plant", co-funded by the THERMIE program. This project aims at the development of pulverized coal-fired plants with live steam temperatures of 700-720°C, compared with up to 600°C for the best plants currently commercially available.

In the author's view, the expected plant efficiency might approach a level of 50% (LHV) for the best seawater-cooled versions. The actual plant efficiency will depend on among others the site conditions, the type of coal used and the steam turbine efficiencies. This project started in 1998 and will enter its last phase in 2006. A demonstration plant (capacity 400-1000 MW) is planned to be in operation by 2010.

2.1.2 The "LEBS" Project

Two representative projects aiming at developing advanced pulverized-coal power systems are underway in the USA: the Low Emission Boiler System (LEBS) and the High Performance Power System (HIPPS). Both technologies should be able to repower or retrofit the existing PCC power plants as well.

The LEBS project uses an integrated-system approach to derive maximum benefit from advances in low-NOx combustion, flue gas cleanup, and power cycle technology. The plant adopts a low-NOx U-fired slagging furnace, a moving bed copper oxide process for SO_2/NOx control, and a supercritical steam cycle (DOE (1999d)). The predicted system efficiency is in the range of 42%-45% (HHV).

2.1.3 The "HIPPS" Project

In contrast to the LEBS, the HIPPS is a highly advanced power system capitalizing on the experience base of power generators and the existing industry support structure. It is based on the indirectly-fired gas turbine combined cycle and hence uses technology more advanced than LEBS to achieve even higher efficiencies and lower emissions. The subsystem in a HIPPS that requires development is a coal-fired high-temperature air furnace (HTF).

Two designs of HIPPS are under development. One HIPPS design uses a fluidized-bed coal pyrolyzer operating at about 927°C and 18 bar. The pyrolyzer converts pulverized coal feedstock into two components: a low-heating-value fuel gas and solid char. The char is separated and burned in the HTF at atmospheric pressure, raising superheated steam and preheating the gas turbine air. The fuel gas is burned with the air from the HTF in a multi-annular swirl burner to further heat this air to the gas turbine inlet temperature.

In the other HIPPS design, the HTF is a direct-fired slagging furnace that utilizes flame radiation to heat air flowing through alloy tubes located within a refractory wall. The HTF is currently designed to heat air to 930°C-1000°C. In order to further boost this temperature, natural gas or another clean fuel can be used (DOE (1999c)). A HIPPS based on this design has been selected for the study in the present work. A sketch of this system is shown in Figure 2.1.

The HIPPS efficiency is expected to exceed 47% (HHV) with total plant cost equal to 95% of that for today's conventional PCC plants. The objectives for the final stage will be the detailed design, construction, and operation of a HIPPS prototype plant. The demonstration project is scheduled to be completed in year 2006.

2.2 PFBC

One of the key components of the pressurized fluidized-bed combustion power plants is the fluidized-bed combustor. In this kind of combustor, jets of air suspend the mixture of sorbent and burning coal during combustion at about 860°C, converting the mixture into a suspension

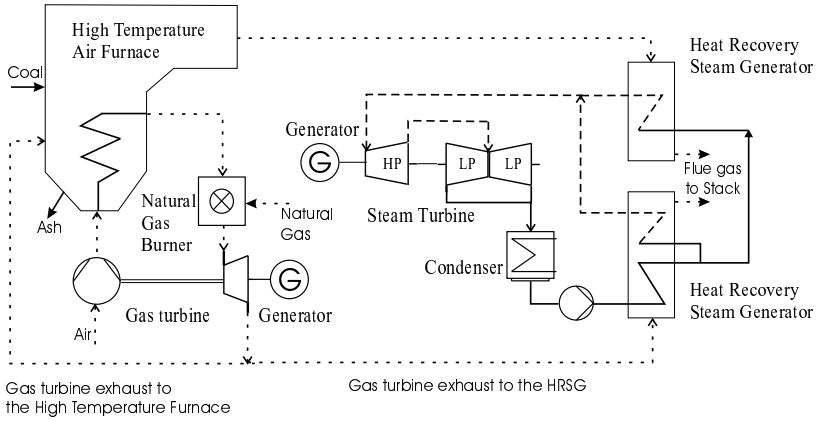

Figure 2.1: Schematic for a HIPPS.

of red-hot particles that flow like a fluid. The primary driving force for the development of fluidized-bed combustion was the reduction in SO_2 and NOx emissions inside the combustor. With typical bed operating temperatures between 815°C and 870°C, inexpensive material such as limestone or dolomite can be used to remove 90% or more of SO_2 from the flue gas. Hence, it is possible to achieve low SO_2 emission levels without additional sulfur removal equipment, even if high sulfur coal is used. Moreover, the NOx formed in the bed is less than in conventional combustors, which operate at higher temperatures. For all the circulating fluidized-bed combustors, further suppression of NOx formation can be accomplished by air staging with less impact on combustion efficiency than in pulverized coal furnaces.

A striking feature of the fluidized-bed combustion is its tolerance to coal feedstock. It allows burning high fouling and slagging fuels, since the bed temperature is below the ash fusion temperatures.

Due to its attractive environmental performance and high fuel flexibility, the fluidized-bed combustion technology has been intensively studied for implementation in the power generation in the last decade (DOE (1989), Buchanan et al. (1994), Campbell et al. (1990), VEAG (1994) and White, Getty & Torpey (1995)). There are basically two versions of PFBC technology approaching the market: The bubbling-bed concept and the circulating fluidized-bed concept. A so-called

second generation PFBC (or advanced PFBC) power plant adopts the latter concept integrated with a carbonizer and a topping combustor (see flow diagram in Figure 2.2). While the first generation PFBC power plants are in early commercial operation stage, the second generation PFBC power plants are in demonstration period. Table A.2 gives an overview of PFBC commercial scale power plants. The data indicate that the efficiency of the first generation PFBC power plants already reaches 42% (HHV).

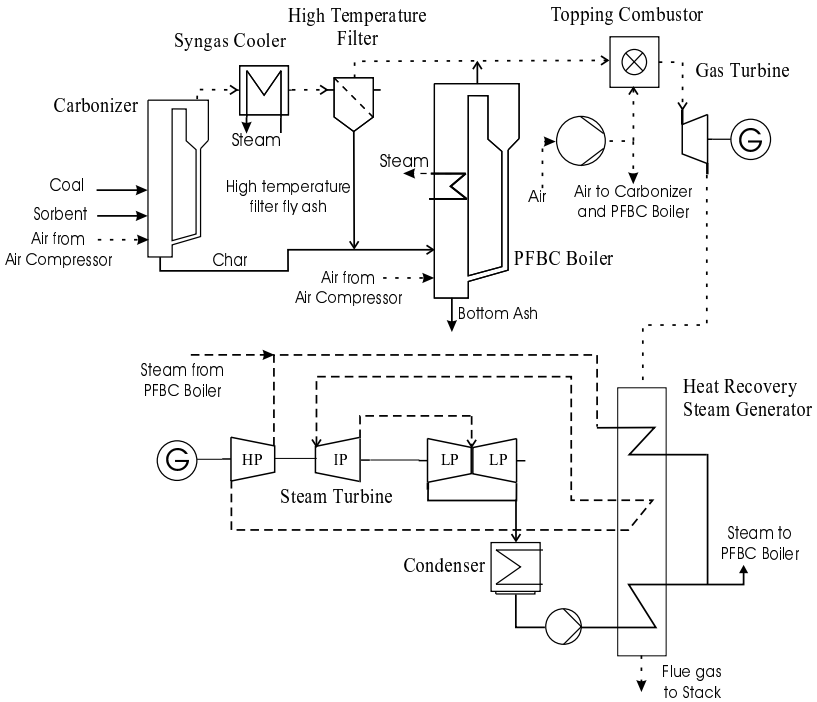

Figure 2.2: Schematic for a PFBC power plant.

Regarding the second generation PFBC technology, a test system started operating in Cottbus, Germany late 2000 (University of Cottbus (2000)). Besides, a fully integrated PFBC power system with net electricity output of 103 MW is scheduled to be in operation in 2005. It is located in Florida, USA and expected to have an efficiency of 45% (HHV) (DOE (1999b)). According to the results of the present work, the ef-

ficiency of a commercial second generation PFBC power plants could reach 46% (HHV) or higher. Components critical to the second generation PFBC power plants are hot gas cleanup system (ceramic barrier filters), advanced carbonizer (gasifier), hot gas piping, solids transfer valves, coal-water paste pumps, and gas turbine optimized for PFBC systems. In the following chapters, the term "PFBC power plant" refers always to the second generation PFBC power plant.

2.3 IGCC

An IGCC power plant consists of a coal gasification unit (*gasification island*), a gas-fired combined-cycle power plant (*power island*), and an air separation unit (ASU), if any. IGCC power plants have the potential of generating electricity from fuels such as coal with high efficiency and with low emissions. These plants are characterized by the type of gasifier (fixed-bed, entrained-bed, or fluidized-bed), the oxidant fed to the gasifier (oxygen or air), and the degree of integration between the ASU and the gasification island as well as the gasification and the power island. A process diagram of a typical IGCC power plant is shown in Figure 2.3, whereby 100% of the ASU air intake is provided by the gas turbine air compressor.

After the first demonstration project in Coolwater (California), the first fully integrated gasification-combined-cycle power plant was the 250 MW unit at Buggenum, Netherlands (Stultz & Kitto (1992)), while the most modern IGCC power plant worldwide is the plant at Puertollano, Spain. IGCC power plants with a sum of over 600 MWe are now in commercial service in the United States. Up to 10% more efficient than conventional pulverized coal plants, these IGCC plants achieve up to 98% SO_2 removal and reduce NOx emissions to approximately $0.043 kg/GJ$ (DOE (1999b)). In addition to its efficiency potential and excellent environmental performance, an IGCC power plant possesses features such as repowering capability, modularity, fuel flexibility, phase construction, low water use, involvement with newest technology, reusable sorbents, marketable by-products, co-products, and good public acceptability.

Table A.3 shows a number of commercial scale coal-based IGCC power plants that entered service in recent years (Lowe (1998) and Univer-

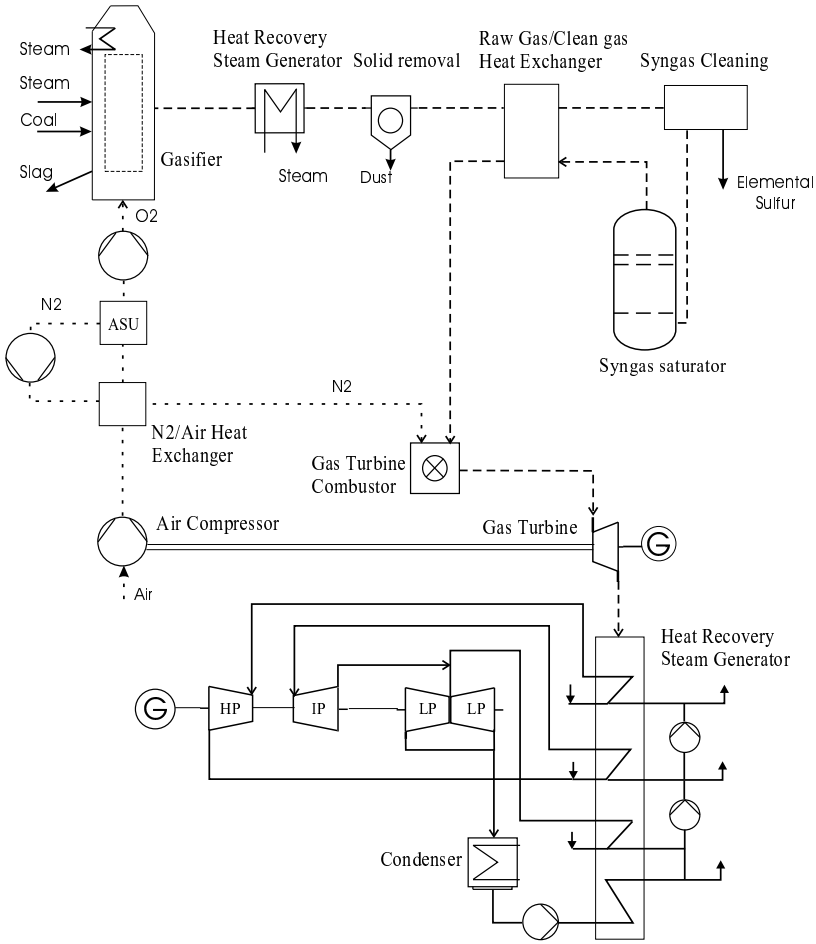

Figure 2.3: Schematic for an IGCC power plant.

sity of Essen (2000)). As can be seen, IGCC power plants achieving efficiencies up to 42% (HHV) are at the commercial demonstration stage of development. It is expected that future IGCC power plants will have even higher efficiencies and lower investment costs than the contemporary ones (Pruschek (1998) and Eurlings (1999)).

Cost reduction is crucial to the market penetration of the IGCC tech-

nology, and capital cost is the main concern. The plant cost for the commercial demonstration IGCC power plants of 250 MW is about 2000 $/kWe (in 1995 dollars) (Lowe (1998)), higher than that of conventional coal-based combustion plants (about 1500 $/kWe (in 1995 dollars)), not to mention the natural gas combined-cycle power plants (about 500 $/kWe (in 1995 dollars)). However, as this technology becomes mature, the associated plant cost will certainly decrease. Using hot gas cleanup in combination with air-blown gasifiers, for example, will further reduce the capital cost of an IGCC power plant.

Additional development efforts are made in areas such as increase in gas turbine inlet temperatures, co-production of both chemicals and electricity, improvement in gasifier designs, and integration of gasification with advanced gas turbine cycles and fuel cells. When three factors - efficiency, cost of electricity, and environmental benefits - are considered simultaneously, IGCC technology precedes all the advanced technologies for power generation to meet the need of coming decades. It is estimated that, by the middle of this century, 30% of electricity generation in USA will be accomplished by IGCC power plants (DOE (2000c)), with 450 GW capacity.

2.4 Other technologies

Over the last 50 years, gas turbine efficiencies have increased from 33% to 38 % (LHV), and those of gas turbine combined-cycles from 48% to 58% (LHV). Towards the end of the 20th century, the worldwide contract awards for natural gas fired power plants averaged 63 GW per year, and about 67 GW per year were forecast over the time period of 2000-2004 (Taud et al. (2000)).

In 1997, the worldwide nuclear capacity was 352 GW, which generated a total of 2276 billion kWh of electricity, providing 17 percent of the world's electricity generation (DOE (1999f)). In 1999, eight countries met at least 40% of their total electricity demand with generation from nuclear reactors (Wesselmann & Unger (2000)). It was projected with uncertainty that the capacity would increase to 356 GW in 2010 and then begin to decline, reaching 311 GW in 2020. While the active nuclear power programs of some countries such as South Korea, Japan, France, and China result in the near-term increase in the overall nu-

clear capacity, plant retirements in the USA and other countries will exceed the capacity additions, contributing to the capacity decline after the year 2010. We should keep in mind that the nuclear industry still faces the challenges of high construction costs and public concern about safety and nuclear waste storage.

In contrast to the nonrenewable fossil fuels, the renewable energy resources are constantly replenished and will never run out. The renewable energy technologies have a much lower environmental impact than conventional energy technologies. The renewable energy sources for electricity generation are most likely to be wind, solar energy (especially solar photovoltaics) and closed-loop biomass.

The fastest growing energy technology in the world, power generation with wind energy showed a capacity surging worldwide from under 2 GW in 1990 to 16.6 GW at the end of 2000. Within the year 1999 alone, more than 3.6 GW of new wind energy generating capacity were installed, thanks to the additions from Germany (1.2 GW), the USA (732 MW), and Spain (650 MW). It was claimed that wind energy would produce 10% of the worldwide energy supply by the year 2020 (American Wind Energy Association (1999)). The current cost of electricity from wind energy lies between 5 and 7 cent/kWh (Flavin (2000)).

While biomass currently provides 35% of the energy in the developing nations, its contributions are much smaller in industrial countries (e.g., 4% in the USA and 2% in Europe in 1998 (Horazak & Brushwood (2000))). In the USA, nevertheless, biomass is the country's leading non-hydro resource of renewable energy. More than 500 electric power plants operate on biomass, with a total capacity of 7.5 GW. Technology development for biomass power can be grouped into two categories: feedstock development and conversion technologies. A reliable feedstock supply available at a predictable price is necessary for the success of any biomass power plant, resulting in much interest in the use of dedicated feedstock. However, the situation is that the crop producer costs are too high, and the price that the electricity producers can pay is too low (Overend (1997)). Another issue is that the efficiencies of biomass power plants are, in general, 20% and 45% for steam plants and IGCC plants, respectively. In view of the high capital cost of a new biomass fired power plant today, around 1500-2000 $/kW in the USA, the increase in plant efficiency would have two effects: It

would reduce the capital cost on a kW basis, and it would reduce the sensitivity of the final cost of electricity to the fuel cost component. The current cost of electricity from biomass plants in the USA varies from 5.5 to 8.5 cent/kWh.

The geothermal resource has been used in many countries. In 1990, electric power plants driven by geothermal energy provided over 44 billion kWh of electricity worldwide per year, and the world capacity was about 6 GW. It was projected that this capacity would be 15 GW in 2000, growing by 9% per year (Horazak & Brushwood (2000)). Most geothermal power plants have availability factors over 90%, and they emit roughly 1000 to 2000 times less carbon dioxide than fossil fueled power plants. However, the high capital costs of geothermal power plants exert negative influence over the exploitation of this resource. In the USA, for example, the typical field and plant cost is around $2000 per installed kilowatt today, and the cost of electricity ranges from 5 to 8 cent/kWh (DOE (2000b)).

With an ancient history, solar energy has emerged as a competitor to fossil fuels. For example, the world photovoltaic shipment increased from almost zero in 1975 to more than 800 MW in 1997, with an average cost reduction of 80% in the last two decades (Flavin (2000)). Concentrating solar power systems, with capacities ranging from 10 kW to 100 MW, are being developed in countries such as the USA, India, Egypt, Mexico, Greece, and Spain. The DOE estimated that by 2005 there will be as much as 500 MW of concentrating solar power capacity installed worldwide. Current technologies correspond to $2000/kW – $3000/kW, resulting in a cost of solar power of 9 – 12 cent/kWh (DOE (2000d)).

Hydro power contributed to about 18.9% of the world electricity generation in 1995 and is expected to grow at an average rate of 2% per year. However, it faces limited prospects for the future. Most of the best available sites in the industrialized countries have long since been exploited, and hydro power is no longer viewed as an environmentally benign energy source. Only developing regions with hydro resources will increase the use of this energy source for generating electricity. The average capital cost of hydro power plants that commenced operation during 1993 was between $1700-2300/kW, and the corresponding cost of electricity has been 2.4 cent/kWh (Rinehart (1999)).

Most renewable energy technologies are still relatively expensive and

cannot consistently provide large amounts of electricity. Although the non-hydro renewable energy is projected to have a very high growth rate over the next twenty years, it starts from a low basis and its share by 2020 will be still less than 1% of the world electricity generation. In contrast, nuclear technology is well developed, and some countries have significant experience in building and operating nuclear power plants. Therefore, it may be a more attractive option for meeting short-term goals of emissions reduction.

3. Methodology and basic assumptions

The performance of the four types of advanced coal-fired electric power plants considered in this study is evaluated through both exergy analysis and economic analysis. A detailed exergetic analysis provides rational criteria for design, evaluation, improvement, and comparison of power plants or of their components from the thermodynamic point of view. In this chapter, the methods of exergy analysis and economic analysis are briefly illustrated. The main assumptions made for the entire thermodynamic and economic analyses are also presented.

3.1 Method of exergy analysis

Exergy is the maximum theoretical useful work attainable from an energy carrier under the conditions imposed by an environment at given pressure p_0 and temperature T_0, and with given amounts of chemical elements.

The purpose of an exergy analysis is generally to identify the location, the source, and the magnitude of true thermodynamic inefficiencies in power plants. Moreover, the results from an exergy analysis constitute a unique base for exergoeconomics, an exergy-aided cost reduction method (Tsatsaronis (1998)). The information provided by an exergy analysis can be thus used as a guide for reducing the thermodynamic inefficiencies of power plants and for improving their performance. Indeed, less destruction and losses associated with a power plant correspond to a higher yield of the power plant.

The key variable resulting from an exergy analysis is the exergetic

efficiency, ϵ. It shows the percentage of the fuel exergy to be found in the product exergy of a power plant or a component. Therefore, the exergetic efficiency gives an unambiguous criterion for judging the performance of a power plant and, more importantly, of its components, from the thermodynamic viewpoint. Depending on the purpose of purchasing and using the *kth* plant component, for example, we define two parameters: fuel $\dot{E}_{F,k}$ and product $\dot{E}_{P,k}$. The fuel represents the net exergy resources spent in this component for generating the product, whereas the product reflects the very purpose of including the component into the power plant. The definition of the fuel and of the product were discussed by Tsatsaronis (1993), Tsatsaronis (1995) and Lazzaretto & Tsatsaronis (1996). The exergetic efficiency of the *kth* component is then defined as:

$$\epsilon_k = \frac{\dot{E}_{P,k}}{\dot{E}_{F,k}}. \tag{3.1}$$

In the case of power plants, the exergetic efficiency can be similarly defined, based on the purpose of operating the plants. For the power plants concerned in this study, the fuel is taken as the exergy supplied to the plant by coal and methane ($\dot{E}_{coal} + \dot{E}_{methane}$), when applicable, plus the exergy in the combustion air ($\dot{E}_{air}$). The product is equal to the net electric output of the plant ($\dot{W}_{net}$). The overall exergetic efficiency ϵ_{tot} of a power plant can be therefore written as:

$$\epsilon_{tot} = \frac{\dot{W}_{net}}{\dot{E}_{coal} + \dot{E}_{methane} + \dot{E}_{air}}. \tag{3.2}$$

In view of exergy analysis, the sources of inefficiency of a power plant are exergy destructions and exergy losses. While the exergy losses refer to the exergy rejected from the power plant to the environment without being further used (e.g., the exergy stream carried out of the plant by the stack flue gases), the exergy destructions within the power plant or component are caused by the irreversibilities inherently associated with phenomena such as chemical reaction, heat transfer, mixing, throttling, friction, and free expansion that take place inevitably in a power plant. It is always beneficial to know the major sources of exergy destruction within a power plant. The exergy destruction rate ($\dot{E}_{D,tot}$) of a power plant can be quantitatively determined through an exergy balance. By assuming that the power plant operates at steady-state, the exergy

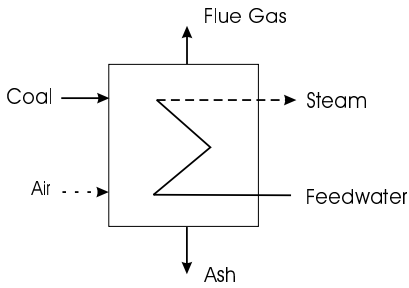

Figure 3.1: Schematic for a conventional boiler.

balance for the plant can be expressed as:

$$\dot{E}_{D,tot} = \dot{E}_{F,tot} - \dot{E}_{P,tot} - \dot{E}_{L,tot}, \tag{3.3}$$

where $\dot{E}_{F,tot}$ and $\dot{E}_{P,tot}$ are the fuel and the product of the power plant, respectively; $\dot{E}_{L,tot}$ denotes the exergy loss rate of the plant.

The exergy balance can be applied at the component level. For the kth component in the plant we obtain

$$\dot{E}_{D,k} = \dot{E}_{F,k} - \dot{E}_{P,k}. \tag{3.4}$$

Here the exergy loss for a component is considered zero and the heat losses, if any, are treated as exergy destruction within the component.

The fuel, the product, and the exergy losses are derived from the exergy values of the material streams of interest, as results of a thermodynamic simulation of the power plant. For instance, the fuel and the product of a boiler shown in Figure 3.1 are formulated as given by Equations 3.5 and 3.6. The basic idea is that the purpose of operating a boiler is to raise steam from the boiler feedwater:

$$\dot{E}_{F,boiler} = (\dot{E}_{coal} + \dot{E}_{air}) - (\dot{E}_{fluegas} + \dot{E}_{ash}); \tag{3.5}$$

$$\dot{E}_{P,boiler} = \dot{E}_{steam} - \dot{E}_{feedwater}. \tag{3.6}$$

Note that the heat loss of the boiler has exergy value of zero, for this heat is rejected to the environment at temperature T_0.

Beside exergetic efficiency and exergy destruction rate, variable such as exergy destruction ratio ($y_{D,k}$) might be also calculated in an exergy analysis. For the kth component in a power plant, $y_{D,k}$ is defined as in Equation 3.7.

$$y_{D,k} = \frac{\dot{E}_{D,k}}{\dot{E}_{F,tot}} \tag{3.7}$$

When comparing the performance of various components in a power plant, the above defined exergy destruction ratio can be useful. However, this variable is usually system structure-dependent (Tsatsaronis (1999)) and therefore should be used with caution for overall effectiveness improvement. This is because of the fact that part of the exergy destruction in a component might be a function of the exergy destruction in some other components of the plant. In this study this variable is used, during the process of exergy analyses, for reference only.

3.2 Tools for a thermodynamic simulation of the power plants

Aspen Plus Flowsheet Simulator (Aspen Plus (9.3-1)) - a commercial software for steady-state chemical/power system simulation - is used in this study for simulating the performance of the power plants. This software calculates thermodynamic variables such as mass flow rate, temperature, pressure, enthalpy, entropy, and the amount of work/heat transfer as well. The major drawback of the commercially available Aspen Plus, in view of this study, lies in the fact that it does not conduct exergy calculations. To address this issue, the author wrote several user subroutines for calculating exergy values and embedded them inside Aspen Plus. The exergy values of the gaseous, liquid, and solid (including coal) streams are then retrieved from the simulation results as are the thermodynamic variables mentioned above.

Due to the fact that no gas turbine model is available in Aspen Plus which allows polytropic efficiency instead of isentropic efficiency as input datum, the author provided a general gas turbine model based on technical data of Siemens' V84.3A gas turbine (Farmer (1997)).

The following correlation is used to calculate the polytropic efficiency of the gas turbine air compressor (DOE (1990) and Wilson (1984)):

$$\eta_{poly} = A - \frac{(r-1)}{B}, \tag{3.8}$$

where r is the pressure ratio of the gas turbine, $A = 0.95$, and $B = 500$.

The polytropic efficiencies of the high and low pressure turbine are likewise estimated with $A = 0.95$ & $B = 300$ and with $A = 0.97$ & $B = 300$, respectively.

Taking into account the air cooling effect, the polytropic efficiency of the high pressure turbine is adjusted by a correction $\Delta\eta$ calculated according to the methodology depicted in Traupel (1988) and a coefficient (C) obtained based on the efficiency of the V84.3A gas turbine under ISO conditions:

$$\eta_{poly,HP,corrected} = \eta_{poly,HP} - C\Delta\eta. \tag{3.9}$$

The coefficient C was introduced by the author to adjust the correction $\Delta\eta$ since the calculated $\Delta\eta$ tends to overstate the adverse effect of the cooling air on the gas turbine polytropic efficiency as the adiabatic combustion temperature increases. The values for C range from 0.55 to 0.75.

The consideration of the cooling air stream results in a fictitious gas turbine inlet temperature (T_{GTIT}), namely the ISO gas turbine firing temperature. If the combustion gases and the entire cooling air flow were mixed before entering the gas turbine, the gas mixture would possess a temperature equal to T_{GTIT}. This temperature is referred to throughout this study when the gas turbine inlet temperature is mentioned. It should be pointed out that this T_{GTIT} is as same as the one used in the above mentioned method for the correction of gas turbine polytropic efficiencies.

Note that it is assumed that the gas turbines involved in this study are of the best technology available. The gas turbine model described above gives, for example, a net LHV efficiency of 38.5% for Siemens' V84.3A gas turbine operating under ISO conditions.

The isentropic efficiency of a steam turbine section is predicted by the Spencer, Cotton, and Cannon method (SCC) method (Spencer,

Cotton & Cannon (1974)), with exception of the first reheat section in the SC power plants. This is accomplished by incorporating several user subroutines in Aspen Plus. The SCC method is used in this study to represent the actual performance of a steam turbine as closely as possible. To reflect the already achieved advances in steam turbine technologies, the calculated isentropic efficiencies are multiplied with a factor ranging from 1.03 to 1.05, as suggested in Cotton (1998). In cases where the prediction of the efficiency is beyond the application range of the SCC method, the turbine section isentropic efficiency is given as a fixed value.

To estimate the exergy destruction associated with coal combustion within a boiler, an adiabatic combustion process has been assumed. That is, this exergy destruction is calculated as if the furnace exit temperature were equal to the maximum combustion temperature. The effect of water-cooled enclosure walls on the temperature of the combustion products leaving the furnace is, in doing so, neglected. Though this exergy destruction is underestimated, the overall value of the exergy destruction relative to the boiler remains correct.

3.3 Economic analysis of the power plants

In this study, the criterion used for the economic comparison among the power plants is the levelized cost of electricity (LCE). It is derived from the levelized total revenue requirement (TRR), the plant net output, and the annual average plant operating hours. The 20-year levelized cost of electricity, in current dollars, has been chosen for this purpose. For calculating the LCE associated with the four types of power plants, the TAG-method of the Electric Power Research Institute (EPRI) – documented in Ramachandran (1993) and applied in Bejan, Tsatsaronis & Moran (1996) – is followed. In this section, the methodology for calculating the LCE is first discussed briefly. The main assumptions and the estimation of the purchased-equipment costs (PEC) are then presented.

3.3.1 Methodology

The annual TRR (or the total product cost) for a power plant is the revenue that must be collected in a given year through sale of the plant products to compensate the owner of the plant for all the expenditures incurred in the same year (Bejan, Tsatsaronis & Moran (1996)). A year-by-year analysis is used to calculate the levelized TRR and hence the LCE of the power plants. The TRR consists of three categories: The levelized fuel costs, operating and maintenance (O&M) costs, and carrying charges (CC). While the fuel costs and the O&M costs simply embody the costs as indicated by the terms, the carrying charges in the TRR comprise items such as the depreciation of the total capital requirement (TCR), the deferred income taxes, the recovery of the allowance for funds used during construction (AFUDC) associated with the common equity, the return on common equity, the interest on debt, the income taxes, and other taxes and insurances.

A concise description of how the total capital requirement has been calculated is included in Section E.2. An elaboration for estimating the TRR, the fuel costs, and the O&M costs can be found in Bejan, Tsatsaronis & Moran (1996). The general assumptions and criteria for the economic analysis are listed in Table 3.1.

3.3.2 The purchased-equipment costs (PEC)

The cost data of the power plants under study are mainly based on those found in several technical reports (Becker et al. (1994), Klara (1994a), Klara (1994b), Buchanan et al. (1994), Bechtel (1995), and Price (1992)). Details are presented in Appendices F, G, H, and I for each type of power plant.

In the process of case analysis, the purchased-equipment cost of an equipment item at a capacity or a size other than the given one, denominated $C_{PE,Y}$, is calculated by following relation:

$$C_{PE,Y} = C_{PE,W} \left(\frac{X_Y}{X_W} \right)^{\alpha}, \tag{3.10}$$

where $C_{PE,W}$ is the PEC at the design capacity; X_W and X_Y are the design capacity or size and the current capacity or size of the equipment item, respectively.

The typical values for the scaling exponent (α), together with the corresponding capacity parameters, are quoted from Bejan, Tsatsaronis & Moran (1996) and given in Section E.1. This scaling method applies also to the required material cost and the labor cost for the purchased equipment.

For bringing all the cost data necessary for the economic analysis to a reference year, 1998 in this study (see Table 3.1), the Chemical Engineering Plant Cost Index published by *Chemical Engineering* is referred to.

3.4 Main assumptions for the power plants

Illinois No. 6 bituminous coal is used as design coal for all types of power plants in this study. Its composition is given in Table B.1. Pure methane with a HHV of 55.52 MJ/kg is burnt in place of natural gas for the HIPPS. The dolomite consists of 80.4% calcium carbonate ($CaCO_3$), 16.1% SiO_2, and 3.5% $MgCO_3$. When limestone is used, it consists of only $CaCO_3$.

Air at 15°C, 1.013 bar and with relative humidity of 60% has been selected for this study. Its composition is listed in Table B.2.

The following assumptions are general for the four types of power plants unless otherwise stated:

- Steady-state, full-load plant performance is evaluated;
- There is no pressure loss in the air intake duct;
- The pressure loss in the gas turbine combustor is 4% ;
- The steam turbine throttle pressure drop is 5%;
- The coal combustion efficiency is 99.5% with 0.5% of carbon unburned;
- The coal combustor heat loss is 0.5% of the coal HHV;
- 3-4% pressure drop is assumed for the heat exchangers;
- The generator efficiency is 98.7%;
- The generator shaft loss is 0.7%;
- The turbo-compressor shaft loss is 1%, if applicable;
- The generator transform loss is 0.24%;
- The steam turbine condensing pressure for all the base cases is 0.083 bar, except for the HIPPS, where 0.051 bar is assumed by DOE for the design case.

The plant-specific assumptions for the four types of power plants are summarized in Appendix B.

The auxiliaries for the power plant were calculated based on the data given in each relevant report. These include in general the power consumption for the boiler feed booster pumps, the circulating water pumps, the cooling tower fans, and the heater drain pumps; the steam turbine auxiliary; the power consumption for coal pulverization, coal handling, limestone handling, and ash handling; the power consumption for the FGD pumps/agitators and for the precipitators; and the miscellaneous balance including plant controls and lighting. The power requirement for auxiliaries was deducted from the plant gross output at end of the thermodynamic simulation.

Table 3.1: Main assumptions and criteria for the economic analysis of the power plants. TPC stands for total plant cost.

Monetary Unit	mid-1998 dollar	
Begin of the design and construction	Jan. 1, 2000	
Constant average general inflation rate of all costs	%	2.5
Real escalation rate of all costs except fuel	%	0.0
Real escalation rate of coal	%	0.1
Real escalation rate of natural gas	%	0.3
Plant economic life	year	30
Plant life for tax purpose	year	20
Project financing		
Common equity	%	50
Debt	%	50
Cost of money		
Required annual return for common equity	%	13.0
Required annual return for debt	%	7.0
Resulting average cost of money	%	10.0
Average combined income tax rate	%	38.0
Average property and tax rate	% of TPC	1.5
Average insurance rate	% of TPC	0.5
Average labor rate	$/year	30.0
Average number of working hours/position	hour/y/po.	2080
Labor overhead charge rate	% of labor	30
Cost of coal (based on HHV)	$/GJ	1.5166
Higher heating value of coal	MJ/kg	27.386
Cost of natural gas (based on HHV)	$/GJ	2.7015
Higher heating value of natural gas	MJ/kg	55.520
- EPRI TAG (Ramachandran (1993)) methodology followed - Current dollars used including effect of inflation - Straight-line depreciation used for company purposes and tax purposes - Net salvage value equal to zero - No investment tax credit and no grants in aid of construction - Revenue levelizing occurs with before-tax average cost of money - Cost of land, working capital, and common equity AFUDC are non-depreciable		

4. Results and Discussion

4.1 Conventional steam power plant

Chosen as a base for comparison, a conventional pulverized coal combustion steam power plant described by Becker et al. (1994) is considered first. The steam conditions for this power plant are 165 bar/538°C /538°C. The feedwater to the steam generator (SG) is heated up to 252.5°C in a 7-stage feedwater preheating system. The pressure drop on the flue gas side within the SG is 12.3%. The plant outlay is shown in Figure 4.1.

The thermodynamic simulation of this conventional steam plant was conducted. The calculated mass flow rates and the corresponding state variables are listed in Table C.1.

This conventional steam power plant has a thermal efficiency of 36.60%, based on the HHV of the coal (LHV 38.28%). The mass flow rate of the coal feedstock is 50.635 kg/s, yielding a plant net power output of 507.6 MW.

The exergetic efficiency of this power plant is 35.8%. About 28% of the plant exergy input is destroyed in the coal combustion process, while some 20% in the heat transfer process within the steam generator. 4.28% and 4.09% of the exergy input is brought away by the stack flue gas and by the condensing water, respectively. For details see Appendix D.1.

4.1.1 Economic analysis

The breakdown of the total direct costs for this power plant is listed in Appendix F.1, based on the data provided by Becker et al. (1994).

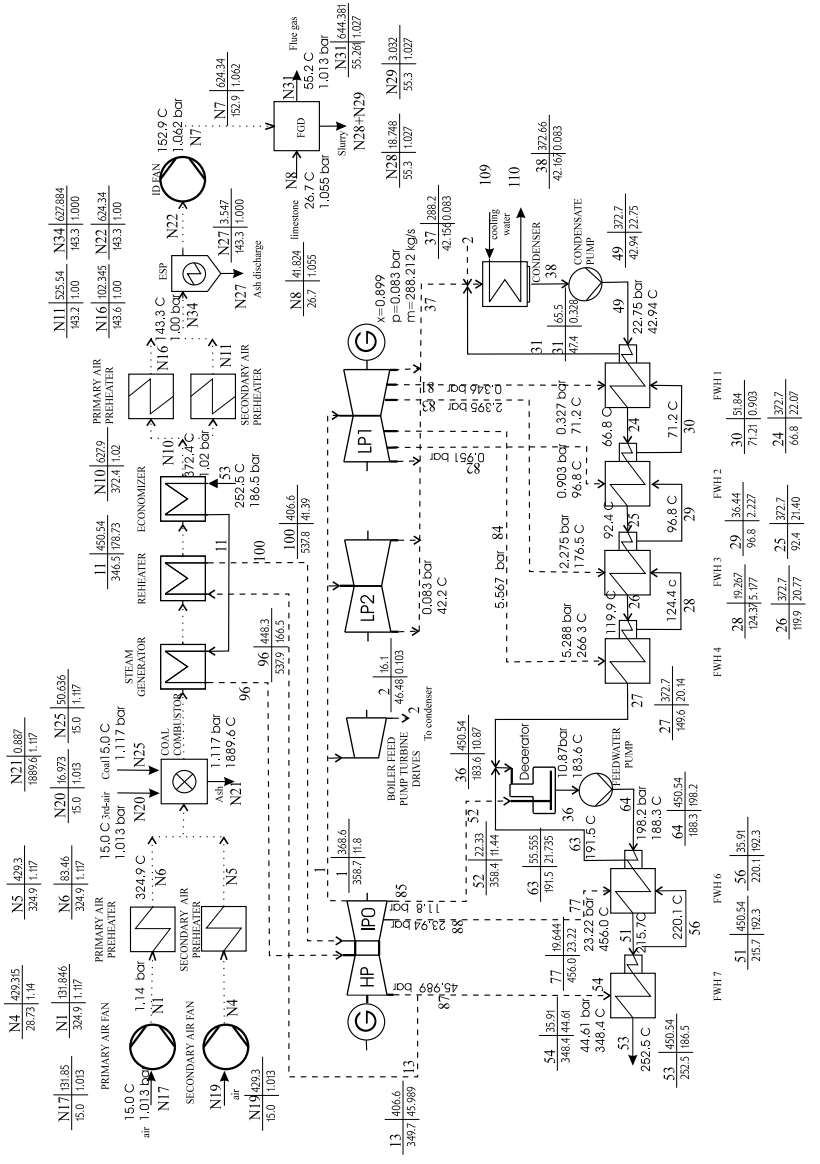

Figure 4.1: Flowsheet for the conventional steam power plant.

The breakdown of the total capital investment for the conventional PCC power plant, as well as the levelized annual costs and total revenue requirement (TRR) in current and constant dollars for levelization time periods of 20 and of 30 years, respectively, is also presented in Appendix F.1, together with the key economic parameters for this power plant.

The total plant cost is 1410 US$(mid-1998)/kW, and the levelized cost of the electricity for a 20-year period is estimated as 6.81 cent/kWh (in current dollars).

4.2 Supercritical steam power plant "580°C"

The power plant Skærbæk unit 3 in Denmark (Kjær (1998)) has been chosen as a reference for the outlay of this supercritical steam power plant described in Section 4.2.1. Next, the results from the exergy analysis are presented (Section 4.2.2), followed by parametric studies concerning the potential influences of some main operating parameters on the overall exergetic efficiency of the plant (Section 4.2.3). An economic analysis is then conducted for this supercritical steam power plant (Section 4.2.4). At the end of this section, performance prediction and economic evaluation of a future supercritical steam power plant "700°C" are presented (Section 4.2.5).

4.2.1 Plant description

In the supercritical steam power plant shown in Figure 4.2, pulverized coal is fed to a once-through boiler (i.e., steam generator) for generating supercritical steam at 290 bar and 582°C. The steam expands first in a very-high-pressure (VHP) steam turbine to 94 bar and is then reheated in the boiler to 580°C before entering a high pressure (HP) turbine. The steam at the outlet of the HP turbine section (19 bar/339°C) is led to the boiler for a second stage of reheating to 580°C. The reheat pressures correspond to the extraction pressure of the last feedwater heater (FWH) and to the operating pressure of the

deaerators, respectively. The pressure losses for the first and the second reheating are assumed to be 5% and 10%, respectively, as in the practice. The steam turbine expansion end pressure is 0.083 bar, with steam exhaust quality of 0.962. A counterflow mechanical draft cooling tower is adopted for condensing the main turbine exhaust steam.

A 10-stage feedwater preheating system is used to preheat the boiler feedwater up to 300°C. The thermal energy in the flue gas leaving the steam generator is recovered in air preheaters of regenerative type. The flue gas leaves the boiler at a temperature of 143.3°C and is, after desulfurization, discharged through a stack to the atmosphere.

4.2.2 Exergetic analysis

This supercritical steam power plant has a net power output of 507.6 MW, same as that of the conventional steam power plant. While the steam mass flow rate reduces from 448.3 kg/s for the conventional power plant to 379.6 kg/s in this power plant, the coal feedstock decreases from 50.635 kg/s to 46.285 kg/s. The calculated mass flow rates and the corresponding state variables are listed in Table C.2.

The isentropic efficiency for the VHP turbine section is calculated by SCC method as 0.862, slightly higher than that in the HP section of the conventional cases (0.86). For the first reheat section, an isentropic efficiency of 0.95 is assumed.

The overall thermal efficiency is 40.05% (HHV), or 41.88% based on LHV. The overall exergetic efficiency is calculated as 39.17%, 3.4 percentage points higher than that of the conventional steam power plant (recall Section 4.1).

The increase in the overall exergetic efficiency results mainly from the reduced exergy destruction in the steam generation, by virtue of the high live steam and reheat steam parameters and of the small turbine steam throughput. The details on the exergy destruction of each major plant area are given in Table D.2. The largest exergy destruction takes place in the fuel combustion process (28.3% of fuel exergy), followed by the exergy destruction associated with the heat transfer inside the steam generator (17.4% of fuel exergy).

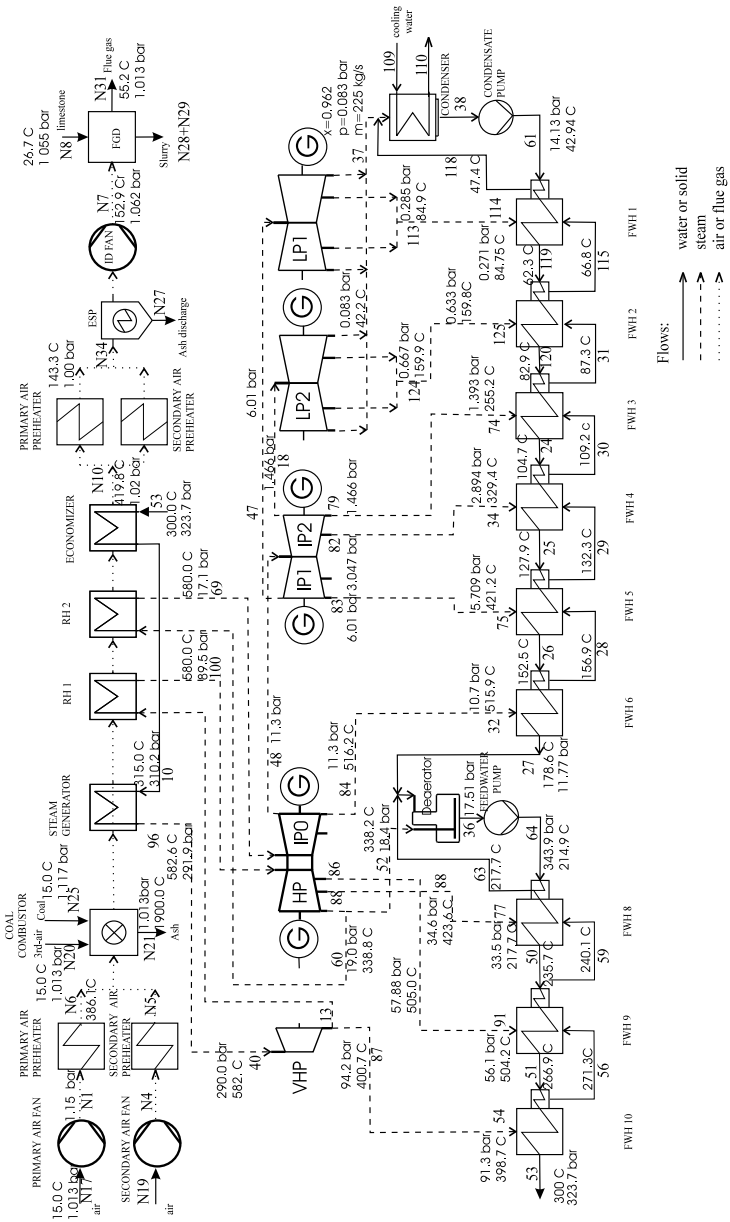

Figure 4.2: Flowsheet for the supercritical steam power plant "580°C".

4.2.3 Parametric studies

In this section, parametric studies are conducted for several parameters that affect the overall performance of a supercritical steam power plant. These are the main steam temperature and pressure, the feedwater preheating temperature, the condenser pressure, and the SG flue gas temperature.

The plant net power output is fixed at 507.6MW, and only one parameter varies at each time.

Effect of steam temperature level

As the exergetic analyses indicate, the second largest exergy destruction in a steam power plant is related with the heat transfer in the steam generation process and amounts to about 14 to 20% of the fuel exergy. This exergy destruction can be most effectively reduced by increasing the steam temperature level (Figure 4.3). Solely increasing the steam temperature level by 20°C results in about 0.4 percentage point gain in the overall exergetic efficiency.

A increase in the steam temperature level results in a reduction in the exergy destruction in the SG heat exchange process, from 17.39% to 15.25% as the temperature level increases from 580°C to 700°C, for example. This is mainly due to the smaller heat transfer temperature difference and the smaller amount of heat transfer in the SG at higher temperature level (about 62 MW less in this case). Moreover, the exergy destruction in the steam turbine (ST) is smaller (2.07% for 580°C and 1.82% for 700°C) due to higher operation parameters, dryer steam exhaust (higher LP section efficiency), and less steam throughput.

At a higher steam temperature level, for example 700°C instead of 580°C, the rate of exergy destruction in the feedwater preheating system has a slightly higher value (1.58% for 580°C and 1.72% for 700°C), since the steam extraction temperatures are normally higher at a higher steam temperature level. Here it is assumed that the feedwater heater terminal temperature differences remain unchanged.

The rate of exergy losses associated with cooling water declines slightly, from 3.74% to 3.55%, as the result of smaller main steam mass flow

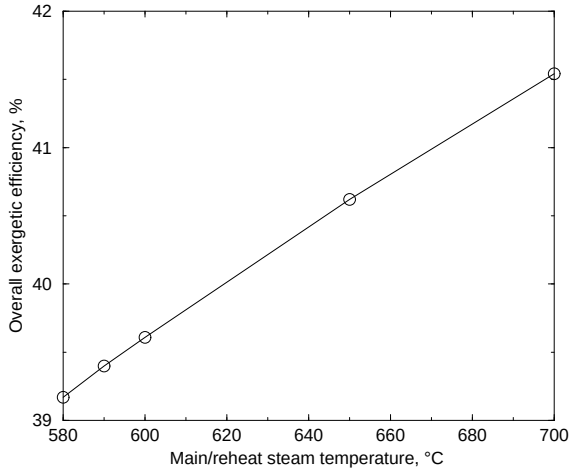

Figure 4.3: SC: Overall efficiency as a function of the steam temperature level.

rate needed at higher main steam temperature level for a given power output.

Effect of main steam pressure

When the the main steam temperature and the reheat temperatures are fixed at 580°C or 700°C, and the two reheat pressures remain constant at 94.2 bar and 19.0 bar, the overall exergetic efficiency changes with the main steam pressure as shown in Figure 4.4. It should be mentioned that, in general, a higher main steam pressure leads to a smaller main steam volume flow rate and hence a worse steam turbine efficiency. In addition, the pressure losses are higher at a higher steam pressure. These have a negative impact on the overall exergetic efficiency, as indicated by the decreasing slope of the lines in Figure 4.4 as the pressure increases. Therefore, it is customary to increase the main steam pressure and temperature at the same time.

The exergy analysis shows that, at a higher main steam pressure, the exergy destruction in the FWHs is smaller, mainly due to the lower first extraction temperature for the last FWH as a consequence of a

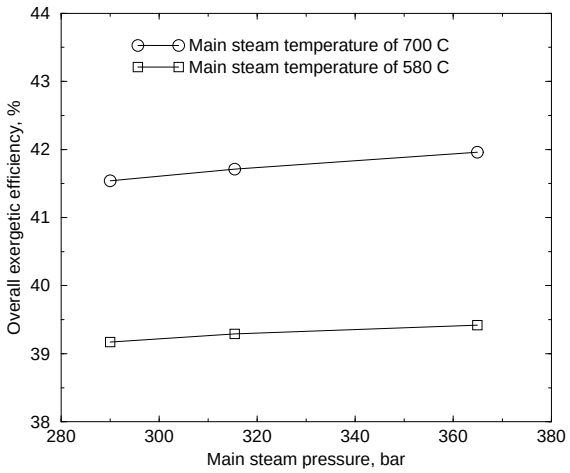

Figure 4.4: SC: Overall efficiency as a function of the main steam pressure.

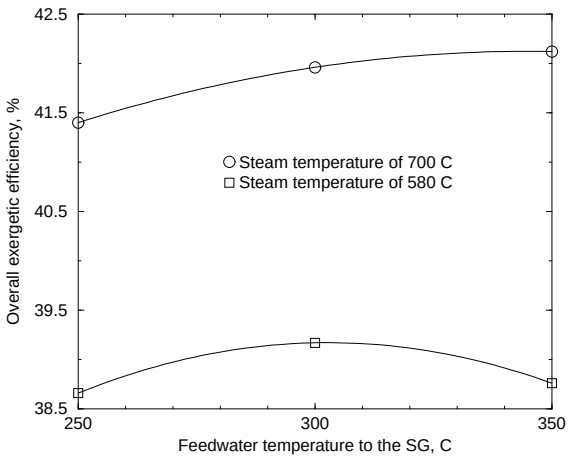

Figure 4.5: SC: Overall efficiency as a function of the feedwater temperature to the steam generator.

higher throttle pressure. In addition, the steam throughput in the ST is smaller. However, the feedwater pump power consumption is higher and the exergy destruction in this component is larger, leading to a higher value of the total exergy destruction in the feedwater preheating system.

When the main steam pressure is higher, the exergy destruction is larger in the HP turbine section (larger portion of power produced at lower section efficiency) and is smaller in the IP and LP turbine sections (smaller steam throughput). With the former dominating, the exergy destruction in the ST increases as the main steam pressure level increases. Here, the two reheat pressures have been kept constant. The higher steam pressure level results in higher pressure losses in the steam generator as well.

At a higher main steam pressure, the first cold reheat temperature is lower. Hence, the exergy destruction in the first reheater (RH) increases. On the contrary, the exergy destructions in the second RH and especially in the superheaters are reduced, due to a smaller steam mass flow rate through these components. This guarantees a higher overall efficiency.

The exergy loss to the cooling water is also smaller at a higher main steam pressure. The reduction of steam turbine throughput at a higher operating pressure leads to a smaller exergy loss associated with the condensate cooling. Note that, on one hand, the first extraction mass flow rate is larger and, on the other hand, the extractions for the remaining HP FWHs are smaller.

As a conclusion, it is more effective that the main steam temperature is increased as well if the main steam pressure is elevated. We consider two main steam temperature levels: 580°C and 700°C, for example. The exergy losses associated with the cooling water and the exergy destruction in the SG heat exchangers decrease by more percentage points for the latter than for the former for the same increase in pressure. This is owing to the fact that the exergy losses associated with the cooling water and the destruction in the steam generator heat exchangers decrease (as a percentage of fuel exergy) with increasing main steam temperatures. The change in exergy destructions in the ST is equivalent for both temperature levels.

Effect of feedwater preheating temperature

As the main steam temperature increases, the preheating temperature of the feedwater to the SG should be increased at the same time. This is indicated by Figure 4.5. The two curves correspond, respectively, to the supercritical power plant "580°C" and to a supercritical steam power plant "700°C" described in Section 4.2.5. As the steam generator feedwater temperature increases, the exergy destruction associated with the heat transfer decreases in the steam generator while it increases in the feedwater preheating system, as discussed in Tsatsaronis & Winhold (1984). There exists, therefore, an optimum, whereby the sum of the two exergy destruction values is minimum. From the thermodynamic viewpoint, the optimal feedwater temperature depends, among others, on the main steam parameters and the feedwater preheating system. While a feedwater preheating temperature of 300°C is reasonable for the supercritical steam power plant "580°C", it seems that this temperature might approach 350°C for the power plant "700°C" (refer to Figure 4.5). In practice, the feedwater temperature is normally limited by the allowable steam temperatures at the boiler furnace exit due to considerations on the furnace enclosure surface (Kjær (1990)).

Effect of condenser pressure

In the supercritical steam power plant "580°C", the condenser pressure is taken as 0.083 bar. If this pressure is reduced to 0.023 bar, the overall exergetic efficiency increases to 41.52%, that is 2.35 percentage points higher than the efficiency achieved when the condenser pressure is 0.083 bar, see Figure 4.6.

This suggests that every 10 mbar increase in the condenser vacuum improves the overall exergetic efficiency by approximately 0.39 percentage points. At a lower condenser pressure, although the exergy destruction in the steam turbine is higher due to lower LP section efficiency and more expansion, the exergy brought away by the cooling water is reduced remarkably. For example, the exergy destructions in the ST amount to 2.07% and 2.57% of the fuel exergy, when the condenser pressure takes values of 0.083 bar and 0.023 bar, respectively. The corresponding exergy losses associated with the cooling water are

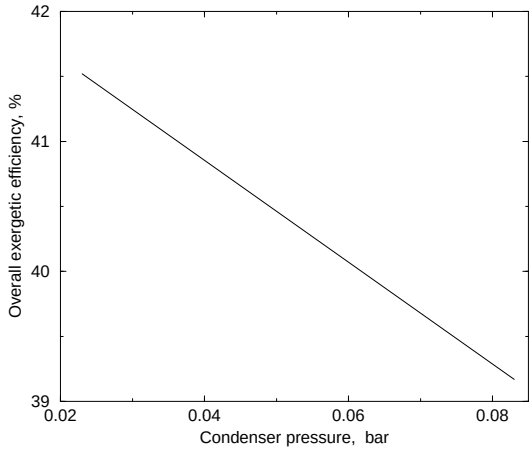

Figure 4.6: SC: Overall efficiency as a function of the condenser pressure.

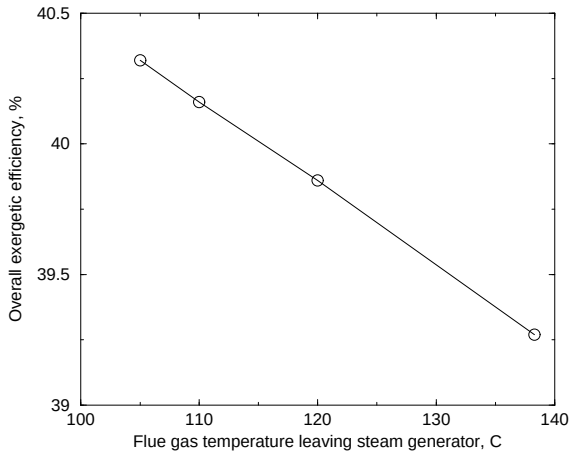

Figure 4.7: SC: Overall efficiency as a function of the steam generator flue gas temperature.

3.74% and 0.84%. It is implied that sea water at 10°C for condensate cooling must be available for achieving a condenser pressure value such as 0.023 bar.

Effect of the steam generator flue gas temperature

In the supercritical power plant "580°C", the flue gas leaves the SG at a temperature of 143.33°C and the plant has an exergetic efficiency of 39.17%.

In Figure 4.7 the change of the overall exergetic efficiency with respect to the above mentioned flue gas temperature is shown. Here the SG pinch temperature difference is assumed to be 30°C and the temperature of the feedwater to the steam generator is 300°C. Figure 4.7 indicates that every 10°C decrease in the SG flue gas temperature improves the overall exergetic efficiency by 0.3 percentage points.

4.2.4 Economic analysis

The economic analysis is based on the cost data available for the conventional steam power plant from Becker et al. (1994). Note that the design and construction period for the supercritical steam power plant is 4 years, one year longer than that for the conventional PCC plant. Other economic criteria remain the same.

To take into account the effect of elevated pressure on the purchased-equipment costs, pressure correction factors are used. For operating pressure levels of 187 bar, 330 bar, and 403 bar, these factors are 1.6, 2.4, and 2.6, respectively (Guthrie (1969)). These numbers are applied to estimate the purchased-equipment cost of the ST, of the FWH, and of the SG. It is assumed that only half of the purchased-equipment cost of the SG is related to the material subject to a cost increase incurred by an elevated operating pressure (Stultz & Kitto (1992)). This applies to the estimate of the purchased-equipment cost of the ST as well. The impact of operating temperatures on the purchased-equipment costs is not considered.

The estimated total direct costs of this supercritical plant are presented in Table F.5. The case-specific economic parameters and costs for the supercritical steam power plant "580°C" are presented in Table F.6.

The levelized annual costs and total revenue requirement in current and constant dollars for levelization time periods of 20 and 30 years, respectively, are presented in Table 4.1. All values are rounded. The key economic parameters are listed in Table 4.2.

Table 4.1: Levelized annual costs and TRR in current and constant dollars for levelization time periods of 20 and 30 years, respectively, for the supercritical steam power plant "580°C". All values in million dollars.

	Current Dollars:	Constant Dollars
20-year period		
Coal costs	71.7 (25.3%)	60.6 (29.3%)
O&M costs	38.4 (13.5%)	32.4 (15.7%)
Carrying Charges	173.7 (61.2%)	113.7 (55.0%)
TRR	283.9 (100.%)	206.6 (100.%)
30-year period		
Coal costs	75.5 (26.9%)	60.7 (31.2%)
O&M costs	40.3 (14.4%)	32.4 (16.7%)
Carrying Charges	164.7 (58.7%)	101.3 (52.1%)
TRR	280.6 (100.%)	194.4 (100.%)

Table 4.2: Key economic parameters for the supercritical steam power plant "580°C".

Net plant power output (MW)	508
Purchased-equipment cost (mid-1998 $/kW)	661
Total plant cost (mid-1998 $/kW)	1666
Total capital requirement (mixed $/kW)	2213
20-year levelized cost of electricity (cent/kWh)	7.51

4.2.5 Advanced supercritical steam power plant

In order to predict the performance of future supercritical steam power plants, a steam power plant with steam conditions 365 bar/700°C/700°C /700°C is analyzed here.

The plant configuration and operating conditions are similar to those of the supercritical steam power plant "580°C", but the feedwater to the steam generator is heated to 350°C. In addition, the reheat pressures are 178.0 bar and 34.3 bar, with corresponding pressure losses of 4% and 6%, respectively. The flowsheet for this supercritical power plant as well as the thermodynamic parameters of material streams are included in Appendix C.3.

The overall efficiency is 43.06% based on the coal HHV (or 45.03% on the LHV). The overall exergetic efficiency is 42.12%, about 3.0 percentage points higher than that of the supercritical steam power plant "580°C". The exhaust steam quality is 0.965. A summary of the key parameters and results for the supercritical steam power plant "700°C", together with those for the power plant "580°C", are listed in Table D.4, whereas the corresponding exergy destructions are given in Table D.3.

Within the heat transfer process in the SG – due to higher steam temperature level (700°C) and higher SG feedwater temperature (350°C) – the exergy destruction reduces significantly, mainly in the reheating processes and in the economizer, compared with the supercritical steam power plant "580°C".

A higher feedwater temperature usually requires a smaller pinch temperature in the economizer, which would increase the cost of the SG. In addition, the exergy destruction in the feedwater preheating system increases by about 0.65 percentage points for a feedwater temperature increase of 50°C. Nevertheless, this exergy destruction increase might be cut down through a more rational feedwater preheating configuration (Kjær (1990)).

The reduction in exergy destruction in the steam turbine for the supercritical steam power plant "700°C" is largely due to a smaller turbine throughput.

Note that at elevated steam parameters, for instance 365 bar/700°C, increasing the feedwater temperature up to 350°C improves the overall efficiency (see Figure 4.5).

The total direct costs, the calculated key economic parameters, the levelized annual costs, and the total revenue requirement (TRR) of this supercritical power plant "700°C" are estimated in a similar way as

in the case of supercritical steam power plant "580°C" (see Table F.7, F.8, and F.9). The key economic parameters are listed in Table 4.3.

A summary of the current-dollar levelized costs of electricity for a 20-year period is presented in Table 4.4 for the three steam power plants, together with the total plant costs. Table 4.4 indicates that the supercritical steam power plants are economically competitive with the conventional steam power plants.

Table 4.3: Key economic parameters for the supercritical power plant "700°C".

Net plant power output (MW)	508
Purchased-equipment cost (mid-1998 $/kW)	693
Total plant cost (mid-1998 $/kW)	1727
Total capital requirement (mixed $/kW)	2290
20-year levelized cost of electricity (cent/kWh)	7.54

Table 4.4: Levelized costs of electricity (20-year, current-dollar), as well as the total plant costs, for the PCC steam power plants.

Power plant	Total plant costs (mid-1998 $/kW)	LCE (cent/kWh)
Conventional PCC	1410	6.81
Supercritical "580°C"	1666	7.51
Supercritical "700°C"	1727	7.54

4.3 HIPPS

HIPPS stands for HIgh Performance Power System. This advanced power system was suggested by the Department of Energy, USA in 1990 and has been intensively studied since then (DOE (1990), Klara (1994b), and Ruth (2001)). A design developed by the United Technologies Research Center (UTRC) team, it is based on an indirectly fired gas turbine combined cycle, with both coal and natural gas as fuel. In this study, a so-called base case is simulated and analyzed.

4.3.1 System description

Air is compressed through a gas turbine compressor to about 11.1 bar. The compressed air is then heated in an air heater to a temperature of 982°C. The air heater is a part of the so-called high temperature furnace (HTF), a key component of the HIPPS. The temperature of the hot air is further boosted by burning an amount of natural gas in an in-duct burner before the air is expanded in a gas turbine. The mass flow of methane is determined so that a desired gas turbine inlet temperature can be obtained (1260°C in this base case). The gas turbine generates about 56.9% of the gross system power output.

About 46% of the gas turbine exhaust at a temperature of 637°C is directed to the HTF as coal combustion air, resulting in an excess air of 16.9%. The coal energy is used to heat up the air expanding in the gas turbine and to raise, with the remaining heat, superheated steam for powering a steam turbine generator. The coal flue gas leaves the HTF at a temperature of 150°C to a gas cleanup unit.

The remaining gas turbine exhaust is led to a HRSG, where the exhaust heat is recovered through steam generation. The steam generated in the HRSG is mixed with the steam from the HTF and expands in the steam turbine. This part of exhaust exits to the stack at a temperature of 95.6°C.

The only steam extraction from the steam turbine is for use in deaerators at about 12 bar. To prevent from potential low-temperature corrosion on the coal flue gas side, the condensate from the condenser at about 33.3°C is preheated solely by the gas turbine exhaust to 98.8°C in the HRSG and then further heated up to 144.5°C by the HTF flue gas.

The flowsheet of the HIPPS is shown in Figure 4.8. The values of the mass flow rates and exergy flow rates are presented in Table C.4.

4.3.2 Exergetic analysis

The thermal efficiency of the HIPPS base case is 48.08%, based on the fuel HHV (51.32% on the LHV). The whole system delivers a net power output of 567.09 MW, 337.11 MW of which is from the gas turbine system. The net steam turbine output is 255.04 MW, accounting for

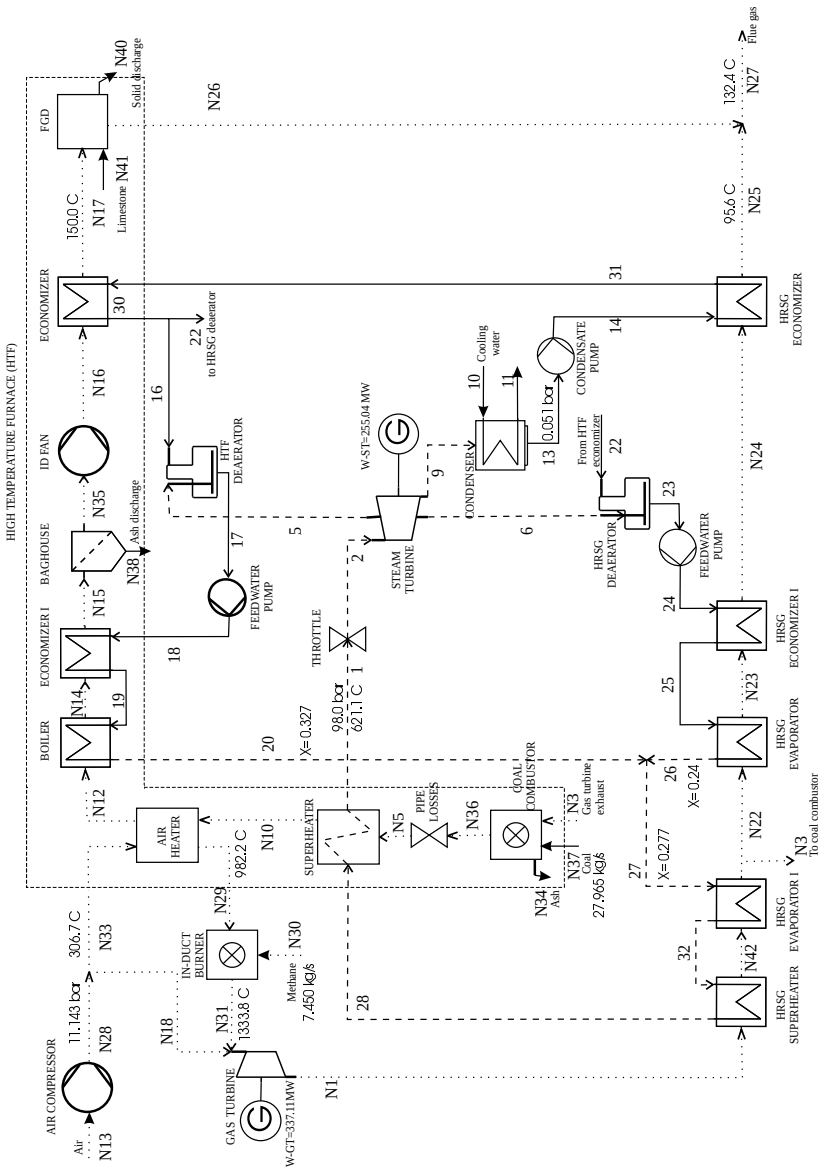

Figure 4.8: Flowsheet for the base case of HIPPS.

43.07% of the system gross output. The auxiliaries amount to 25.06 MW, 4.23% of the gross output (592.15 MW).

The mass flow of the coal feedstock is 27.965 kg/s and that of methane is 7.450 kg/s. This methane flow provides about 35.07% of the total thermal input (HHV).

The system exergetic efficiency is 48.53%. The exergy destructions in the major plant areas, as well as the exergy losses with the effluents, are shown in Table D.5, together with the corresponding percentage of the coal exergy input.

About 25% of the system exergy input is destroyed in the combustion process for both coal (17.16%) and methane (8.04%). The exergy destruction in the HTF, in the gas turbine system excluding the combustor, and in the HRSG are the remaining major shares of total exergy destruction. The condensate cooling brings away approximately 1.90% of the total fuel exergy.

4.3.3 Parametric studies

Parametric studies are conducted to assess the impact of parameters such as air temperature at air heater exit, gas turbine efficiency, main steam parameters, and condenser pressure on the overall plant performance.

Effect of the air temperature at air heater exit

In the HIPPS base case, the gas turbine combustion air is first heated up in the air heater to 982°C. Temperatures higher than 982°C are not considered in the present design in view of the materials available today. However, it is of importance to know how this temperature affects the overall efficiency.

To exclude the effect of the gas turbine section on the overall efficiency, the mass flow of the intake air to the gas turbine air compressor is kept the same as that in the base case, i.e. 866.9 kg/s. The amount of the gas turbine exhaust for coal combustion is adjusted so that the excess air in the HTF remains 16.9%. The pinch temperature difference for the HTF and HRSG is fixed at 30°C.

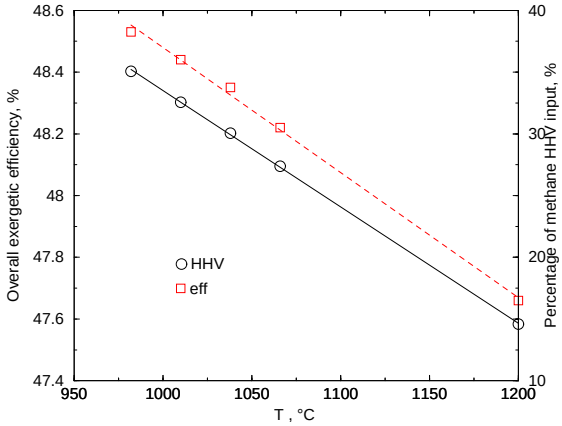

Figure 4.9: HIPPS: Overall efficiency and percentage of methane HHV input as a function of the air temperature at the air heater exit.

For a given gas turbine inlet temperature, 1260°C in this case, the relative methane consumption decreases when the air temperature at the furnace exit increases. At the same time, more coal is burnt in the HTF. For example, the percentage of HHV input by methane is reduced from 35.07% in the base case to 32.55% if the air temperature in question is 1010°C instead of 982°C; the mass flow rate of the coal feedstock increases from 27.96 kg/s to 29.00 kg/s accordingly. The system exergetic efficiency decreases slightly from 48.53% to 48.44%, while the gas turbine exhaust temperature remains essentially unchanged (637°C).

The variation of the overall exergetic efficiency and of the percentage of methane thermal input with respect to the air heating temperature are shown in Figure 4.9, respectively.

Consider the case when the air heating temperature is 1200°C instead of 982°C. At a higher air heating temperature, a smaller amount of methane fed to the in-duct burner and a higher air temperature lead to less exergy destruction in the CH_4 burner (3.43% versus 8.04%) and in the expander (3.75% versus 4.02%). The total exergy destruction in the gas turbine system is reduced by 4.89 percentage points.

Let us now consider the changes in the exergy destruction associated with coal combustion: On one hand, the gas turbine exhaust contains more oxygen and less gas turbine exhaust is needed for combusting one unit of coal input. Hence, the temperature of the coal combustion products is higher, which reduces the exergy destruction associated with the coal combustor. Here the excess air for the coal combustion is kept unchanged. On the other hand, a larger coal feedstock results in a larger amount of exergy destruction associated with coal combustion. The combination of the above two effects leads to a higher exergy destruction associated with coal combustion (21.89% versus 17.16%) at a higher air heating temperature (1200°C versus 982°C). Taking into account the reduction in exergy destruction associated with methane combustion, the overall exergy destruction associated with fuel combustion increases by 0.12 percentage points.

As mentioned in Section 4.3, the flue gas leaves the HTF at a temperature of 150 °C, while the gas turbine exhaust exits from the HRSG at 95.6 °C. At the higher HTF air temperature achieved through a higher coal input, the mass flow rate of the flue gas is larger. The exergy losses with the flue gases are therefore larger (+0.32 percentage points in this case) at the higher air heating temperature.

As the air heating temperature increases, the exergy destruction per unit heat transfer in the HTF air heater decreases. This is due to the higher average temperature on the cold side. However, the total exergy destruction in this component is larger. The heat transfer conditions on the HRSG side remain basically the same, except for the smaller amount of heat transfer. The higher temperature level of the hot side in the HTF heat exchangers results in a larger net exergy destruction in the heat exchange processes inside the HTF/HRSG (+0.37 percentage points).

The exergy loss with the solid discharge is higher (+0.12 percentage points) at the higher air heating temperature. A lower feedwater temperature to the deaerators requires more steam extraction and causes a higher exergy destruction (+0.07 percentage points). Note that in this case less heat from the gas turbine exhaust is available for the feedwater preheating.

Fully coal-fired HIPPS

If the HIPPS is fueled only with coal, the temperature at the air heater exit must be about 1340°C so that the gas turbine temperature can be maintained at 1260°C. In this case, called HIPPSC, the system exergetic efficiency is 46.72%. The net system output is 568.1 MW, equivalent to that in the base case.

The coal mass flow rate is now 43.45 kg/s, whereas the air flow rate remains the same as in the base case. About 57.6% of the gas turbine exhaust is led to the coal combustion (44% in the base case), at a temperature of 387.4°C (405.7°C in the base case). The excess air of 16.9% equals that in the base case.

Because of the larger share of gross power output from the steam turbine cycle when the system is only fueled with coal (44.59% compared with 43.01% in the base case), a larger amount of feedwater is needed for a given net system power output (186.392 kg/s compared with 177.992 kg/s in the base case). Consequently, the exergy brought away by the condensate cooling water amounts to 23.20 MW, which is 1.04 MW more than that in the base case. The auxiliaries are also higher due to the larger coal input and the higher feedwater flow rate.

Figure 4.10 gives a prediction of how the overall exergetic efficiency increases with the air heating temperature. The curve indicates that every 50°C increase in this temperature results in an increase in the overall efficiency by about 0.5 percentage points.

Effect of GT expander polytropic efficiency

In the HIPPS base case, the gas turbine expander polytropic efficiency is 0.90 and the compressor polytropic efficiency 0.93. In Figure 4.11, the variation of overall exergetic efficiency with the gas turbine expander polytropic efficiency is shown, where the polytropic efficiency of the air compressor is kept at 0.93.

The results indicate that the overall efficiency has a fairly strong dependency on the polytropic efficiency of the gas turbine expander. As the expander polytropic efficiency increases from 0.87 to 0.92, the overall exergetic efficiency increases by 1.23 percentage points. This is

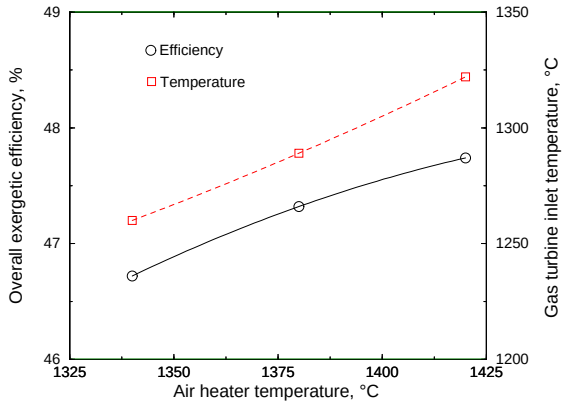

Figure 4.10: HIPPSC: Overall efficiency, as well as the gas turbine inlet temperature, as a function of the air temperature at air heater exit for the wholly coal-fired HIPPS.

because about 57% of the system gross output is contributed by the gas turbine system.

Effect of main steam parameters

In the HIPPS base case, main steam of 621°C/93 bar is chosen. The condenser pressure is 0.051 bar and the steam exhaust quality is 0.86. The pinch temperature differences in both the HRSG and the HTF are 30°C. The system exergetic efficiency is 48.53%. To achieve a higher system efficiency, the steam conditions should be elevated. Figure 4.12 shows the relationship between the main steam temperature and the overall exergetic efficiency under three main steam pressures: 93 bar, 128 bar, and 162 bar.

It should be mentioned that when the main steam temperature is increased to above 650°C, the total feedwater mass flow rate decreases remarkably for a given pinch temperature difference and a given exhaust temperature at the HRSG exit. This means that there is more low level heat available and the condensate to the deaerators can be heated up to such an extent that no steam extraction from the steam

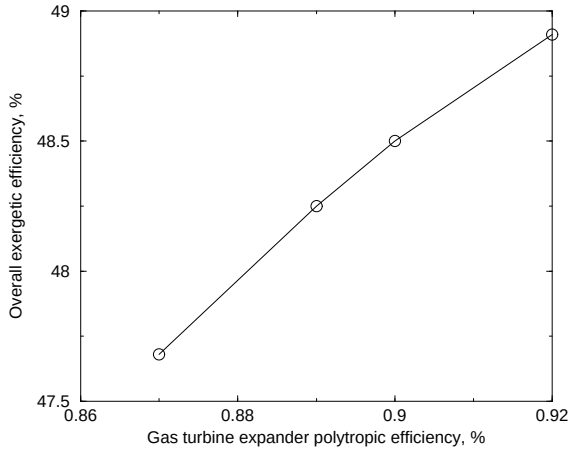

Figure 4.11: HIPPS: Overall efficiency as a function of the gas turbine expander polytropic efficiency (conditions: $T_{GTIT} = 1260°C$; methane HHV input=35.1%).

turbine is needed. In this case, to ensure a proper operation of the condensate/feedwater preheating section, the flue gas temperature on the HRSG exit has to be increased and the system has a lower exergetic efficiency. Alternatives are to lower the pinch temperature difference for the HTF and HRSG train or to generate low pressure steam, with penalties of investment cost and complexity, respectively.

Less steam throughput at higher steam parameters results in less heat transferred to the cooling water. The steam turbine has a higher efficiency and a higher net output, and the system efficiency improves slightly. Note that the slope of the curves in Figure 4.12 decreases as the main temperature increases, which can be explained by the higher flue gas temperatures.

At a main steam pressure of about 93 bar, the system exergetic efficiency benefits from the elevation of the main steam temperature up to approximately 650°C. Further increasing this temperature reduces the overall efficiency due to the increasing HRSG exhaust stack temperature. Since more main steam can be generated at higher main steam pressures, it is possible to raise the main steam temperature

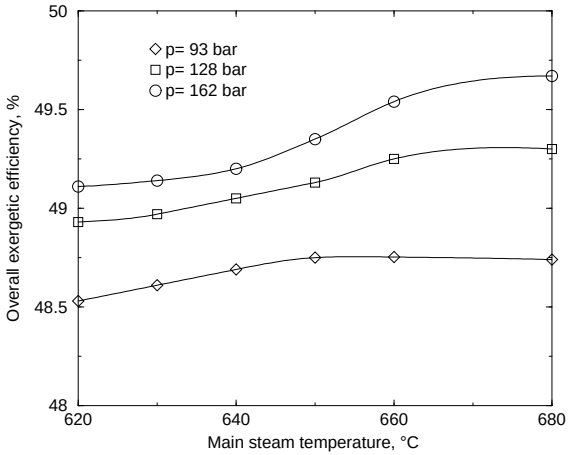

Figure 4.12: HIPPS: Overall exergetic efficiency as a function of the main steam temperature level at different main steam pressures.

above 650°C to improve the overall system efficiency. However, for a certain percentage of efficiency improvement, a larger main steam temperature increase is required at a higher main steam pressure than at a lower main steam pressure. This is because of the high pressure losses and the low exhaust steam quality associated with high main steam pressures.

Effect of condenser pressure

In the HIPPS base case, the condenser pressure is set at 0.051 bar. Figure 4.13 gives an estimation of how the overall exergetic efficiency is affected by the condenser pressure.

From Figure 4.13 we see that an increase of 10 mbar vacuum in the condenser results in some 0.17 to 0.3 percentage point increase in the overall exergetic efficiency, depending on the condenser pressure level. Note, however, that at high condenser pressures (such as 0.083 bar) the system operation conditions need slight modifications. For example, either the pinch temperatures should be decreased or the flue gas

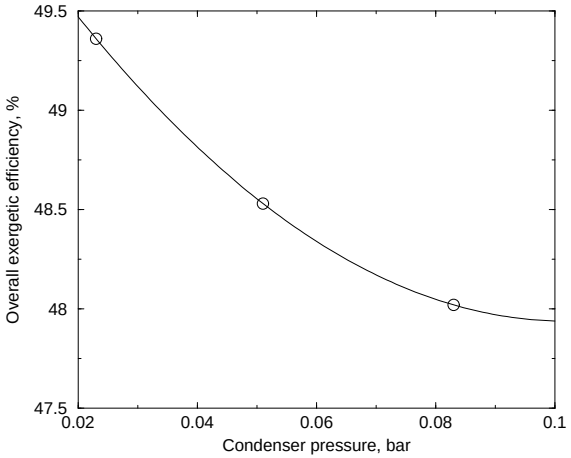

Figure 4.13: HIPPS: Overall efficiency as a function of the condenser pressure.

temperatures increased so that the deaerators function properly. This explains the slope change in the curve of Figure 4.13.

4.3.4 Economic analysis

For the HIPPS base case, the total direct costs are provided by Klara (1994a). These costs and the breakdown of the total capital investment of the HIPPS base case are listed in Tables G.1 and G.2. The case specific economic parameters and the costs for the HIPPS base case are presented in Table G.3.

The levelized annual costs and total revenue requirement (TRR) in current and constant dollars for levelization time periods of 20 and 30 years, respectively, for the HIPPS base case are presented in Table 4.5. The key economic parameters are listed in Table 4.6.

Table 4.5: Levelized annual costs and TRR in current and constant dollars for levelization time periods of 20 and 30 years, respectively, for the HIPPS base case. All values in million dollars.

	Current Dollars:	Constant Dollars:
20-year period		
Coal costs	40.8	34.4
Gas costs	40.3	34.0
Fuel costs	81.1 (28.9%)	68.4 (33.5%)
O&M costs	39.2 (14.0%)	33.1 (16.2%)
Carrying Charges	160.2 (57.1%)	102.6 (50.3%)
TRR	280.5 (100.%)	204.1 (100.%)
30-year period		
Coal costs	42.9	34.5
Gas costs	42.6	34.3
Fuel costs	85.6 (30.7%)	68.8 (35.6%)
O&M costs	41.2 (14.8%)	33.1 (17.1%)
Carrying Charges	151.9 (54.5%)	91.2 (47.3%)
TRR	278.7 (100.%)	193.1 (100.%)

Table 4.6: Key economic parameters for the HIPPS base case.

Net plant power output (MW)	567
Purchased-equipment cost (mid-1998 $/kW)	652
Total plant costs (mid-1998 $/kW)	1370
Total capital requirement (mixed $/kW)	1827
20-year levelized cost of electricity (cent/kWh)	7.06

4.4 PFBC power plant

4.4.1 Plant description

The design configuration of the PFBC power plant considered in this study is based on several sources (Buchanan et al. (1994), Dodd et al. (1997), White, Getty & Torpey (1995), Rehmat & Goyal (1993), Ambrose et al. (1993), Beer & Garland (1997), Sellakumar & Lamar (1995), and Robertson & Bonk (1993)). Figure 4.14 illustrates the

configuration of a base case of this PFBC power plant. The mass flow rates and the exergy flow rates of the streams are presented in Table C.5.

The plant air intake is compressed in a low pressure compressor to 3.82 bar, inter-cooled from 166.3°C to 79.4°C by the condensate, and then compressed in a high pressure compressor to 16.44 bar (Buchanan et al. (1994)). The compressed air is split by control valves and fed to a carbonizer (14%), a PFBC combustor (20%), and a gas turbine topping combustor (66%).

Dried crushed coal (50 μs) and dolomite (100 μs) are fed into a circulating carbonizer, together with a substoichiometric amount of the gas turbine compressor discharge air (Dodd et al. (1997)) which has been preheated in a recuperator by the gas turbine exhaust. It is assumed that the carbon conversion in the carbonizer is proportional to the amount of air fed to the carbonizer (White, Getty & Torpey (1995)). With an excess air ratio of 0.298 of the stoichiometry (0.30 given in Rehmat & Goyal (1993) for Illinois No.6 coal), about 73.1% of the total carbon input is converted into CO and CO_2. The carbonizer bed operates at a temperature of 860°C (Rehmat & Goyal (1993) and White, Getty & Torpey (1995)), with a pressure of 16.24 bar.

The solid part, mainly the char, of the partially gasified products from the carbonizer is then sent to a pressurized circulating fluidized-bed combustor. The char combustion takes place at 860°C and 15.48 bar (Dodd et al. (1997), Rehmat & Goyal (1993)), whereby the sulfide sorbent is oxidized to sulfate. The bed ash is removed at the bottom of the cyclone and then cooled to 261°C in an ash cooler by combustion air and depressurized in an ash removal system. Owing to the cyclone trains and to the hot gas filter downstream, 99% of the fly ash in the combustion flue gas can be further removed (Buchanan et al. (1994)). The cleaned flue gas is then directed to a so-called topping combustor.

Note that no gas cooler is used between the PFBC and the hot gas filter, for the fluidized-bed combustion temperature is low enough so that the filter with a working temperature between 871°C and 899°C can be used directly (Ambrose et al. (1993), Beer & Garland (1997)).

The syngas having a higher heating value of 5.451 MJ/kg from the carbonizer passes through a cyclone system and is cooled down to 643°C (Sellakumar & Lamar (1995) and Dodd et al. (1997)) in a hot

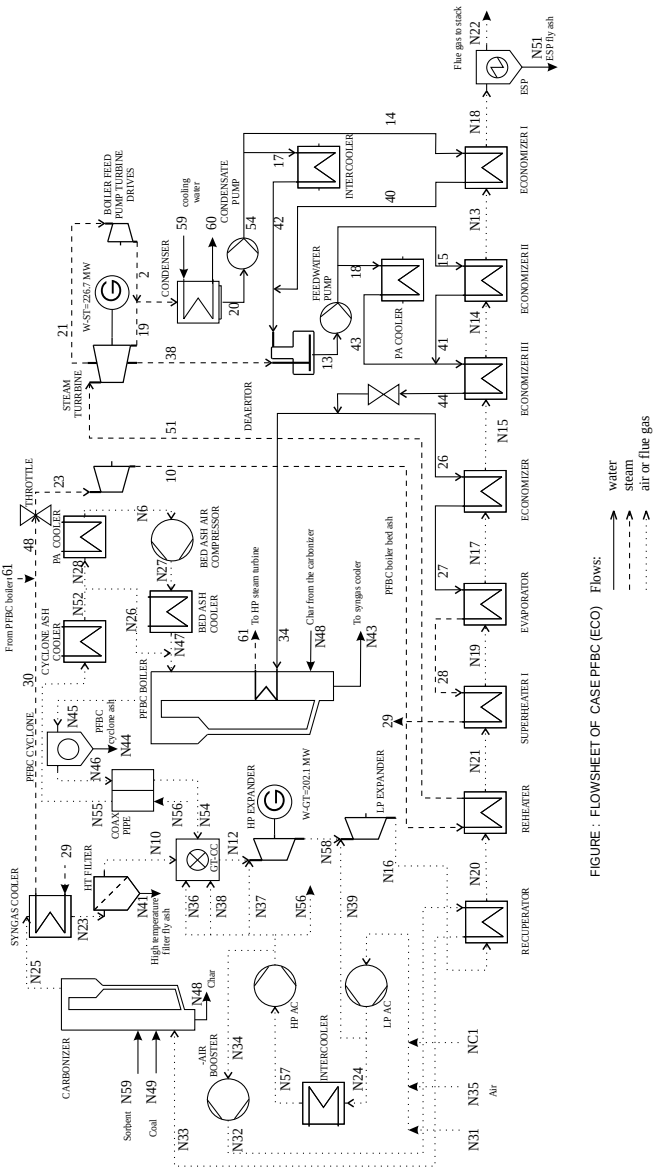

Figure 4.14: Flowsheet for the PFBC plant.

gas cooler by steam superheating. It is then guided through gas filters, where the entrained char and sulfur-absorbing compounds are removed. The clean syngas is then, together with the PFBC flue gas and some air from the air compressor, fired in the topping combustor for final oxidation, raising the gas turbine inlet temperature to 1260°C (Dodd et al. (1997)). The combustion products are expanded through a gas turbine to 656.°C, cooled down in an HRSG, cleaned in an electrostatic precipitator (ESP) at 138°C, and finally discharged to the stack (Rehmat & Goyal (1993) and Robertson & Bonk (1993)). As shown in Figure 4.14, the steam turbine receives two streams of steam. The condensate from the condenser is first heated in the economizer I and in the air compressor intercooler. After flowing through the deaerator, the economizer II and the process air cooler in parallel, and then through the economizer III, the feedwater is split into two flows: one is sent to the PFBC boiler; the other passes through the HRSG evaporator/superheater and then the syngas cooler. The steam from the PFBC boiler and that from the HRSG/syngas cooler (about 40% of the entire stream) merge before entering the steam turbine at throttle temperature and pressure of 538 °C and 166.5 bar, respectively. Single reheating is adopted for this Rankine cycle and the reheater is located in the HRSG.

It should be pointed out that the smallest temperature difference in the HRSG (i.e., the smallest temperature difference between the exhaust and feedwater) is on the cold end of the economizer II. For a given HRSG exhaust exit temperature, this temperature difference determines the total steam turbine throughput. The amount of the steam production in the PFBC boiler is set so that the bed temperature is maintained at 860°C.

4.4.2 Exergetic analysis

The plant has an overall exergetic efficiency of 45.70%; the thermal efficiency is 46.73/48.87% (HHV/LHV). The net plant power output is 417.2 MW, 201.9 MW of which is from the gas turbine system, 47% of the plant gross power. The net power output of the steam turbine is 226.7 MW. The auxiliaries are 11.6 MW, 2.71% of the plant gross output.

The isentropic efficiencies for the HP and reheat steam turbine sections

are predicted by the SCC method as 86.32% and 94.78%, respectively. The steam exhaust quality is 0.907 at a condenser pressure of 0.083 bar.

The exergy destruction in the major plant areas, as well as the exergy losses with the effluents, are shown in Table D.6, together with their percentage with respect to the plant exergy input.

Table D.6 shows that about 32% of the total plant exergy input is destroyed in the carbonization/combustion process. More than 6% of the exergy input is carried away by the flue gas and condensate cooling water.

4.4.3 Parametric studies

In this section, the effect of some major plant parameters on the overall efficiency is investigated. These parameters include the carbon conversion ratio in the carbonizer, the gas turbine inlet temperature, the condenser pressure, the main steam temperature, and the isentropic efficiencies of the gas turbine and the steam turbine.

Effect of carbon conversion ratio (CCR)

The CCR is defined as the ratio of the carbon converted in the carbonizer to the total carbon present in the coal. At higher CCRs, the plant is expected to have a higher exergetic efficiency, see Figure 4.15.

The higher the CCR, the higher the carbonizer bed temperature, and the better the overall efficiency. The advantage in overall efficiency at a higher CCR results from the fact that a larger amount of coal exergy is transferred to the gas turbine system, whose performance surpasses that of the PFBC boiler/steam turbine system. In addition to that, higher bed temperatures allow faster char gasification and hence smaller carbonizer bed volume. Nevertheless, some low-level heat can hardly be recovered with the present plant configuration and the flue gas temperature to the ESP has to be increased as the bed temperature increases.

It should be mentioned that the carbonizer bed temperature is to be kept in a range of 820°C - 900°C to allow a proper sulfur retention

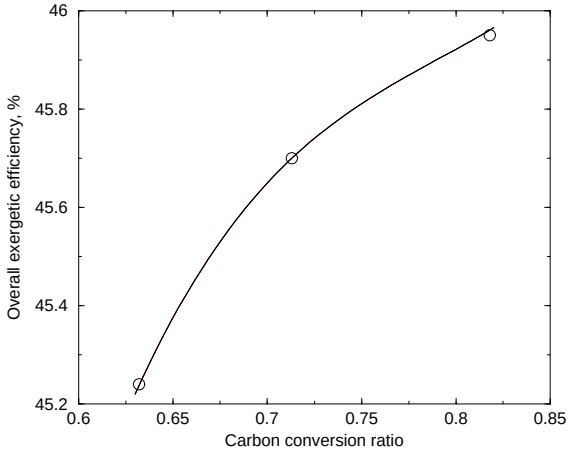

Figure 4.15: PFBC: Overall efficiency as a function of the carbon conversion ratio in the carbonizer.

and calcium utilization and to prevent the alkali from being evaporized (Campbell et al. (1990)). Apart from that, the heating value of the product gas will drop as the bed temperature increases.

To a certain degree, the carbonizer bed temperature can be adjusted by the air temperature at the recuperator exit. When the CCR is high, the air should be less preheated in the recuperator so that the bed temperature can be kept lower. However, above certain CCR values, the recuperator will be by-passed and too much low-level heat is left to be recovered in the HRSG. For instance, the bed temperature reaches 908 °C when the CCR is 0.818. Should the CCR be further increased, the carbonizer bed temperature would be so high that the carbonizer malfunctions. At low CCRs, the air is heated in the recuperator as much as possible to sustain a high enough bed temperature. Yet the gas turbine exhaust temperature of 656°C limits the extent of air preheating and hence restrains the rise in the carbonizer bed temperature. At CCR values below 0.5, the carbonizer bed temperature will be too low to maintain normal performance in the carbonizer.

The benefit brought by a high CCR is balanced out, to some extent, by the decreasing gas turbine efficiency. While the bed temperature of the fluidized-bed combustor stays constant, the syngas from the carbonizer

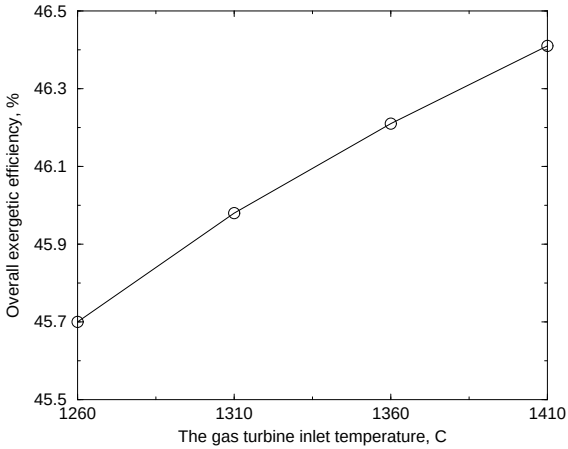

Figure 4.16: PFBC: Overall efficiency as a function of the gas turbine inlet temperature (CCR=0.731).

at a higher bed temperature requires a larger air mass flow for the gas turbine to hold the turbine inlet temperature in an accessible range. As a result, the relevant exergy destructions caused by mixing and by cooling air increase. So does the exergy loss with the flue gas.

Effect of the gas turbine inlet temperature

The amount of air diverted from the air compressor to the gas turbine combustor is a function of, among others, the permitted gas turbine inlet temperature, 1260°C in the PFBC base case. If this air mass flow rate is reduced from 345.8 kg/s in the base case to 314.1 kg/s while the other operation parameters remain unchanged, the gas turbine inlet temperature will be 1310°C, boosting the overall exergetic efficiency from 45.70% to 45.98%. Figure 4.16 shows the overall exergetic efficiency as a function of the gas turbine inlet temperature. The CCR is kept at 0.731 and the flue gas to the stack has a temperature of 137.5°C.

Figure 4.16 indicates that every 50°C increase in the gas turbine inlet temperature boosts the overall efficiency by about 0.25 percentage

points. A higher gas turbine inlet temperature permits a smaller exergy destruction in the topping combustor and a larger gas turbine output. However, as this inlet temperature increases, the gas turbine polytropic efficiency decreases due to the higher air requirement for the turbine blade cooling. It should be mentioned that, for the simulation purpose, it was assumed that the gas turbine polytropic efficiency without cooling is only a function of the turbine pressure ratio. An eventual improvement on the PFBC plant efficiency through elevated turbine inlet temperatures relies strongly on gas turbine technology.

Effect of the condenser pressure

In the PFBC base case, with a steam cycle of 166.5 bar/537.8°C/537.8°C, the exergetic efficiency is 45.70%. The corresponding condenser pressure is 0.083 bar (1.2 psia) with steam quality of 0.907.

Figure 4.17 gives the variation of the overall exergetic efficiency with respect to the condenser pressure. It shows that every 10 mbar decrease in this pressure increases the overall exergetic efficiency by about 0.16 percentage points.

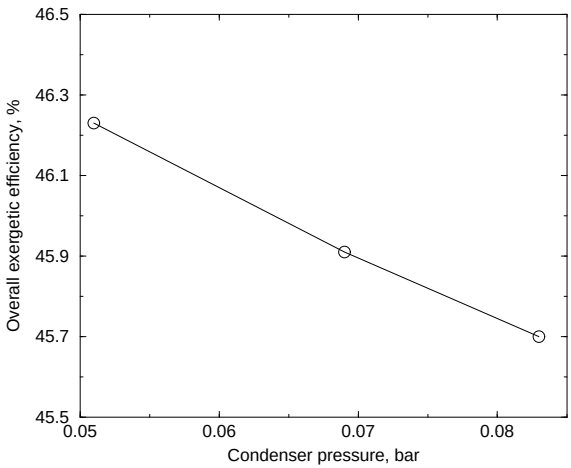

Figure 4.17: PFBC: Overall exergetic efficiency as a function of condenser pressure.

At a lower condenser pressure of 0.051 bar, the steam turbine gross output is higher, 231.3 MW compared with 226.7 MW in the PFBC base case, with a lower exhaust steam quality of 0.893 (compared with 0.907 in the base case). The condensate has a correspondingly lower temperature (about 35°C instead of 43°C). This means that, for a given pinch temperature difference in the HRSG, a smaller amount of steam is raised in the HRSG. A smaller steam throughput produces less power output in the steam turbine sections except the last one. The exergy destruction in the steam turbine increases slightly due to degraded performance of the last steam turbine section. All in all, the plant net power increases in this case from 417.2 MW in the base case to 422.0 MW.

A lower condenser pressure leads to more condensate heating, therefore to a higher exergy destruction in the HRSG train.

The condenser pressure affects indirectly the temperature of the syngas to the gas turbine topping combustor as well. This temperature is higher due to less cooling steam passing through the syngas cooler when the condenser pressure is lower. Hence, more air is needed for the gas turbine combustion to control the turbine inlet temperature. Consequently, a larger exergy destruction occurs in the gas turbine system (the exergy destruction in the GT combustor is the same, 12.40% of the exergy input).

Though a lower condenser pressure leads to higher condensate heating, and therefore higher exergy destruction in the HRSG train, the exergy losses with the cooling water reduce significantly, resulting in a higher overall exergetic efficiency, as shown in Figure 4.17.

Effect of the main steam temperature

Figure 4.18 shows how the overall exergetic efficiency varies with the steam temperature level. The steam pressures are not changed. From Figure 4.18 we see that an increase of 100°C in the steam temperature level corresponds to approximately 1 percentage point improvement in the overall exergetic efficiency.

At a higher main steam temperature, the amount of steam generated in the PFBC boiler reduces for a given bed temperature. The contradictory effect of lowered gas turbine exhaust temperature and of

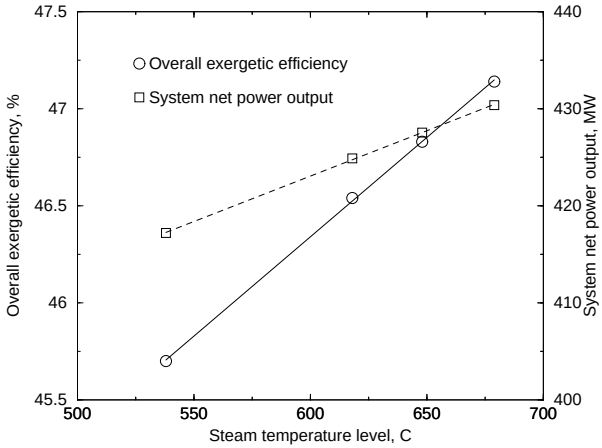

Figure 4.18: PFBC: Overall exergetic efficiency and plant net power output as a function of steam temperature level. The carbon conversion ratio is 0.731.

reduced total amount of feedwater result in a constant steam mass flow raised in the HRSG. Consequently, the steam turbine throughput is reduced. However, the steam turbine power output is increased due to the higher steam temperature, and the turbine performance improves because of the higher turbine section efficiencies and the drier exhaust steam as well.

The syngas to the topping combustor has a lower temperature at a higher main steam temperature. Recall that the syngas cooler acts as the last stage of superheater for the steam raised in the HRSG. Therefore, the gas turbine output decreases as the main steam temperature increases. Still, the net gain in the plant power generation is positive, as indicated by Figure 4.18.

Thermodynamically, the main steam temperature is looser restrained here than in an IGCC power plant. In both cases, steam is used to cool down the coal-derived syngas, which sets principally a limitation to the main steam temperature as well as to its pressure. Nevertheless, a PFBC boiler renders better in-bed sulfur removal than a gasifier in an IGCC power plant and therefore imposes less danger of corrosion

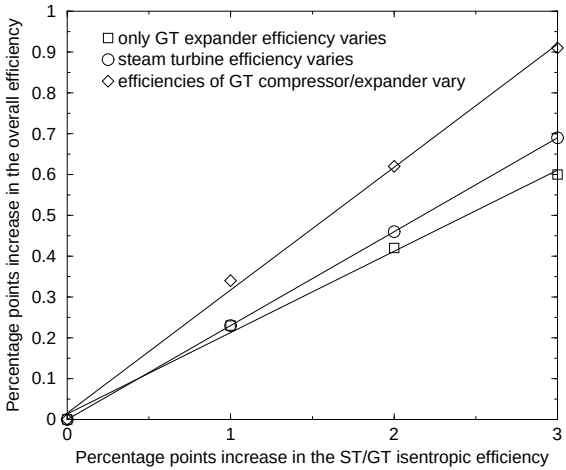

Figure 4.19: PFBC: The percentage point increase in the overall efficiency as a function of the increase in gas turbine/steam turbine isentropic efficiency. The carbon conversion ratio is 0.731

on the steel pipes (Sahan (1997) and Bechtel (1995)). This allows potentially higher steam parameters of the steam turbine cycle and a higher overall efficiency for a PFBC power plant.

Effect of the gas turbine isentropic efficiency

In the PFBC base case, the LP and HP air compressors have isentropic efficiencies of 0.85 and 0.87, respectively, and the gas turbine expanders 0.865. The overall exergetic efficiency reaches 45.70%. Figure 4.19 presents the increase, expressed by percentage points, of the overall exergetic efficiency obtained by increasing only the efficiency of gas turbine expanders as well as by increasing the efficiencies of both the expanders and the compressors, respectively.

When the efficiency of both the air compressors and the expanders increase simultaneously, the overall efficiency gains a significant improvement. Note that an increase in the air compressor efficiency leads to less heat rejection from the intercooler so that the heat required in the

HRSG for feedwater heating is larger, resulting in a minor increase in the exergy destruction in the HRSG. However, less steam is generated and less exergy is lost to the cooling water.

Effect of the steam turbine isentropic efficiency

As mentioned in Section 4.4.2, the isentropic efficiencies of the HP steam section and the reheat section for the base case are 86.32% and 94.78%, respectively.

Figure 4.19 gives also the change in the overall exergetic efficiency as a function of the steam turbine isentropic efficiency. The influence of the steam turbine performance on the overall plant efficiency is slightly more significant than that of the gas turbine expander. This can be explained by the fact that about 47% of the gross plant power output is generated in the gas turbine. It should be mentioned that the higher the CCR, the stronger the impact of the gas turbine efficiency on the overall exergetic efficiency.

Except for the HRSG, where the amount of heat transfer in the reheater increases and larger exergy destruction occurs, the exergy destruction/ losses in every area reduce when the isentropic efficiency of the steam turbine increases.

4.4.4 Economic analysis

For the PFBC base case, the cost estimation was made based on the cost data from a first generation PFBC power plant (Buchanan et al. (1994)) as well as from other sources such as Klara (1994a), Price (1992), and Bechtel (1995).

The estimated total direct costs for the PFBC base case are summarized in Table H.2, while the breakdown of the total capital investment is given in Table H.3. The case specific economic parameters and costs for the base case are presented in Table H.1.

The cost of the combustion gas turbine was evaluated according to the cost information of the HIPPS. The cost of the intercooler was estimated separately and then added to the gas turbine generator.

The cost for the carbonizer was estimated based on cost data for gasifiers (Price (1992) and Bechtel (1995)). It is estimated to be, based on coal mass flow rate, 25×10^6 mid-1993 US$. The basic argument is that the carbonizer used in PFBC power plants is simpler and therefore 30% cheaper than those involved in IGCC power plants.

For the recuperator, the cost was calculated in the same way as for the air preheater.

The levelized annual costs and TRR in current and constant dollars for levelization time periods of 20 and 30 years, respectively, for the PFBC base case are presented in Table 4.7. The key economic parameters are listed in Table 4.8

Table 4.7: Levelized annual costs and TRR in current and constant dollars for levelization time periods of 20 and 30 years, respectively, for the PFBC base case. All values in million dollars.

	Current Dollars:	Constant Dollars:
20-year period		
Fuel costs	46.3 (22.8%)	39.1 (25.8%)
O&M costs	31.0 (15.3%)	26.2 (17.3%)
Carrying Charges	125.6 (61.9%)	86.1 (56.9%)
TRR	203.0 (100.%)	151.4 (100.%)
30-year period		
Fuel costs	48.8 (24.3%)	39.2 (27.5%)
O&M costs	32.6 (16.3%)	26.2 (18.4%)
Carrying Charges	119.1 (59.4%)	77.0 (54.1%)
TRR	200.5 (100.%)	142.4 (100.%)

Table 4.8: Calculated key economic parameters for the PFBC base case.

Net plant power output (MW)	417
Purchased-equipment cost (mid-1998 $/kW)	552
Total plant costs (mid-1998 $/kW)	1498
Total capital requirement (mixed $/kW)	1942
20-year levelized cost of electricity (cent/kWh)	6.94

4.5 IGCC power plant

In this section, a Shell-based integrated gasification-combined-cycle (IGCC) power plant with a capacity of 255 MW is studied. The plant configuration is laid out mainly according to the IGCC power plants proposed by Bechtel (1995) and by Hartman et al. (1983), respectively. Basically, this IGCC power plant consists of a gasification island, a syngas cleaning-up system, an air separation unit, and a gas turbine combined-cycle.

A brief description of the IGCC power plant is given in Section 4.5.1, followed by the exergetic analysis and the economic analysis included in Sections 4.5.2 and 4.5.3, respectively. No parametric analysis is conducted for the IGCC power plant, for this power plant is mainly used here for the purpose of comparison among the different power generation technologies concerned in this study.

4.5.1 Plant description

The coal is ground and then dried by heated nitrogen. The pressurized dry coal, oxygen of 95% mole purity, and high pressure steam are fed into an oxygen-blown gasifier, which operates at 28 bar and 1400°C, as shown schematically in Figure 4.20. Saturated steam at 129 bar is generated in the water-cooled membrane wall of the gasifier. A portion of this steam is fed to the gasifier as reaction steam, while the remaining is directed to the HP turbine section of a steam turbine for power production. The gasifier slag flows down through the gasifier chamber to a water bath located at the bottom of the vessel.

The hot raw syngas produced in the gasifier is quenched to 1040°C by mixing with a stream of cool, clean recycled raw syngas (Price (1992)). The quenched raw syngas then enters a high temperature syngas cooling section, where it is cooled successively to 330°C in a radiant and in a convective high pressure steam boiler to generate saturated, high pressure steam at 119 bar.

The cooled raw syngas passes through cyclones and a wet scrubber for solid removal. It is then directed to a hydrolysis unit, where the HCN and COS contained in the syngas are hydrolyzed to NH_3 and H_2S, respectively (see Figure 4.21). The raw syngas leaving the hydrolysis

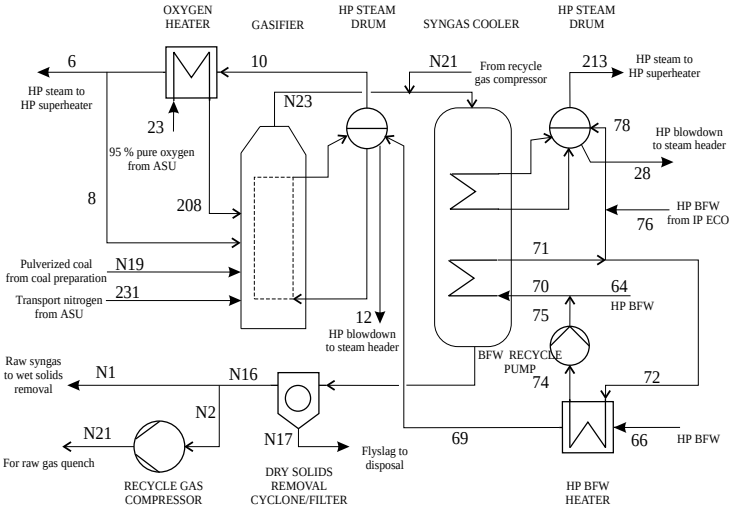

Figure 4.20: Flowsheet for the coal gasification island of the IGCC power plant.

unit is cooled in a clean gas heater, a condensate heater and a trim cooler, through which the ammonia is brought away by the blowdown to a sour water stripper. The cold syngas is sent to an acid gas removal (AGR) unit, where the H_2S is removed in a so-called Sulfinol-M process. The clean syngas has, after sulfur removal, a composition of approximately 62.5% CO, 26.5% H_2, 10% N_2, and small amounts of Ar, CO, and CH_4, respectively. The acid gas from the regenerator of the AGR unit and the sour gas from the sour water stripper are sent to a Claus sulfur recovery unit, where ammonia is burnt and the sulfur is recovered with purity exceeding 99%. The off-gas from the Claus plant is treated in a Shell Claus Offgas Treating (SCOT) unit and sulfur species in the gas are catalytically converted to H_2S. The effluent is cooled to generate LP steam and quenched in a quench column. The bleed from the quench column is led back to the sour water stripper, while the overhead is routed to an amine absorber where H_2S is absorbed by a circulating amine solution.

The amine absorber overheat is burned in an incinerator to convert the residual H_2S and COS to SO_2. The incinerator exhaust is vented

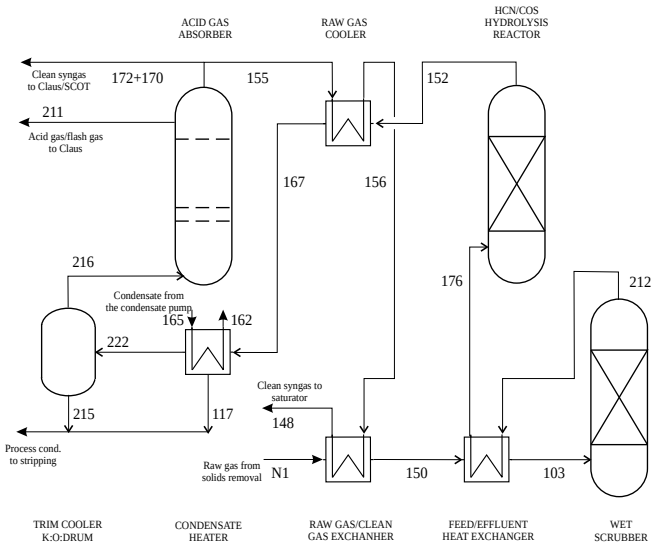

Figure 4.21: Flowsheet for the scrubbing of the IGCC power plant.

to the atmosphere. The bottom of the amine absorber is directed to the AGR unit.

The air separation unit (ASU) adopted here is based on a medium pressure traditional cryogenic process, making use of the pressure of the extracted air from the gas turbine (refer to Figure 4.22). All the required air for the ASU is supplied from the gas turbine extraction. The produced oxygen with a purity of 95% (mole) is compressed and heated up to 250°C before being fed to the gasifier. Nitrogen is produced at high purity for coal preparation/transportation and for pressure delivery. The residual nitrogen remaining after oxygen and nitrogen requirements for the gasification have been met is compressed and returned to the gas turbine combustor. A syngas saturator is used to raise the moisture content of the syngas. The main purpose of the saturator is to use in the process low-temperature heat that would otherwise be rejected to the environment. The added moisture also lowers the heating value of the syngas, and hence mitigates the NOx emissions associated with the gas turbine combustion. Before entering the gas turbine combustor, the saturated syngas of 169.5°C is further

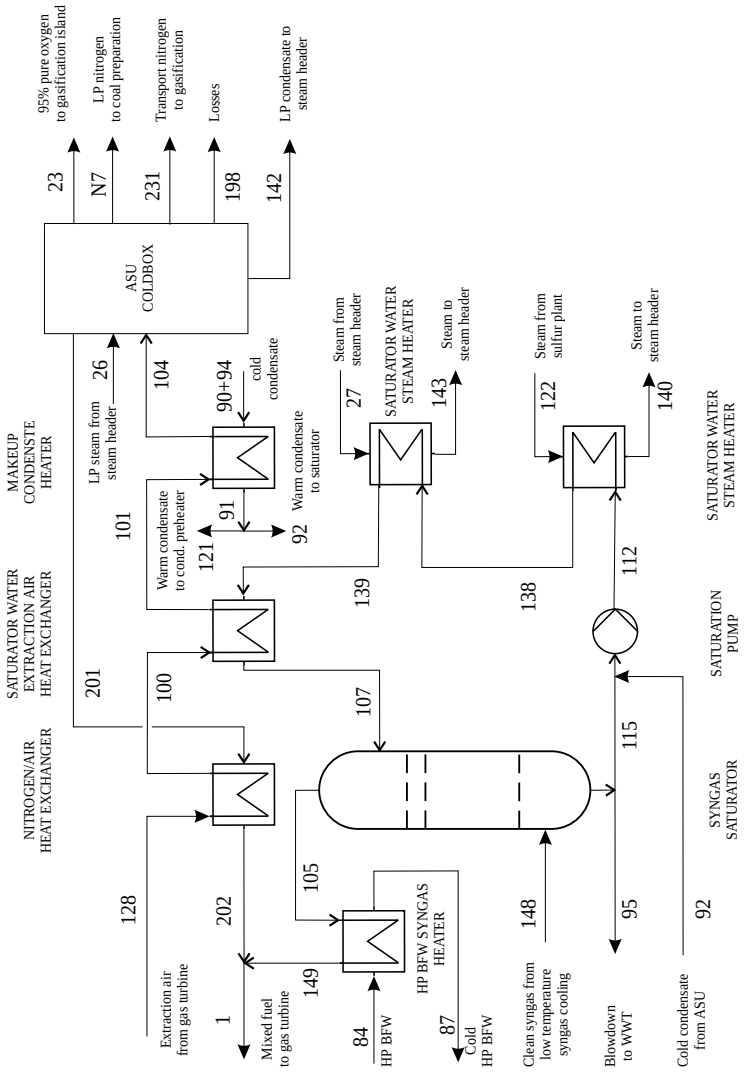

Figure 4.22: Flowsheet for the air separation unit of the IGCC power plant.

heated to 246.5°C by a stream of hot high pressure feedwater from the HRSG.

An overview of the combined-cycle power island is given in Figure 4.23. A single shaft combined cycle is chosen. The steam cycle – with steam conditions 104.6 bar/538°C/538°C – is integrated with the gasification and with the gas cleanup to enhance the overall efficiency and to lower the cost of electricity. A gas turbine with a pressure ratio of 17.1 is used for the syngas application. The turbine inlet temperature is 1285°C.

The HRSG adopted here is a three-pressure, reheat, and natural circulation type. The condensate is heated in the ASU and in the gasification island to recover low-temperature heat. Besides, hot high pressure feedwater from the HRSG is sent to the syngas cooler to facilitate the high level heat recovery and to the ASU to heat up the clean syngas to the gas turbine system. The main steam condenser is cooled by circulating water, maintaining a pressure of 0.051 bar.

The values of the mass flow rates and the exergy flow rates are presented in Table C.6.

4.5.2 Exergetic analysis

The calculated overall exergetic efficiency is 43.2%. The thermal efficiencies are 44.7% and 46.8%, based on the HHV and LHV of the coal, respectively. The net power output amounts to 254.7 MW and the gas turbine provides 62.6% of the plant gross power output. The auxiliaries sum to 22.04 MW, 7.97% of the gross power. About 16 MW of the auxiliaries is consumed in the ASU.

The exergy destructions in the major plant areas, as well as the exergy losses with the effluents, are shown in Table D.7, together with the corresponding percentage of the coal exergy input.

Out of the total exergy input of 589.66 MW, 130.07 MW and 108.52 MW are destroyed within the gas turbine system and the gasification island, respectively. These numbers correspond to 39.3% and 32.8% of the total exergy destruction and losses, and 22.06% and 18.40% of the total plant exergy input, respectively. Cumulatively 61.2 MW of exergy, or 10.38% of the fuel exergy, is carried out of the plant by

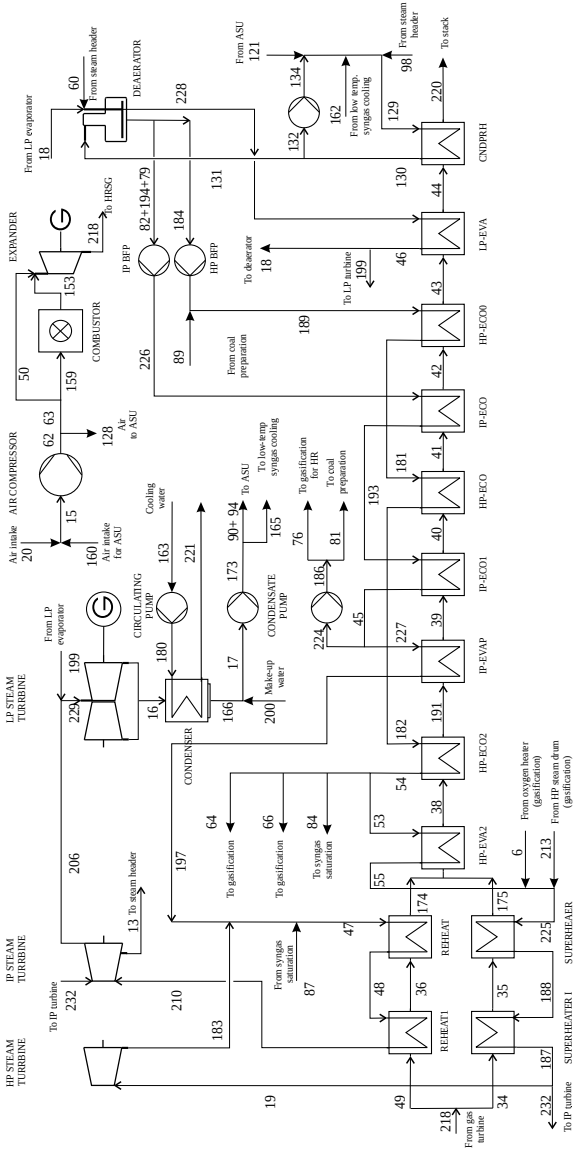

Figure 4.23: Flowsheet for the power island of the IGCC power plant.

effluent, stack flue gas, cooling water, and solid discharge. The sulfur recovery plant is responsible for the destruction of 1.77% of the exergy input, while the steam turbine for 0.95% (5.6 MW).

The exergy destruction associated with cold gas cleanup is 2.42% of the fuel exergy. If the hot gas cleanup is adopted and the syngas is cooled only to 600°C, the overall exergetic efficiency can be approximately 0.9 percentage points higher.

The overall exergetic efficiency of this IGCC power plant is not as sensitive to the gas turbine inlet temperature as the that of the PFBC power plant investigated in Section 4.4. A 25°C difference in this temperature will cause approximately a deviation of 0.1 percentage points of the overall efficiency, compared with about 0.14 percentage points in case of the PFBC power plant (see Section 4.4.3). This can be explained by the different higher heating values of the fuel gases that are burnt in the gas turbine combustor. The steam-saturated, nitrogen-diluted syngas produced in this IGCC power plant has a higher heating value of 4.88 MJ/kg, about 1.68 times that of the fuel gas (syngas mixed with the exhaust from the PFBC boiler) fed into the topping combustor in the PFBC base case. More cooling air is needed in the case of the IGCC plant than in the PFBC case. The adverse impact of the cooling air flow on the gas turbine efficiency is more significant for the former than for the latter, when the gas turbine inlet temperature is increased. Moreover, the IGCC power plant has a better HRSG system (three-pressure system) and a lower flue gas temperature, compared with the PFBC power plant. The energy of the gas turbine exhaust is recovered better in the IGCC plant than in the PFBC one.

4.5.3 Economic analysis

For this IGCC power plant, the total direct costs are derived based on the cost data given in Bechtel (1995) and Price (1992). The total direct costs and the breakdown of the total capital investment of the plant are listed in Tables I.1 and I.2, respectively. The case specific economic parameters and costs are presented in Table I.3.

The levelized annual costs and total revenue requirement in current and constant dollars for levelization time periods of 20 and 30 years, respectively, for the IGCC power plant are presented in Table 4.9. The

key economic parameters are listed in Table 4.10.

Table 4.9: Levelized annual costs and TRR in current and constant dollars for levelization time periods of 20 and 30 years, respectively, for the IGCC power plant. All values in million dollars.

	Current Dollars:	Constant Dollars:
20-year period		
Coal costs	32.2 (20.9%)	27.2 (24.3%)
O&M costs	32.9 (21.4%)	27.8 (24.8%)
Carrying Charges	88.8 (57.7%)	57.1 (50.9%)
TRR	154.0 (100.%)	112.1 (100.%)
30-year period		
Coal costs	33.9 (22.2%)	27.3 (25.8%)
O&M costs	34.6 (22.6%)	27.8 (26.2%)
Carrying chargers	84.2 (55.2%)	50.8 (48.0%)
TRR	152.8 (100.%)	105.9 (100.%)

Table 4.10: Calculated key economic parameters for the IGCC power plant.

Net plant power output (MW)	255
Purchased-equipment cost (mid-1998 $/kW)	1011
Total plant costs (mid-1998 $/kW)	1687
Total capital requirement (mixed $/kW)	2256
20-year levelized cost of electricity (cent/kWh)	8.12

5. Comparative Evaluation of the Power Plants

5.1 Exergetic evaluation

Compared with the exergetic efficiency of the conventional steam power plant (see Section 4.1), the exergetic advantages of the four types of power plants are apparent (refer to Table 5.1). Among these advanced power plants, the HIPPS has the highest overall exergetic efficiency.

The HIPPS is the only one among the power plants under study that is partly fueled with natural gas. About 35.07% of the fuel HHV input is provided by natural gas. Its overall system efficiency therefore benefits from the high power contribution from the gas turbine, about 56.9% of the system gross power output (see Table 5.2). Another advantage

Table 5.1: Overall system exergetic efficiencies of the power plants under study (the corresponding overall thermal efficiencies on a LHV basis are given in the brackets).

Plant	Overall exergetic efficiency [%]	Net power [MW]
HIPPS	48.53 (51.3)	567.1
HIPPSC	46.72 (49.9)	568.1
PFBC	45.70 (48.9)	417.2
IGCC	43.19 (46.8)	254.7
SC 700°C	42.12 (45.0)	507.8
SC 580°C	39.17 (41.9)	507.6
Conventional PCC	35.80 (38.3)	507.6

Table 5.2: Percentages of gas turbine power with respect to the plant gross output, gas turbine inlet temperatures, and steam conditions for the power plants under study.

Plant	$\dot{W}_{GT}/\dot{W}_{gross}$ [%]	T_{GTIT} [°C]	Steam conditions
HIPPS	56.9	1260	93 bar/620°C
HIPPSC	55.4	1260	93 bar/620°C
PFBC	47.1	1260	166 bar/538°C/538°C
IGCC	62.6	1285	100 bar/536°C/540°C
SC 700°C	0.0	-	365 bar/700°C/700°C/700°C
SC 580°C	0.0	-	290 bar/582°C/580°C/580°C
Conv. PCC	0.0	-	165 bar/538°C/538°C

of using natural gas is that the exergy destruction associated with the combustion is relatively low, estimated at 25.2% of the total system exergy input (see Section 4.3.2), less than those of other plants in question, as indicated by Table 5.3. Note that the maximum combustion temperature of the HIPPS is, in fact, lower than that of the steam power plants, since the gas turbine exhaust is used as coal combustion air in case of the HIPPS. Moreover, a portion of gas turbine exhaust (about 54% of the total flue gas) leaves the HIPPS at 95.6°C, which lowers the exergy lost with the flue gas to 3.5%. Hence, even if the steam cycle in the HIPPS operates under relatively low parameters, the HIPPS has the highest overall exergetic efficiency (48.53%) among the four types of power plants.

Note that for the HIPPS the condenser pressure is 0.051 bar, same as that of the IGCC plant but lower than that of the steam power plant and of the PFBC plant (0.083 bar). If 0.083 bar is assumed also for the HIPPS, the overall exergetic efficiency becomes 48.02%, 0.51 percentage points lower (see Section 4.3.3). Nevertheless, the HIPPS still possesses its leading position in system efficiency.

If the HIPPS is fueled only with coal, as in the case HIPPSC, the overall system exergetic efficiency is 46.72% (see Section 4.3.3). All the system operating conditions for the gas turbine and steam turbine remain the same as those for the HIPPS, with exception of the air heater exit temperature being increased to 1340°C (compared with

Table 5.3: Combustion and/or gasification/carbonization temperatures, if applicable, and the exergy destruction ratios associated with these processes.

Plant	$T_{SG,max}$ [°C]	$T_{GT,comb}$ [°C]	$T_{carb/gasif}$ [°C]	$\frac{\dot{E}_D}{\dot{E}_{F,tot}}$ [%]
HIPPS	<1720	1334	-	25.19
HIPPSC	<1950	-	-	24.98
PFBC	< 900	1266	860	32.04
IGCC	-	1413	1400	28.59
SC 700°C	<1930	-	-	27.33
SC 580°C	<1930	-	-	27.33
Conv. PCC	<1900	-	-	28.04

982.2°C for the HIPPS). A further increase in this air heater exit temperature requires higher levels of gas turbine inlet temperature. For example, at an air heater exit temperature of 1420°C, the HIPPSC has an exergetic efficiency of 47.74%, as indicated in Figure 4.10. Apparently, the improvement of the system efficiency of such HIPPSC depends strongly on the advances in materials for the air heater.

The PFBC plant has the second highest overall system efficiency (45.7%). The only fuel to the plant is coal. Approximately half of the system power output comes from the gas turbine system. It should be pointed out that the PFBC plant has the highest percentage of fuel exergy that is destroyed in the combustion/carbonization processes. This is caused by the low temperatures at which the processes take place (see Table 5.3).

Compared with the gas turbine in the HIPPS, the gas turbine in the PFBC plant contributes a smaller portion to the gross plant power output. This is partly responsible for the lower plant efficiency of the latter. The low operation temperature of the fluidized bed requires more heat transfer to the steam side. Thus, a large portion of the coal energy bypasses the gas turbine and is used only in the steam turbine, with the remaining energy used in both the gas turbine and the steam turbine.

From the exergetic point view, low combustion temperatures generally imply high exergy destruction associated with the combustion/

carbonization process (refer to Table 5.3). However, the moderate operation temperature is the very feature of a fluidized bed combustion system that allows better environmental performance than other combustion technologies.

The IGCC power plant has the highest share of gas turbine power output in the total system power generation. This is due to the gasification of the entire coal feedstock at a relatively high temperature. In addition, the syngas from the gasifier is saturated with water before entering the gas turbine combustor. This increases the specific power output of the gas turbine, but requires a clean water source.

The air separation unit's high power consumption results in a high auxiliary requirement (about 7.97% of the system gross output, see Table 5.4). This is one of the major factors leading to an overall system efficiency lower than that of both the HIPPS and the PFBC power plant. It should be mentioned that the air intake for the ASU is fully supplied from the gas turbine air compressor and the ASU operates at medium pressure (about 13.8 bar). Without a stand-alone air compressor, the ASU has a power consumption slightly lower than that of the low pressure ASU (generally at 4-6 bar) requiring a separate air compressor. Another adverse factor is the adoption of the cold gas cleanup in this IGCC power plant. The overall efficiency might be by about 1 percentage point higher if a hot syngas cleanup technology were involved (see Section 4.5.2).

For the IGCC plant, the highest steam pressure in the HRSG is basically limited by the pressure in the HP syngas cooler. This is because

Table 5.4: Overall plant auxiliaries as a percentage of the gross plant power output for the power plants under study.

Plant	Auxiliaries [%]	Gross plant power output [MW]
HIPPS	4.23	592
PFBC	2.69	429
IGCC	7.97	277
SC 700°C	7.37	548
SC 580°C	6.94	545
Conv. PCC	6.09	540

the water tubes of the cooler operate in a severely corrosive environment due to the presence of H_2S in the syngas. The tube temperature is kept under 300°C to prevent a dramatic increase in the corrosion rate. Therefore, a main steam pressure of 100 bar is chosen for the HRSG in this plant. This affects, in turn, the steam turbine efficiency and the IGCC overall plant efficiency.

The SC steam power plants, both the "580°C" concept and the "700°C" one, have the lowest system efficiency among the four advanced coal-fired power generation technologies (refer to Table 5.1). There are several factors that account for it.

First, the highest temperatures of the working fluids in SC steam power plants are much lower, compared with those in the remaining power plants under study (see Table 5.5). Owing to the material technologies available today, it is not feasible to further increase the steam temperature beyond this level.

Second, being one of the inherent disadvantages of steam turbine power plants, the flue gas temperatures leaving the power generation section ($T_{fluegas}$) are set higher for the steam plants than for the other three types of power plants. This is because the desulfurization takes place after the coal combustion and there is a substantial amount of sulfur in the flue gas leaving the steam generator to the desulfurization unit (FGD). The actual allowable value of the flue gas temperature depends

Table 5.5: Highest working fluid temperatures, assumed temperatures of the flue gas leaving the power generation section, and the associated exergy destruction ratios for the power plants under study.

Plant	$T_{max,workingfluid}$ [°C]	$T_{fluegas}$ [°C]	$\frac{\dot{E}_{L,fluegas}}{\dot{E}_{F,tot}}$ [%]
HIPPS	1260 (gas)	121	3.50
PFBC	1260 (gas)	138	3.23
IGCC	1285 (gas)	105	3.05
SC 700°C	700 (steam)	143	4.59
SC 580°C	580 (steam)	143	4.60
Conv. PCC	538 (steam)	143	4.24

on the sulfur content in the coal fired, the moisture content in the flue gas, and the type of FGD. The flue gas temperature for each type of power plant under study is given also in Table 5.5.

Third, the auxiliary consumption for the two SC steam power plants is high, almost equivalent to that of the IGCC power plant (see Table 5.4). This is mainly the result of the high feedwater pump power consumption at elevated steam pressures of 290 bar for SC "580°C" and of 365 bar for SC "700°C", respectively. In general, the high auxiliary consumption of steam power plants is inevitable due to the additional equipment for emissions control.

5.2 Potential of thermodynamic improvements

5.2.1 Supercritical steam power plants

For the supercritical steam power plant, an increase in steam temperature/pressure has the highest potential for improving system efficiency (see Section 4.2.3). A supercritical steam power plant under steam conditions 365 bar/700°C/700°C/700°C is expected to yield an overall exergetic efficiency of 42.12% (45.03% based on LHV) at a condenser pressure of 0.083 bar (see Section 4.2.5).

Low condenser pressure is a decisive prerequisite for a high efficiency of SC steam power plants. Every 10 mbar increase in the condenser vacuum would bring approximately 0.39 percentage points to the plant exergetic efficiency under the conditions provided in the "580°C" case studied here (see Section 4.2.3). In addition, the low flue gas temperature is important for better system efficiencies (see Section 4.2.3).

Since 6.0-7.3% of gross power output of a supercritical steam power plant is consumed as auxiliaries (see Table 5.4), reduction of boiler auxiliary power consumption is worth of further consideration.

5.2.2 HIPPS

The advances in air heater material technologies are the key factor for reducing the percentage of methane input to the system. The higher the allowable HTF air exit temperature, the higher the fuel input from coal, at a moderate penalty of the system efficiency (refer to Figure 4.9).

A HIPPS that is fueled fully with coal has an overall exergetic efficiency of 46.72% or higher, provided that the air temperature at the air heater can be as high as 1340°C and that the gas turbine inlet temperature is 1260°C. Further improvements on the overall system efficiency require an increase in both the air temperature at the air heater exit and the gas turbine inlet temperature (see Figure 4.10).

The advanced gas turbine technologies that result in high polytropic efficiencies have significant influence on the overall exergetic efficiency (see Figure 4.11).

Moreover, the overall exergetic efficiency can be further improved by raising the live steam condition level (see Figure 4.12).

The condenser pressure of a HIPPS is not as important a parameter, in view of the overall efficiency, as that of a supercritical steam power plant. Every 10 mbar decrease in the condensing pressure improve the system efficiency of a HIPPS system by less than 0.3 percentage points (see Section 4.3.3). This suggests that the HIPPS are more suitable than the SC steam power plants for areas where a low condenser pressure cannot be achieved.

5.2.3 PFBC power plant

The main parameter affecting both system operation and overall efficiency is the carbon conversion ratio (CCR). The higher the CCR, the higher the carbonizer bed operation temperature and the better the overall efficiency (see Section 4.4.3). Note that the carbonizer operates under approximately adiabatic conditions. Indeed, a higher CCR permits more coal energy to be used in both the gas turbine and the steam turbine. As the CCR increases from about 0.6 to 0.8, there can be about 1 percentage point increase in the overall efficiency of this PFBC power plant.

The limits to the CCR are set so that the carbonizer can function properly. In addition, the part-load behavior of the PFBC plant imposes certain constraints on the CCR.

The major factor that hinders the improvement of the plant efficiency is the gas turbine inlet temperature. The higher this temperature, the better the system efficiency. As the gas turbine inlet temperature increases from 1260°C to 1360°C, the system efficiency might have an increase by 0.51 percentage points at a CCR of 0.731 (see Figure 4.16).

While the condenser pressure has a moderate influence on the overall efficiency (see Figure 4.17), the steam temperature affects relatively strongly the system performance (see Figure 4.18).

When possible, steam turbines of better performance should be used to effectively improve the overall efficiency, especially at low carbon conversion ratios. This can be seen in Figure 4.19, which shows that the overall efficiency depends more on the steam turbine performance than on that of the gas turbine. Apparently, the higher the carbon conversion ratio, the more important is the gas turbine efficiency to the overall efficiency.

5.2.4 IGCC power plant

A parametric study was not conducted for this IGCC power plant. Unlike the SC steam power plants, the PFBC power plants, and the HIPPS, the IGCC power plants are distinguished into several types, each of them having its peculiar features and characteristics. Therefore, evaluation and conclusions made for an IGCC power plant are very case specific.

Generally, the overall system efficiency of an IGCC plant depends mainly on the cold gas efficiency of the gasification process and on the overall heat integration among the steam streams, the air streams, and the saturator. The IGCC power plant with a Shell gasification process considered in this study uses a cold gas cleanup process, which has a negative impact on the system efficiency (see Section 4.5.2). However, the adoption of a hot gas cleanup introduces a penalty of emissions and might increase the plant costs. Using advanced gas turbines and reducing the ASU power consumption (5.77% of the plant gross power

output) will further increase the overall efficiency of an IGCC power plant.

5.3 Economic evaluation

5.3.1 Levelized cost of electricity (LCE)

The levelized costs of electricity for the four types of power plants are summarized in Table 5.6. Note that, although the PFBC plant has a lower overall efficiency and a higher total plant cost (see Table 5.7) than the HIPPS does, its LCE is still competitive compared with that of the HIPPS. This is due to the favorable cost of coal over that of natural gas. The IGCC power plant has the highest value of the LCE among all the power plants.

Apart from its highest overall system efficiency, the low LCE for the HIPPS is also due to its lowest total plant cost (1370 $/kW), see Table 5.7. The reasons for that are the high share of power production in the gas turbine and the large plant size. The IGCC plant has the highest LCE, a consequence of a relatively high total plant cost and of high operating and maintenance costs.

Table 5.6: Overview of the levelized costs of electricity of the power plants under study (20-year, current dollars).

Plant	LCE [cent/kWh]	Exergetic efficiency [%]
HIPPS	7.06	48.53
HIPPSC	6.93	46.72
PFBC	6.94	45.70
IGCC	8.12	43.19
SC 700°C	7.54	42.12
SC 580°C	7.51	39.17
Conv. PCC	6.81	35.80

Table 5.7: Total plant cost (in mid-1998 dollars) and the total capital requirement (in mixed-dollars), together with the net plant output and the gas turbine's share to it.

Plant	TPC [$/kW]	TCR [$/kW]	$\dot{W}_{net}$ [MW]	$\dot{W}_{GT}/\dot{W}_{gross}$ [%]
HIPPS	1370	1872	567	56.9
HIPPSC	1464	1945	568	55.4
PFBC	1498	1942	417	47.1
IGCC	1687	2256	255	62.6
SC 700°C	1727	2290	508	-
SC 580°C	1666	2213	508	-
Conv. PCC	1410	1837	508	-

5.3.2 Total plant cost (TPC)

The major component of the TPC of a power plant is its total direct costs (TDC). About 70% of the TPC is incurred by the TDC for the power plants under study. Further, the cost associated with the purchased-equipment (PEC), inclusive of installation, constitutes approximately 65% of the TPC for all the plants, except for the HIPPS where this percentage is 48.2% (see Table 5.8). Therefore, the PEC exerts a dominating impact on the end-product costs of a power plant.

Table 5.8: Ratios of the purchased-equipment costs to the total plant cost, of the total direct costs to the total plant cost, and of the purchased-equipment costs to the total direct costs.

Plant	PEC/TPC [%]	TDC/TPC [%]	PEC/TDC [%]
HIPPS	48	69	70
HIPPSC	49	69	71
PFBC	59	70	93
IGCC	64	70	94
SC 700°C	66	70	94
SC 580°C	66	70	94
Conv. PCC	65	70	93

Table 5.9: Breakdown of the total purchased-equipment costs for the power plants under study (in percentage).

Area	HIPPS	HIPPSC	IGCC	SC 700°C	PFBC
SG/boiler	-	-	-	47.4	35.7
HTF	39.3	41.3	-	-	-
Gasification	-	-	39.5	-	-
Carbonizer	-	-	-	-	8.2
ST	10.0	9.5	43.8	19.8	11.5
GT	21.3	19.1	with ST	-	24.0
HRSG&stack	5.0	4.2	with ST	5.6	9.7
Gas cleanup	21.7	23.2	-	14.2	6.7
CD&FWH	2.7	2.7	3.7	13.0	4.2
ASU	-	-	9.3	-	-
Saturator	-	-	3.7	-	-
Entire plant	100.0	100.0	100.0	100.0	100.0

For the HIPPS, about 39.3% of the PEC is related with the HTF, while 21.7%, 21.3%, and 12.8% result from the FGD/ESP, GT and ST, respectively. The LCE of this type of power plants is strongly dependent on the costs of the HTF and of the GT. An overview of the distribution of the PEC among the major areas is given for the four types of power plants in Table 5.9. Note that the percentage of the cost for the HTF in the HIPPS is approximately the same as that of the gasification island in the IGCC plant. The portion of cost of the flue gas cleanup is significantly high for HIPPS and "700°C" plants, 21.7% and 14.2% respectively.

5.3.3 Total capital investment (TCI)

The TCI of a power plant is the basis for calculating the plant's total capital requirement (TCR). The constitution of the TCI for the power plants is presented in Table 5.10. We see that about 87% of the TCI is incurred by the total plant cost; 10% comes from the allowance for funds used during construction (AFUDC); and the rest is related with organization and startup costs, working capital, and cost of land.

While 80% of the organization and startup costs comes from the 2%

Table 5.10: Breakdown of the total capital investment (in mid-1998 dollars) for the advanced power plants under study.

Source	Percent
Total plant cost	86.15 - 87.30
AFUDC	9.00 - 9.58
Organization and startup costs	2.12 - 2.18
Working capital	1.61 - 2.05
Cost of land	0.04 - 0.07
Total capital investment	100.0

of total plant cost, 37% to 55% of the working capital stems from the 2 months of fuel costs at full load. The AFUDC depends on both the total plant cost and the length of the design and construction period.

The TCR is one of the major contributors to the total revenue requirement of a power plant. The economic study here indicates that the ratios between the the TCR and the TCI are 1.12 and 1.16 for the four types of power plants when the design and construction period takes 3 and 4 years, respectively. Apparently these numbers change with the assumed average cost of money.

5.3.4 Total revenue requirement (TRR)

The percentage of the levelized fuel costs, the O&M costs, and the carrying charges (CC) are presented in Table 5.11. The O&M costs constitute about 14% of the total revenue requirement (except 21.4% for the IGCC plant), while the percentages of the fuel costs vary from 21% to 30%. Here current dollars with a 20-year levelization period are used for the costs.

The high percentage of fuel cost for the HIPPS is caused by the use of methane as fuel, contributing 50% of the total fuel costs. Note that, because of its low plant efficiency, the conventional PCC power plant has an equally high share of fuel costs to that of the HIPPS.

The levelized fuel cost per unit coal mass flow (kg/s) of a power plant excludes the effect of the plant thermal efficiency on the levelized fuel costs. Thus defined fuel costs vary only with the construction years

Table 5.11: The shares of the levelized fuel costs, the O&M costs and the carrying charges, respectively, to the total revenue requirement for the power plants under study.

Type of power plant	Fuel costs [%]	O&M costs [%]	Carrying charges [%]
HIPPS	28.9	14.0	57.1
HIPPSC	23.0	15.1	61.9
PFBC	22.8	15.3	61.9
IGCC	20.9	21.4	57.7
SC 700°C	23.4	13.5	63.1
SC 580°C	25.3	13.5	61.2
Conv. PCC	29.7	14.1	56.2

and with the plant capacity factor (PCF). If the construction period is one year longer – 4 years instead of 3 – the fuel costs per unit coal mass flow will increase by 2.6% (same for PCF of 0.8 and 0.85), at an average nominal escalation rate of coal costs of 2.6025% as assumed in this study. If the PCF changes from 0.80 to 0.85, the levelized fuel costs per unit coal mass flow are 6.25% higher (for both 3 and 4 years of construction).

The PCF for the PFBC power plant is 0.80, lower than the 0.85 in case of SC steam power plants and of the IGCC power plant. Moreover, the design and construction period of the PFBC plant, 3 years, is assumed one year shorter than those of the SC steam/IGCC power plants, respectively. The PFBC plant possesses in addition high overall exergetic efficiency, directly below that of the HIPPS. Hence, the PFBC plant has a low percentage of fuel costs, just above that of the IGCC plant.

As indicated by Table 5.6, the PFBC power plant and the HIPPSC have practically the same value of the LCE (about 6.9 cent/kWh), though the latter has a higher plant efficiency and a lower total plant cost than the former. The main reason is the assumed number of years for the design and construction period. It is of 3 years for the PFBC plant and of 4 years for the HIPPSC, and the total capital requirements of the two plants become even (see Table 5.7). Moreover, the fuel costs for the first operation year become higher for the HIPPSC

(1.334 cent/kWh) than for the PFBC plant (1.328 cent/kWh). Note that the HIPPSC has a lower fuel cost (1.143 cent/kWh) at the base year 1998 than the PFBC plant (1.168 cent/kWh). As a result, the LCE of the PFBC plant approaches that of the HIPPSC, in spite of the fact that the former has higher levelized O&M costs (1.061 cent/kWh) than the latter (1.049 cent/kWh). It can be seen from Table 5.11 that while the percentage of the carrying charges in the TRR is 61.9% for both plants, the HIPPSC has a slightly higher percentage of fuel costs and a lower percentage of O&M costs than the PFBC plant. It should be mentioned that should the cost for the air heater in the HIPPSC be higher than assumed here, the PFBC plant would have lower LCE than the HIPPSC, as indicated later by Figure 5.2.

The highest percentage of O&M costs for the IGCC plant is due to its large number of operation positions required (high fixed O&M costs) and to its high expenses for major overhaul (high variable O&M costs). Besides, the large percentage of the GT power output contributes to high costs for the gas turbine maintenance (high variable O&M costs). This and the high investment cost account for the lowest percentage of fuel costs among all.

If we compare the HIPPSC with the HIPPS, we see that the former has a lower percentage of fuel costs and a higher percentage of carrying charges than the latter. Indeed, the PEC for all the components of the HIPPSC increases by 4% to 35%, except for the GT and the HRSG, by which the PEC decreases by 2% and 8%, respectively. However, the benefit introduced by burning solely coal compensates the increase in the capital investment, allowing for the HIPPSC a lower LCE than for the HIPPS.

5.3.5 Sensitivity studies

In order to conduct the economic analysis in this study, some important parameters such as plant capacity factor, costs of coal and natural gas, and returns on common equity and debt had to be assumed. These parameters may affect, to a certain extent, the calculated levelized cost of electricity (LCE). Besides, the estimated purchased-equipment costs of the power plants may be inaccurate. This section deals with the effects of assumptions and inaccuracies on the LCE.

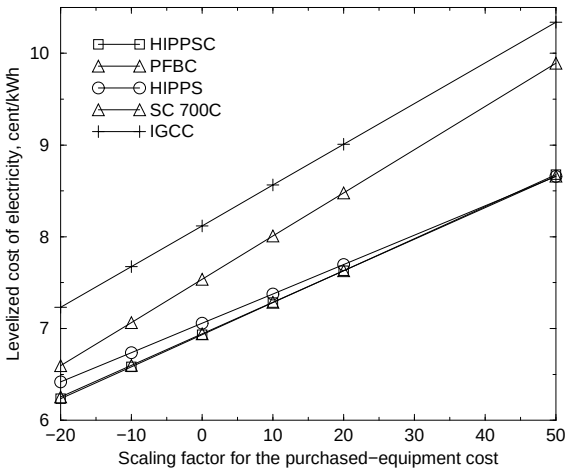

Figure 5.1: LCE as a function of the change in the estimated PEC.

Effect of purchased-equipment costs

The first step and the most difficult task in an economic analysis is the estimation of the purchased-equipment costs for a new power plant. The accuracy of the estimates is subject to many uncertainties associated with the available cost information, the involved novel technologies, and various contingencies. The calculated LCE of the power plants varies linearly with the estimated purchased-equipment costs including installation, as shown in Figure 5.1. Here it is assumed that the efficiencies of the power plants remain unchanged. Approximately every 10% variation of the PEC leads to about 4% to 7% change on the LCE, depending on the efficiency of the respective power plant. As Figure 5.1 indicates, the higher the plant efficiency, the lower the LCE dependency on the PEC.

Effect of the cost for the air heater for the HIPPSC

If the HIPPS is 100% fueled with coal (i.e., HIPPSC), the system exergetic efficiency is 46.72% (see Section 4.3.3). The corresponding calculated LCE is 6.93 cent/kWh, compared with 7.06 for the HIPPS.

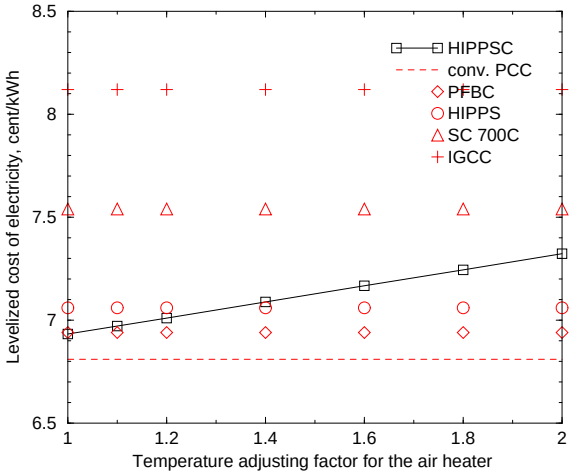

Figure 5.2: LCE for the HIPPSC as a function of the temperature adjusting factor for the cost of the air heater/HTF (20-year, current dollars).

This is the cost estimated when the elevated temperature level in the air heater/HTF (from 1260°C to 1340°C) is not accounted for . Figure 5.2 shows the calculated LCE for the HIPPSC at different values of an adjusting factor for the cost estimation of the air heater.

If the cost of the air heater for the HIPPSC is about 35% higher than that assumed for the air heater in the HIPPS, the calculated LCE is equal for both systems. We notice that, even in case the cost of the air heater is doubled, the LCE of the HIPPSC is still lower than those of the SC and IGCC power plants.

Effect of plant capacity factor

Figure 5.3 shows the levelized cost of electricity of a power plant as a function of the plant capacity factor (PCF). If the PCF increases from 80% to 85%, the LCE of the power plants decreases by about 4%. We notice that the order of the LCEs of the power plants under study remains unchanged when the plant capacity varies from 75% to 90%.

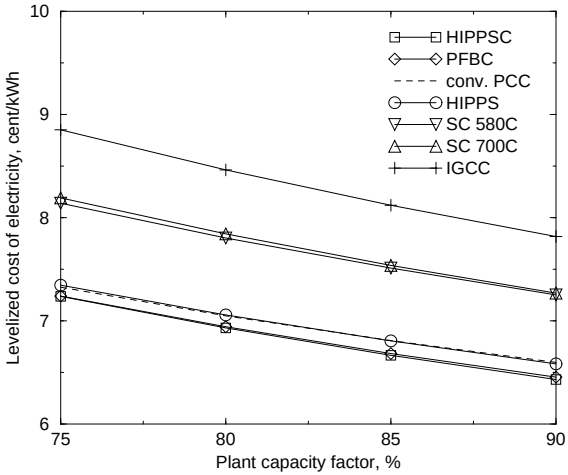

Figure 5.3: LCE as a function of plant capacity factor.

For a given PCF, the HIPPSC has the lowest LCE among all the advanced power plants under study here, which indicates that the HIPPSC is a very attractive option for electricity generation with coal. The PFBC plant has an equivalent value of LCE to that of the HIPPSC. These plants even obtain a LCE slightly lower than that of the conventional PCC plant. The HIPPS exhibits a comparable LCE to that of the conventional PCC plant. We should keep it in mind that the actually assumed PCF is by 5% higher for the conventional PCC plant than for the HIPPS and the PFBC power plant.

The SC steam power plants can only be competitive with the HIPPS /PFBC power plants if they operate with very high plant capacity factors. The IGCC plant has a too high LCE, 7.7% and 15.0% higher than those of the supercritical plant and the HIPPS, respectively. Therefore, the IGCC plant is not economically acceptable. If the total plant cost of the IGCC plant can be reduced by about 13%, this plant has a LCE in the same order of that of the SC steam power plant.

Note that the levelized fuel costs are independent of the PCF. Hence, the LCE is more sensitive to the PCF for plants with low fuel costs than for plants with high fuel costs. This explains why the power plants with high capital investment ought to operate with high PCF.

Effect of natural gas cost

Figure 5.4 shows the dependence of the LCE of the HIPPS on natural gas cost. The assumed cost of natural gas for this study is 2.70 $/GJ-HHV, or 2.85 $/MBtu-HHV (in mid-1998 dollars). In case the actual cost of natural gas is higher than the assumed one, the superiority of the HIPPS in its LCE is reduced. If the cost of natural gas is 10% cheaper than the assumed one, the HIPPS has a LCE comparable to those of the HIPPSC and the PFBC power plants. When the cost of natural gas increases by 50% and by 100%, the LCE of the HIPPS reaches those of the SC "700°C" power plant and the IGCC power plant, respectively.

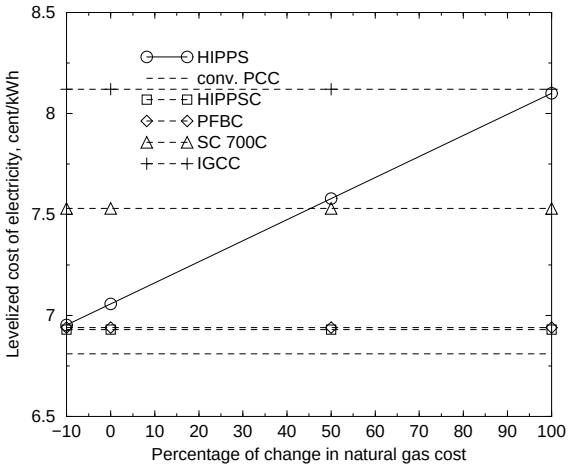

Figure 5.4: Dependence of LCE of the HIPPS on natural gas cost.

Effect of real escalation rate of natural gas cost

The real annual escalation rate of natural gas cost has been set to 0.3% for the economic evaluation of the HIPPS. Since about 35% of the higher heating value of the fuel input to the HIPPS is provided by natural gas, the real escalation rate assumed for the natural gas influences the calculated LCE of the HIPPS. However, as Figure 5.5 reveals, this influence is rather low. An increase of 1% in this rate brings merely a 1.98% growth in the LCE. The real annual escalation rates of natural gas between 0% and 1% correspond to values of 2.50% and 3.53% for the average annual nominal escalation rate of the cost of natural gas, respectively.

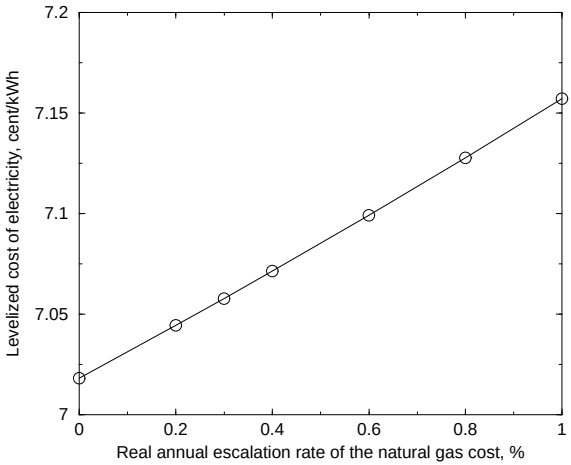

Figure 5.5: Dependence of LCE of the HIPPS on the real annual escalation rate of natural gas cost.

Effect of coal cost

The cost of coal assumed for the Illinois No.6 coal in this study is 1.52$/GJ-HHV, or 1.60$/MBtu-HHV (in mid-1998 dollars). Figure 5.6 shows the effect of coal cost on the LCE of the power plants. The LCE values are calculated based on the assumed plant capacity factors. When the assumed coal cost varies by 10%, the calculated changes of LCE are within 2-3%. We notice that the LCE for the conventional PCC, the HIPPSC, and the PFBC plants reaches that of the HIPPS when the coal cost is by 20% higher than the assumed one.

The effect of the plant efficiency, or of the coal mass flow rate, on the LCE is similar to that of coal cost. A minor difference (within 0.03 cent/kWh for a ±10% variation in efficiency) exists in that there is a weak relation between the plant efficiency and the purchased-equipment costs (especially the purchased-equipment cost of the coal/ash handling system), while the PEC is basically independent of coal cost.

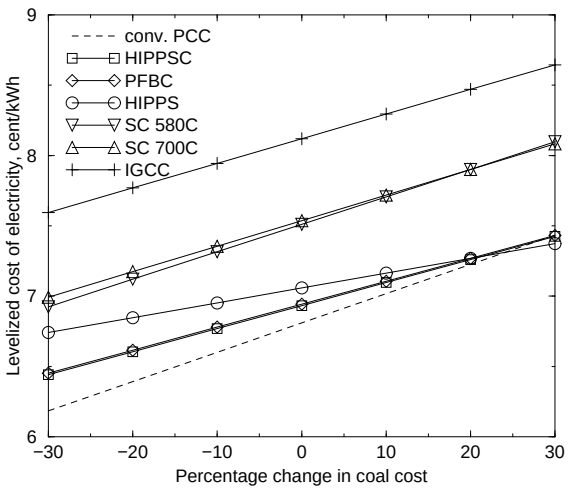

Figure 5.6: Dependence of LCE on coal cost.

Effect of the real escalation rate of coal cost

In the economic analysis a real annual escalation rate of 0.1% was assumed for the cost of coal, resulting in a coal nominal escalation rate of 2.60%. Note that the assumed constant average inflation rate is 2.50%. If the real annual escalation rate of coal cost varies from 0% to 1.0%, i.e., the nominal escalation rate of coal cost from 2.50% to 3.53%, the LCE changes by only 2% to 3% for the advanced power plants (see Figure 5.7).

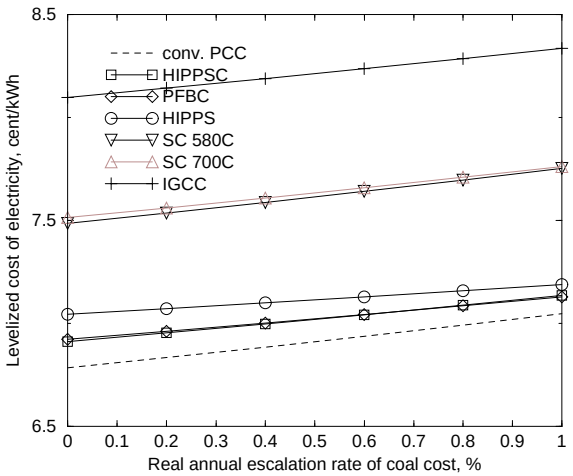

Figure 5.7: Dependence of LCE on the real annual escalation rate of coal cost.

Effect of returns on equity and debt

It was assumed that financing is provided by common equity (50%) and debt (50%). The assumed minimum returns on equity and debt are 13% and 7%, respectively. If these values vary by 10% from the assumed ones, the calculated LCE changes by about 4% and 1.4%, respectively, for all the power plants under study (see Figure 5.8).

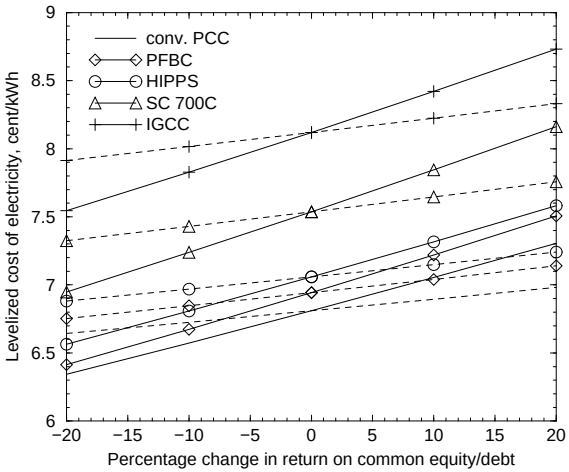

Figure 5.8: Dependence of LCE on returns on common equity (solid lines) and on debt (dashed lines), respectively.

5.4 Emissions evaluation

The estimation of NOx emissions is beyond the scope of this study. The NOx emission values mentioned here are based on information from literature. It should be mentioned that the maximum combustion temperature reaches the highest value in the pulverized coal steam power plant, while it is lowest in the PFBC power plant (Table 5.3).

Based on today's technology, the desulfurization efficiency for each type of power plant is shown in the last column of Table 5.12. Note that the Illinois No. 6 coal involved in this study has a sulfur content of 3.65%, as received. The sulfur dioxide (SO_2) emissions per unit of electricity generated depend on both the desulfurization technologies involved and the plant efficiency, for a given coal. Unlike SO_2 emissions, the specific carbon oxide emissions of a power plant are determined by a single factor, i.e., the plant efficiency, when fueled with a given type of coal.

Table 5.12 provides an overview of the emissions of the power plants under study. The values for SO_2 and CO_2 are given in grams per kWh of electricity generated. As far as the SO_2/CO_2 emissions are concerned, the HIPPS provides the best performance. Operating a HIPPS instead of a conventional PCC power plant results in annual reductions of SO_2 emissions of 8000 tons and CO_2 of one million tons (assuming a PCF of 0.80 and plant capacity of 500 MW). The following sections deal with the emission issues of each type of power plant.

5.4.1 Supercritical steam power plants

Without emissions control, a pulverized coal combustion power plant burning 2.5% sulphur coal would release flue gas containing around 4700 mg/m^3 of SO_2, 800-2000 mg/m^3 of NOx, and about 8 g/m^3 of dust (Scott (1997)). For the new power plants, these values may be of 400 mg/m^3 of SO_2, 650 mg/m^3 of NOx, and 50 mg/m^3 of dust. Local NOx emission limits of 200 mg/m^3 are widely required and dust emission limits can be as low as 10 mg/m^3.

In this study, it is assumed that the desulfurization efficiency is 90%. The resulting SO_2/CO_2 emissions are 2.183/781.1 g/kWh$_{el}$ for the "580°C" case, respectively (see Table 5.12). This means that these

Table 5.12: CO_2 and SO_2 emissions for the power plants under study. Numbers in parentheses are the respective rough percentages with regard to the values for the conventional PCC power plant.

System	CO_2 [g/kWh$_{el}$]	SO_2 [g/kWh$_{el}$]	Desulfurization [%]
HIPPS	552 (65)	0.118 (5)	99
PFBC	669 (78)	0.187 (8)	99
IGCC	709 (83)	0.198 (8)	99
SC 700°C	726 (85)	2.031 (85)	90
SC 580°C	781 (91)	2.183 (91)	90
Conv. PCC	854 (100)	2.389 (100)	90

emissions are about 8.5% lower than those of the conventional PCC power plant.

The emission control options for the SC steam power plants are flue gas desulfurization with a 95% efficiency or higher, selective catalytic reduction or equivalent technology to control NOx emissions, and possibly a final wet electrostatic precipitator or baghouse for particulate emission control. The equipment adds cost to the power generation, lowers the system efficiency (high parasitic consumption) and increases the plant specific CO_2 emissions. For this type of power plants, the overall efficiency is hence a key factor for being competitive with other types of technologies.

5.4.2 HIPPS

The NOx and SO_2 emissions for HIPPS are set less than 0.0258 kg/GJ-LHV and the particulates 0.0013 kg/GJ-LHV, respectively. These limits correspond to 0.181 g/kWh$_{el}$ and 0.009 g/kWh$_{el}$, respectively. Even if high-sulfur coal such as the Illinois No.6 coal is used, a desulfurization efficiency of 98.5% suffices. The desulfurization is accomplished by using a conventional wet flue gas desulfurization system.

The NOx emissions of a HIPPS depend on the design of the high temperature furnace. Controlled fuel distribution and multiple, long-axial flames are the options for controlling NOx and managing wall

ash deposition in the furnace.

5.4.3 PFBC power plant

The target level for SO_2, NOx and particle removals is set at one-fifth of that required under the New Source Performance Standards (NSPS) with system efficiency above 45% (DOE (1999b)). That is, the SO_2 and the NOx emissions should not be higher than 0.181 g/kWh$_{el}$ and the particle emissions 0.007 g/kWh$_{el}$. Due to the fact that the maximum temperature involved in this power plant is below 1400°C (refer to Table 5.3), practically no thermal NOx are formed. However, about 10% fuel-nitrogen will convert to NOx.

The in-bed sulfur absorption by limestone or dolomite injection is enhanced by the elevated operation pressure. Within the bed operation temperature range, hydrogen sulfide and sulfur dioxide evolved from fuel-sulfur can be absorbed by calcium bearing solid particles within the beds. Sulfur exits the PFBC system as solid sulphate with ash, a granular solid material allowing easy handling. 98-99% of SO_2 can be thus removed.

Moreover, NOx, SOx, and CO are very weakly linked in a pressurized process, thus very low emissions of all three pollutants can be achieved simultaneously. The availability of excess oxygen in the fluidized bed means that the hydrogen-sulfide levels are at or below detectable levels. Similarly, no carbonyl-sulfide can be detected either. The bed carbon monoxide levels are negligible as well, less than 20ppm, under the pressurized operation where the oxidation rate of CO is approximately proportional to pressure (Johansson, Bodlund & Willians (1989)).

The particle removal upstream of the gas turbine is achieved possibly by hot gas cleanup (HGCU) filtration devices, with an efficiency over 98%. Filters using ceramic material in various shapes and sizes are under testing. A conventional electrostatic precipitator or equivalent will accomplish further cleanup before the flue gas enters the atmosphere.

5.4.4 IGCC power plant

The polluting substances in the syngas from the gasifier can be eliminated with two types of gas treatment units: Cold gas cleanup (CGCU)

and hot gas cleanup (HGCU). The IGCC power plant studied here (see Section 4.5) utilizes a CGCU system, a Claus sulfur recovery unit, and a Shell Claus Offgas Treating (SCOT) unit. 99.5% of the fuel sulfur can be recovered as elementary sulfur.

In the reducing atmosphere of the gasifier, the elementary nitrogen in the fuel is converted into molecular nitrogen (N_2), ammonia (NH_3), and hydrocyanic acid (HCN). The latter two can be integrally eliminated by the gas treatment (with CGCU, for example). Nevertheless, the formation of thermal NOx needs special attention for an IGCC system due to the carbon monoxide and hydrogen present in the syngas. Since dry low NOx combustors are not suitable for syngas fuel, nitrogen injection and syngas/nitrogen saturation are preferred for NOx control in an IGCC power plant. The NOx emission can be as low as 10 to 25 ppm (15% O_2) or less (Bechtel (1995)).

The inherent penalty on system efficiency caused by syngas cooling in the CGCU unit can be avoided if the CGCU is substituted by a HGCU unit. It has been claimed that the overall efficiency is expected to increase by at least 1 percentage point (Pilleul (1994)) and for an IGCC system based on entrained bed gasification process by 2-3 percentage points (Alderliesten (1990)). However, additional NOx might be formed due to the absence of NH_3 elimination. Metals present in the syngas are of concern as well.

It should be noted that, for combined power plants that involve gas turbines, gasification processes with CGCU are able to remove troublesome impurities such as vanadium, sodium, and potassium, which cause corrosion in the gas turbine blades.

Among the four power plants evaluated in this study, the IGCC power plant has the best environmental performance.

5.5 Plant operation

The SC power plants have significantly better partial load performance than the remaining three types of power plants. Thanks to the once-through steam generator adopted in the SC power plant, the dynamic behavior of the SC is superior to that of the conventional PCC. The operation characteristics of a SC power plant are essentially the same

as those of a conventional PCC steam power plant, except for more strict water treatment requirements.

From the operation standpoint, the PFBC system is similar to the IGCC system, except that a larger fraction of coal energy in the PFBC system is shunted around the gas turbine and transferred directly to the steam turbine. In the PFBC power plant studied here, about 60% of the superheated steam fed to the steam turbine is raised in the the circulating bed combustor. Since this occurs before the gas turbine rather than in the gas turbine exhaust, the steam conditions are relatively independent. The system is therefore more limited by the material considerations than by the process conditions. Another characteristic of the PFBC system is the interaction among the carbonizer, the fluidized bed combustor, and the fluidized bed heat exchangers. This presents unique challenges for operating this type of power plants.

The hot gas cooling for the syngas temperature to the gas turbine combustor is limited by the control valve at the gas turbine burner. This temperature is about 400°C nowadays. Another problem is that the available hot booster compressors are relatively small (Campbell et al. (1990)).

For IGCC power plants, the integration between the gas turbine air compressor and the air separation unit (ASU) plays a major role in the optimization of the system in terms of efficiency, flexibility, and operation. The dependency of gas turbine on ASU, as well as involvement of syngas saturator, gives rise to problems when the fuel switches between syngas and natural gas.

There is no operation experience for the HIPPS. The cycle performance should not be difficult. A potential problem could be ash deposition in the high temperature furnace.

6. Conclusions and future outlook

Coal has played an important role in the power generation sector worldwide, and it will probably remain so for several decades. In an era when the demand for electricity grows and the emission standards become increasingly strict, clean coal technologies emerge as duty-bound countermeasures to cope with this tough situation. However, these technologies will only be adopted if they are competitive for power generation, allowing high efficiencies, reasonable costs, low emissions, and high plant availabilities.

The clean coal technologies include supercritical steam power plants (SC), indirectly coal-fired power systems (i.e., the HIPPS), advanced pressurized fluidized-bed combustion power plants (PFBC), and integrated gasification-combined-cycle power plants (IGCC), among others. They represent options for power generation with coal into the distant future and have therefore been studied here.

The present work aimed at identifying, among the four types of power plants, the option which attains the possibly highest overall efficiency, provides electricity at reasonable cost, and allows acceptably low emissions. As a result, the relative positions of the four advanced technologies on the potential electricity market can be located. Hence, an exergetic analysis and an economic analysis have been conducted on each of the four types of plants, together with parametric studies. A conventional PCC steam power plant with a thermal efficiency of 36.6% (HHV) was used to represent today's technology standard of coal-fired power plants. Attention was also paid to two special cases: the supercritical steam power plant "700°C" (SC 700°C) and the fully coal-fueled HIPPS (i.e., the HIPPSC).

6.1 Overall performance

The HIPPS seems to be the most promising power system. The HIPPS base case shows an overall exergetic efficiency of 48.5% (or an energetic one of 51.3% on a LHV basis). This efficiency is about 26% higher than that of the conventional PCC power plant. The corresponding LCE is estimated at 7.06 cent/kWh, slightly higher than that of the conventional power plant (6.81 cent/kWh) and that of the PFBC power plant (6.94 cent/kWh). In case the coal price is 20% higher than the assumed one (1.5166$/GJ-HHV), these three power plants will have the same LCE (see Figure 5.6) and the HIPPS gains some priority. However, if the natural gas price goes up to 1.5 and 2 times the assumed one (2.7015$/GJ-HHV), the LCE of the HIPPS will be as high as those of the SC 700°C power plant and the IGCC power plant, respectively (see Figure 5.4). The emissions of the HIPPS are very low: The CO_2 emissions (552.2 g/kWh$_{el}$), for example, are 35% lower in the HIPPS than in the conventional PCC plant (see Table 5.12).

For the HIPPS base case, 35.07% of the fuel input is provided by methane, the air temperature at the HTF exit is 982°C, and the gas turbine inlet temperature is 1260°C (Section 4.3.2). If this system is fueled only with coal (case HIPPSC), the overall exergetic efficiency decreases by 1.8 percentage points down to 46.72% (Section 4.3.3), while the LCE remains unchanged. Still, this efficiency is the highest among all the coal-fired power plants involved in this study. The key prerequisite for this HIPPSC is an air temperature of 1340°C or higher at the HTF exit, so that a gas turbine inlet temperature of 1260°C can be reached. Starting from the air temperature of 1340°C, every 50°C increase will improve the system efficiency by 0.5 percentage point, provided that the gas turbine inlet temperature can be elevated accordingly (see Figure 4.10).

The only critical and risky component in the HIPPS is the high temperature furnace (HTF), which is undergoing intensive research. The cost of the HTF accounts for 39.3% of the PEC of the HIPPS, more than half of which comes from the air heater. The uncertainty in estimating the PEC of the air heater affects certainly the LCE of the HIPPSC. This effect is, however, not significant (see Figure 5.2). If the cost of the air heater is about 35% higher than the assumed one for the HIPPSC, the LCE of the HIPPSC becomes equal to that of the

HIPPS base case; the LCE of the HIPPSC remains lower than those of the SC/IGCC power plants even if the assumed cost of the air heater is doubled.

Basically, the advances in material (both for the HTF and for the gas turbine), the design of the HTF, and the natural gas price determine the prospect of the HIPPS. It should be pointed out that the HIPPS has the lowest specific total plant cost (1370 $/kW), very close to that of the conventional PCC power plant (see Table 5.7). In addition, it possesses the largest plant capacity (567 MW) among the four types of power plants. All this favors the overall performance of the HIPPS. The exact cost effectiveness of the HIPPS will depend on the actual cost of the HTF incurred in the future.

The PFBC power plant proves to be the second best option. It attains an exergetic efficiency of 45.70% or a thermal efficiency of 48.87% (LHV). The key parameter affecting both the plant efficiency and the plant operation is the carbon conversion ratio (CCR, see Section 4.4.3). From the thermodynamic view point, this ratio should be kept as high as possible so that the coal energy can be exploited in both the gas turbine and the steam turbine. As indicated in Figure 4.15, as this ratio increases from 0.6 to 0.8, the overall plant efficiency gains one percentage point.

However, the CCR is coupled with the carbonizer bed temperature, or the sulfur retention. As pointed out in Section 4.4.3, the carbonizer bed temperature should be kept within a range of 820 - 900°C to ensure a sound bed operation. At too high values of CCR, cooling becomes necessary to control the bed temperature, and this affects the overall efficiency adversely. Moreover, the fuel gas produced at a higher carbonizer bed temperature has a lower heating value, which is undesired from the economic view point. In addition, the CCR is restricted by the allowable gas turbine inlet temperature, which affects in turn the overall efficiency. With a CCR of 0.731, an increase of 50°C in this temperature raises the overall efficiency by about 0.25 percentage points (see Section 4.4.3). Note that the decrease in this inlet temperature is done here by cutting down the air feed to the gas turbine combustor. If the CCR and the gas turbine inlet temperature are increased simultaneously, the resulting impact on the overall efficiency will be significant. In the sense of the overall efficiency of this type of PFBC power plants, the design of carbonizers that operate

with high CCR at moderate temperatures and the advances in turbine technology are the most decisive factors. In the author's opinion, the optimal CCR of a PFBC plant can only be determined through on-site operation, taking into account the impact of part-load operation.

The LCE of the PFBC power plant is 6.94 cent/kWh, the same as that of the HIPPSC and lower than those of the remaining advanced power plants (7.06-8.12 cent/kWh). It should be mentioned that the PCF for this power plant is assumed to be 0.80. As stated in Section 5.3.5, the LCE is to be reduced by about 8% if the plant operates with a PCF of 0.9. We notice also that the PEC of the PFBC boiler/ST holds 47.2% of the PEC of this PFBC plant (see Table 5.9), although the gas turbine contributes 47.1% of the plant gross power output (see Table 5.7). Efforts on reducing the cost of the PFBC boiler might be cost effective.

Ranking last, the supercritical steam power plant "580°C" is able to yield an overall exergetic efficiency of 39.17%, or 41.88% on a lower heating value basis, at a condenser pressure 0.083 bar (see Section 4.3.2). The efficiency of this power plant is by 9.4% higher than that of the conventional PCC power plant, while by 19.3% and 14.3% lower than those of the HIPPS and the PFBC power plant, respectively. If the steam parameters are further elevated to 365 bar and 700°, the overall exergetic efficiency may reach 42.12%, or the energetic efficiency 45.03% (LHV) (refer to Section 4.2.5), about 3 percentage points higher than that of the SC power plant "580°C".

As pointed out earlier, the condenser pressure is a key factor to the overall efficiency of this steam power plant. If sea-water cooling is possible and a condenser pressure of 0.023 bar is achievable, the exergetic efficiency of the SC power plant "580°C" will increase to 41.52% (Section 4.2.3). However, such low condenser pressure should be considered as an extreme case and not be used as a general condition upon evaluating supercritical steam power plants. The author would like to state that an overall thermal efficiency of 55% (LHV) for future SC steam power plants "700°C", as claimed in Kjær (1998), should be unattainable.

The estimated LCE is basically the same for both the SC "580°C" and the SC "700°C", i.e. 7.5 cent/kWh. Compared with the conventional PCC plant, it means some 10% increase in the LCE. Moreover, the LCE of the SC power plants lies between those of the HIPPS/PFBC

plant and that of the IGCC plant (see Table 5.6), due to the high investment costs of the steam generator and the steam turbine, 47.4% and 19.8% of the plant PEC for the SC "700°C", respectively (Table 5.9). It is worth to note that the PEC for the steam generator and for the steam turbine of the SC steam power plants in this study were evaluated based on the data from the conventional PCC power plant. Since the emission reduction associated with a SC power plant can always be accomplished using stack gas cleanup systems, the purchased-equipment costs of future SC steam plants ("700°C") will depend on the price of the introduced superalloys, on the manufacturing costs of steam generators and steam turbines, and on the emission regulations.

The IGCC power plant has an overall exergetic efficiency of 43.2% or an energetic one of 46.8% (LHV), see Section 4.5.2. This efficiency is by about 21% and 10% higher than those of the conventional PCC plant and the SC plant "580°C", respectively, and lower than that of the HIPPS and that of the PFBC power plant (Table 5.1). However, the LCE of the IGCC plant is the highest among all options analyzed here (about 7.7%-19.2% higher, see Table 5.6). This is mainly the result of the high specific investment costs and the high O&M costs. It should be underlined that the IGCC technology renders outstanding capability for reducing emissions, especially when gas turbines are involved.

From the economic view point, it is essential for the plants studied here to cut down the plant capital investment, as indicated by the high carrying charges, which amount to 58%-63% of the TTR on average (see Table 5.11). The probably most meaningful solution addressing this issue might be the combined techniques of preengineered design and modular construction (Maude (1996)). While the average fuel costs contribute to 23% of the TRR for the coal-based power plants, the share of the O&M costs in the TRR varies from 13.5% to 15.3%, with the exception of the IGCC plant, where it lies around 21.4%. The fuel costs depend on the overall plant efficiency, and the O&M costs are getting lower as modern control techniques are developed and applied.

6.2 Technology perspectives

One of the most critical issues facing the operators of coal-based power plants today is how to retain the well proven and familiar operating characteristics of pulverized coal-fired steam power plants and at the same time meet increasingly demanding limits on emissions.

Compared with pulverized coal combustion technology, there is much less operating experience both with HIPPS, PFBC, and IGCC power plants and with the steam cycles incorporated in these systems. This is especially the case with large scale plants, which are favored worldwide for power generation to achieve low cost of electricity.

Therefore, the supercritical steam power plants will probably be a preferred coal-based power generation technology for the short-term addition of new capacity, with the overall drive towards more advanced steam conditions. While relative high plant efficiencies are guaranteed with the technology available today, the identical operation to the conventional PCC plants and the high performance at part load ensure immediate market acceptance.

For long-term applications, the HIPPS system should be the best candidate by virtue of its supreme efficiency, simple configuration, similar operation to pulverized coal steam power plants, and intensive involvement with advancement in material and gas turbine technology.

The PFBC and IGCC power plants for power generation based on coal, as studied in this work, will play a significant role in the coming years if quick maturity of these technologies is reached before commercial HIPPS technology enters the power market, probably in a decade. Hence, these two types of power plants might serve as options for middle-term base-load power generation, provided that the cost reduction of the IGCC plants can be achieved. Besides, PFBC and IGCC power plants are capable of efficiently using fuel feedstock such as biomass and refinery residual, due to their relative flexibility on fuel and outstanding environmental performance. In addition, an IGCC system will be an indispensable module, integrated with advanced gas turbines and fuel cells, in an extremely clean power plant park for future electricity generation. In this sense, the PFBC and IGCC technologies have a very promising future.

Appendix

A. State-of-the-art of the four types of power plants

Table A.1: Representative supercritical steam power plants worldwide.

Plant	Capacity [MW]	Steam state bar/°C/°C	Startup	η(LHV) [%]
Schwarze Pumpe (D)	2x800	250/544/562	1992	41.0
Esbjerg 3 (DK)	415	250/560/560	1992	45.3
Staudinger Unit 5 (D)	500	250/540/560	1993	43.0
Nordjylland 3 (DK)	410	290/582/580	1998	47.0
Lippendorf (D)	2x800	268/554/583	2000	42.4
Waigaoqiao (China)	2x900	279/542/562	2002	42.7

Table A.2: Commercial scale PFBC power plants.

Plant	Capacity [MW]	Steam Conditions	Startup [%]	η(HHV)
Wärtan (S)	135(225)	137bar/530°C	1990	33.5
Escatrón (E)	75	94bar/513°C	1990	36.4
Tidd (USA)	70	90bar/496°C	1990	35.0
Warkamatsu (JP)	70	103bar/593°C/593°C	1993	37.5
Cottbus (D)	65(90)	142bar/537°C/537°C	1999	42.0
Karita (JP)	350	241bar/565°C/593°C	1999	42.0

Table A.3: Commercial scale coal-fired IGCC power plants

Plant	Capacity [MW]	Gasifier Type	Startup	η(HHV) [%]
Cool Water (USA)	96	entrained-flow	1984	31.2
Plaquemine (USA)	160	2-entrained-flow	1987	36.0
Buggenum (NL)	253	entrained-flow	1994	41.3
Wabash River (USA)	262	2-entrained-flow	1995	39.2
Polk County (USA)	250	entrained-flow	1996	40.0
Piñon Pine (USA)	99	fluidized-bed	1997	38.0
Puertollano (E)	300	entrained-flow	1997	42.5
Litinov (Czech)	350	fixed-bed	1997	-

B. Main assumptions for the thermodynamic analyses

B.1 Composition of coal and air

Table B.1: Coal analysis for the Illinois No. 6 coal (in weight %)

ULTIMATE ANALYSIS (dry basis)	
Carbon	71.20%
Hydrogen	4.98%
Nitrogen	1.27%
Sulfur	3.65%
Oxygen	9.30%
Ash	9.60%
Total	100.00%
MOISTURE (as received)	8.8%
PROXIMATE ANALYSIS (dry basis)	
Fixed Carbon	53.6%
Volatile Matter	36.8%
Ash	9.6%
Total	100.0%
HIGHER HEATING VALUE (as received)	27.386 MJ/kg (11774 Btu/lbm)
LOWER HEATING VALUE (as received)	26.189 MJ/kg (11259 Btu/lbm)
CHEMICAL EXERGY (Ahrendts' model)	27.997 MJ/kg
CHEMICAL EXERGY/HHV	1.0223

Table B.2: Assumed mole composition of air at 15°C and 1.013 bar.

Nitrogen	77.3300%
Oxygen	20.7380%
Water	1.0096%
Argon	0.9210%
Carbon dioxide	0.0014%
Total	100.0000%

B.2 Assumptions

Here the most important assumptions made for each power plant are presented. The assumptions valid for all power plants are given in Section 3.4.

B.2.1 Assumptions for the steam power plants

The basic assumptions for the steam power plants are as follows:

- The pressure drop in the steam generator is 10%;
- The steam turbine throttle pressure drop is 0.6%;
- The pressure drop in the conventional reheater is 10%;
- The pressure drop in the 1st and 2nd reheater for "580°C"is 5% and 10%, respectively;
- The pressure drop in the 1st and 2nd reheater for "700°C"is 4% and 6%, respectively;
- 28.8% excess air is used in the coal combustor;
- The net plant power output is kept at 508 MW;
- For all feedwater heaters the terminal temperature difference is 4.44°C;
- The flue gas temperature at the steam generator exit is 143.3°C.

B.2.2 Assumptions for the HIPPS

The basic assumptions for the HIPPS are as follows:

- The pinch temperature difference is 30°C for both HRSG and high temperature furnace;
- The gas turbine inlet temperature is 1260°C ;
- The main steam conditions are 93 bar/620°C;
- The pressure drop in the steam generator is 10%;
- 17% excess air is assumed for the coal combustion;
- The steam turbine generator losses are 2%;
- The flue gases leave the HRSG and the high temperature furnace at 95.6°C and 150°C, respectively.

B.2.3 Assumptions for the PFBC power plant

The basic assumptions for the PFBC power plant are as follows:

- The carbonizer bed temperature is fixed at 860°C;
- The circulated fluidized bed operates at 860°C;
- The gas turbine inlet temperature is 1260°C;
- The mole ratio of the calcium in the limestone to the sulfur in the coal is 2 (Ambrose et al. (1993), Rehmat & Goyal (1993));
- The fuel gas from the carbonizer is cooled to 643°C;
- There is no hot syngas cooling after the fluidized bed;
- 46% of bed ash is removed from the fluidized bed;
- 99% of fly ash in the fluidized bed flue gas is removed by cyclone/filter;
- The bed solids are discharged at a temperature of 261°C;
- There is 0.0076 % of gas entrained with the cyclone fly ash;
- 99% of coal sulfur is captured in bed;
- The steam conditions are 166 bar/538°C;
- The pressure drop in the cyclone system is 5-10%;
- The flue gas leaves the HRSG at 137.5°C.

B.2.4 Assumptions for the IGCC power plant

The basic assumptions for the IGCC power plant are as follows:

- The oxygen/water mass flow ratio for the gasifier feeds is 25.0;
- The mass flow ratio of oxygen to nitrogen for the gasifier feeds is 7.138 (Hartman et al. (1983));
- Oxygen feedstock of 95 mole purity is used;
- The gasifier outlet temperature is 1400°C;
- The gasifier carbon conversion ratio is 99%;
- The operating pressure of the gasifier is 28 bar;
- 100 % of slag is discharged to the gasifier slag hopper;
- 100 % of fly ash is captured by the gasifier cyclone;
- 1.8% of coal HHV is carried away by the jacket cooling water;
- 0.5% of coal HHV is lost in the gasifier;
- The gas turbine inlet temperature is 1285°C;
- 1% of fuel LHV to the gas turbine combustion chamber is lost;
- The pinch temperature difference for HP, IP, and LP evaporator is 8°C, respectively ;
- The pressure losses in the heat exchangers in both the gasification section and the HRSG are 3% and 3.2%, respectively;
- Flue gas leaves the HRSG at 105.0°C.

C. Tables and flowsheets for the power plants

C.1 Conventional steam power plant

Table C.1: Mass flow rate, temperature, pressure and flow rates of enthalpy, entropy and exergy for each stream of the conventional PCC plant.

$No.$	$\dot{m}$ $[kg/s]$	T $[^{\circ}C]$	p $[bar]$	$\dot{H}$ $[MW]$	$\dot{S}$ $[kW/K]$	$\dot{E}$ $[MW]$
1	368.62	358.7	11.8	-4717.55	-800.83	400.88
2	450.54	346.5	178.7	-6461.59	-2575.36	254.38
13	406.58	349.7	46.0	-5242.23	-1189.00	491.38
24	372.66	66.8	22.1	-5846.60	-3170.64	8.19
25	372.66	92.4	21.4	-5806.62	-3057.18	15.48
26	372.66	119.9	20.8	-5763.30	-2942.86	25.86
27	372.66	149.6	20.1	-5716.15	-2827.15	39.67
28	19.27	124.4	5.2	-297.62	-151.20	1.41
29	36.44	96.8	2.2	-567.16	-297.03	1.59
30	51.84	71.2	0.9	-812.43	-438.17	1.18
31	65.45	47.4	0.3	-1032.28	-572.86	0.62
36	450.54	183.6	10.9	-6844.26	-3265.54	70.58
37	288.21	42.2	0.1	-3929.70	-568.96	55.74
38	372.66	42.2	0.1	-5885.62	-3287.26	2.78
49	450.54	252.5	184.3	-6700.64	-2991.59	135.26
51	450.54	215.7	192.3	-6776.51	-3142.04	102.74
52	22.33	358.4	11.4	-285.77	-48.20	24.20
53	450.54	252.5	186.5	-6700.64	-2991.83	135.33

$No.$	$\dot{m}$ $[kg/s]$	T $[°C]$	p $[bar]$	$\dot{H}$ $[MW]$	$\dot{S}$ $[kW/K]$	$\dot{E}$ $[MW]$
54	35.91	348.4	44.6	-463.01	-104.56	43.27
56	35.91	220.1	42.5	-539.59	-248.05	8.04
63	55.56	191.5	21.7	-841.97	-398.52	9.49
64	450.54	188.3	198.2	-6830.80	-3256.95	81.57
77	19.64	456.1	23.2	-247.59	-43.07	25.29
81	12.47	72.4	0.3	-167.81	-25.34	4.88
82	15.40	98.2	1.0	-204.91	-31.87	8.47
83	17.17	176.9	2.4	-225.80	-36.14	12.31
84	19.27	266.7	5.6	-250.03	-41.22	17.31
85	22.33	358.7	11.8	-285.77	-48.51	24.28
87	35.91	349.7	46.0	-463.01	-105.02	43.40
88	19.64	456.5	23.9	-247.59	-43.34	25.37
96	448.29	537.9	166.5	-5636.44	-1348.72	696.20
100	406.58	537.8	41.4	-5057.81	-910.73	595.62
109	13575.53	23.9	1.1	-215444.02	0.00	41.66
110	13575.53	35.5	1.0	-214783.29	0.00	73.57
N1	131.85	28.7	1.1	-11.56	18.48	1.24
N4	429.32	28.7	1.1	-37.63	60.16	4.05
N5	429.32	324.9	1.1	94.08	365.71	47.72
N6	83.46	324.9	1.1	18.29	71.09	9.28
N7	624.34	152.9	1.1	-1369.85	330.06	83.91
N8	41.82	26.7	1.1	-670.28	-395.53	0.15
N10	627.88	372.4	1.0	-1221.36	625.79	150.76
N11	525.54	143.2	1.0	-1153.99	275.34	66.06
N16	102.35	143.6	1.0	-224.69	53.73	12.88
N17	131.85	15.0	1.0	-13.38	16.77	-0.09
N19	429.32	15.0	1.0	-43.58	54.61	-0.30
N20	16.97	15.0	1.1	-1.72	1.68	0.13
N21	0.89	1889.6	1.1	1.46	2.64	1.59
N22	624.34	143.3	1.0	-1376.16	325.60	78.88
N25	50.64	15.0	1.1	-102.84	-191.06	1417.67
N27	3.55	143.3	1.0	-2.51	3.47	0.06
N28	18.75	55.3	1.0	-297.87	-169.06	0.28
N29	3.03	55.3	1.0	-13.99	0.70	14.29
N31	644.38	55.3	1.0	-1728.58	132.65	60.63
N34	627.88	143.3	1.0	-1378.68	329.07	78.94

Table C.1 (Cont'd)

C.2 SC steam power plant “580 °C”

Table C.2: Mass flow, temperature, pressure and flow rates of enthalpy, entropy and exergy for the SC “580 °C” base case.

$No.$	$\dot{m}$ $[kg/s]$	T $[°C]$	p $[bar]$	$\dot{H}$ $[MW]$	$\dot{S}$ $[kW/K]$	$\dot{E}$ $[MW]$
10	379.65	315.0	310.20	-5529.6	-2322.55	173.45
13	342.61	400.7	94.16	-4405.8	-1084.52	449.46
18	242.34	241.9	1.47	-3153.9	-387.70	171.13
24	300.87	104.7	12.90	-4672.6	-2425.97	15.76
25	300.87	127.9	12.51	-4643.1	-2350.05	23.43
26	300.87	152.5	12.14	-4611.4	-2273.28	33.02
27	300.87	178.6	11.77	-4577.2	-2195.32	44.74
28	12.13	156.9	10.62	-185.7	-91.13	1.41
29	23.29	132.3	5.66	-359.0	-180.84	1.92
30	33.62	109.2	2.89	-521.5	-269.39	1.88
31	43.10	87.3	1.39	-672.5	-356.00	1.52
32	12.13	515.9	10.74	-151.2	-20.01	15.49
34	10.32	329.4	2.89	-132.6	-16.54	9.08
36	381.55	205.8	17.51	-5758.3	-2685.02	74.53
37	225.33	42.2	0.08	-3038.5	-337.73	46.49
38	300.87	42.2	0.08	-4751.9	-2654.05	2.24
40	379.14	582.0	290.08	-4767.5	-1225.24	612.64
47	261.21	421.4	6.01	-3305.6	-430.84	281.99
48	272.37	516.2	11.30	-3393.1	-455.62	349.56
50	381.55	235.7	337.02	-5702.8	-2601.49	106.00
51	381.55	266.9	330.28	-5648.4	-2497.16	130.33
52	14.93	338.2	18.43	-192.0	-36.84	16.63
53	381.55	300.0	323.68	-5587.2	-2386.63	159.69
54	32.13	398.7	91.33	-413.2	-101.31	42.04
56	32.13	271.3	89.26	-474.9	-207.06	10.81
59	53.00	240.1	54.77	-791.4	-356.38	14.03
60	297.83	338.8	19.00	-3829.1	-738.90	332.86
61	300.87	42.9	14.13	-4750.5	-2651.09	2.75
63	65.75	217.7	32.03	-988.7	-455.53	14.37
64	381.55	214.9	343.90	-5737.9	-2672.51	91.37
69	455.63	366.6	48.54	-5857.4	-1315.63	562.96
74	9.48	255.2	1.39	-123.1	-14.45	6.74
75	11.16	421.2	5.71	-141.2	-18.15	11.97

$No.$	$\dot{m}$ $[kg/s]$	T $[°C]$	p $[bar]$	$\dot{H}$ $[MW]$	$\dot{S}$ $[kW/K]$	$\dot{E}$ $[MW]$
77	12.76	422.9	33.52	-161.9	-31.66	16.35
79	9.48	255.3	1.47	-123.1	-14.67	6.81
82	10.32	329.5	3.05	-132.6	-16.78	9.15
83	11.16	421.4	6.01	-141.2	-18.41	12.05
84	12.13	516.2	11.30	-151.2	-20.30	15.57
86	20.87	505.0	57.88	-261.6	-52.33	30.23
87	32.13	400.7	94.16	-413.2	-101.70	42.15
88	12.76	423.6	34.56	-161.9	-31.83	16.40
91	20.87	504.2	56.15	-261.6	-52.05	30.15
96	379.65	582.6	291.87	-4773.9	-1227.80	613.73
100	342.61	580.0	89.45	-4243.3	-862.39	547.96
109	13575.53	10.0	1.10	-216232.9	-125862.74	36.52
110	13575.53	19.8	1.01	-215679.1	-123939.45	36.14
113	8.21	84.9	0.28	-109.3	-12.66	3.19
114	8.21	84.8	0.27	-109.3	-12.47	3.14
115	51.91	66.8	0.63	-814.5	-441.57	1.03
118	60.11	47.4	0.27	-948.1	-526.14	0.57
119	300.87	62.3	13.71	-4726.1	-2576.26	5.54
120	300.87	82.9	13.30	-4700.2	-2501.30	9.84
124	8.81	159.9	0.67	-116.1	-13.86	4.76
125	8.81	159.8	0.63	-116.1	-13.65	4.70
N1	120.52	28.7	1.14	-10.6	16.89	1.14
N4	392.42	28.7	1.14	-34.4	54.99	3.70
N5	392.42	386.1	1.12	111.8	375.35	57.58
N6	76.29	386.1	1.12	21.7	72.97	11.19
N7	570.69	152.9	1.06	-1247.2	304.03	80.91
N8	41.82	26.7	1.05	-670.3	-395.53	0.15
N10	573.93	419.8	1.02	-1080.7	620.38	159.56
N17	120.52	15.0	1.01	-12.2	15.33	-0.09
N19	392.42	15.0	1.01	-39.8	49.91	-0.28
N20	15.51	15.0	1.12	-1.6	1.53	0.12
N21	0.81	1922.5	1.12	1.4	2.44	1.50
N22	570.69	143.3	1.00	-1253.0	299.95	76.30
N25	46.29	15.0	1.12	-94.0	-174.64	1295.85
N27	3.24	143.3	1.00	-2.3	3.17	0.06
N28	20.89	55.2	1.03	-331.9	-188.39	0.31
N29	2.77	55.2	1.03	-12.8	0.64	13.06
N31	588.85	55.2	1.03	-1573.1	123.56	59.55
N34	573.93	143.3	1.00	-1255.3	303.12	76.36

Table C.2 (Cont'd)

C.3 SC steam power plant “700 °C”

Table C.3: Mass flow, temperature, pressure and flow rates of enthalpy, entropy and exergy for the SC “700 °C” base case.

$No.$	$\dot{m}$ $[kg/s]$	T $[°C]$	p $[bar]$	$\dot{H}$ $[MW]$	$\dot{S}$ $[kW/K]$	$\dot{E}$ $[MW]$
10	355.91	354.9	390.32	-5108.0	-2059.33	204.48
13	313.35	571.1	177.95	-3914.6	-920.86	505.55
18	209.46	285.2	2.01	-2708.1	-332.05	164.92
24	266.85	114.3	20.77	-4133.3	-2123.54	16.86
25	266.85	141.5	20.14	-4102.4	-2046.38	25.54
26	266.85	170.7	19.54	-4068.8	-1968.05	36.57
27	266.85	201.8	18.95	-4032.0	-1887.87	50.27
28	12.55	175.1	17.57	-191.1	-91.99	1.80
29	23.91	146.0	8.89	-367.1	-182.22	2.40
30	34.26	118.8	4.27	-530.1	-270.93	2.28
31	43.59	93.3	1.91	-679.1	-357.06	1.76
32	12.55	606.7	17.68	-153.9	-20.63	18.44
34	10.35	388.5	4.27	-131.7	-16.46	10.31
36	357.70	236.7	31.57	-5347.0	-2414.71	91.59
37	192.48	42.2	0.08	-2594.0	-283.38	39.85
38	266.85	42.2	0.08	-4214.6	-2353.93	1.99
40	355.43	699.9	365.00	-4362.4	-1064.10	656.99
47	228.28	493.4	9.22	-2854.6	-374.43	280.03
48	239.64	607.0	18.61	-2938.7	-399.64	353.87
50	357.70	270.9	419.74	-5288.2	-2335.43	127.57
51	357.70	309.1	411.35	-5222.6	-2218.34	159.38
52	17.79	417.0	33.23	-226.0	-44.42	22.64
53	357.70	350.0	403.12	-5144.6	-2088.27	199.92
54	37.96	569.8	174.39	-474.2	-111.22	61.14
56	37.96	313.6	172.32	-552.6	-230.56	17.10
59	62.11	275.3	102.09	-916.8	-398.24	21.54
60	264.00	417.7	34.26	-3354.4	-662.87	337.08
61	266.85	42.9	22.75	-4213.2	-2351.43	2.67
63	73.06	246.7	58.25	-1088.6	-486.89	20.38
64	357.70	249.8	428.31	-5322.6	-2400.59	111.95
69	45.14	313.6	172.32	-657.2	-274.23	20.33
74	9.33	308.3	1.91	-120.2	-13.80	7.50
75	11.36	493.2	8.94	-142.1	-18.48	13.89

$No.$	$\dot{m}$ $[kg/s]$	T $[°C]$	p $[bar]$	$\dot{H}$ $[MW]$	$\dot{S}$ $[kW/K]$	$\dot{E}$ $[MW]$
77	10.95	509.8	59.74	-137.1	-27.47	15.96
79	9.33	308.5	2.01	-120.2	-14.02	7.56
82	10.35	388.7	4.49	-131.7	-16.71	10.38
83	11.36	493.4	9.22	-142.1	-18.63	13.94
84	12.55	607.0	18.61	-153.9	-20.93	18.53
86	24.16	606.4	105.58	-298.0	-61.15	39.96
87	37.96	571.1	177.95	-474.2	-111.54	61.24
88	10.95	510.7	61.59	-137.1	-27.62	16.00
91	24.16	605.7	103.47	-298.0	-60.94	39.90
96	355.91	700.4	367.25	-4368.3	-1066.44	658.14
100	313.35	700.0	170.83	-3806.0	-795.49	578.09
109	13575.53	10.0	1.10	-216232.9	-125862.74	36.52
110	13575.53	18.4	1.01	-215756.3	-124203.68	35.07
113	8.15	99.9	0.32	-108.3	-12.40	3.36
114	8.15	99.8	0.31	-108.3	-12.21	3.30
115	52.42	69.6	0.80	-821.9	-444.12	1.14
118	60.57	47.4	0.31	-955.4	-530.17	0.58
119	266.85	65.1	22.07	-4188.4	-2275.76	5.59
120	266.85	88.9	21.41	-4161.9	-2199.90	10.27
124	8.83	188.3	0.84	-115.8	-13.73	5.21
125	8.83	188.2	0.80	-115.8	-13.52	5.15
N1	112.16	28.7	1.14	-9.8	15.72	1.06
N4	365.21	28.7	1.14	-32.0	51.18	3.44
N5	365.21	386.9	1.12	104.4	349.78	53.76
N6	71.00	386.9	1.12	20.3	68.00	10.45
N7	531.09	152.9	1.06	-1160.4	282.93	75.28
N8	41.82	26.7	1.05	-670.3	-395.53	0.15
N10	534.11	420.4	1.02	-1005.0	577.88	148.69
N17	112.16	15.0	1.01	-11.4	14.27	-0.08
N19	365.21	15.0	1.01	-37.1	46.45	-0.26
N20	14.44	15.0	1.12	-1.5	1.43	0.11
N21	0.75	1922.7	1.12	1.3	2.27	1.40
N22	531.09	143.3	1.00	-1165.8	279.13	71.00
N25	43.06	15.0	1.12	-87.5	-162.48	1205.62
N27	3.02	143.3	1.00	-2.1	2.95	0.05
N28	22.49	55.1	1.03	-357.3	-202.83	0.34
N29	2.58	55.1	1.03	-11.9	0.60	12.15
N31	547.85	55.1	1.03	-1461.7	115.10	55.36
N34	534.11	143.3	1.00	-1167.9	282.08	71.05

Table C.3 (Cont'd)

C.4 HIPPS

Table C.4: Mass flow rate, temperature, pressure and flow rates of enthalpy, entropy and exergy for each stream of the HIPPS base case.

$No.$	$\dot{m}$ $[kg/s]$	T $[°C]$	p $[bar]$	$\dot{H}$ $[MW]$	$\dot{S}$ $[kW/K]$	$\dot{E}$ $[MW]$
1	180.17	621.1	97.98	-2213.8	-440.03	301.92
2	180.17	619.5	93.08	-2213.8	-435.95	300.75
5	0.93	316.1	11.86	-11.9	-2.15	0.96
6	1.25	316.1	11.86	-16.1	-2.91	1.30
9	177.99	33.3	0.05	-2446.0	-377.96	22.99
10	10513.76	21.1	0.97	-166978.0	-95790.39	29.01
11	10513.76	29.6	0.97	-166606.2	-94544.60	41.88
13	177.99	33.3	0.05	-2817.8	-1591.51	0.83
14	177.99	33.3	4.94	-2817.7	-1591.44	0.94
16	75.56	144.5	4.94	-1160.8	-577.13	7.42
17	76.49	151.4	4.94	-1172.7	-578.80	8.23
18	76.49	153.9	108.86	-1171.4	-577.81	9.24
19	76.49	317.3	108.86	-1110.8	-458.78	35.52
20	76.49	317.3	108.86	-1079.2	-405.18	51.73
22	102.43	144.5	4.94	-1573.5	-782.33	10.06
23	103.68	151.4	4.94	-1589.7	-784.59	11.15
24	103.68	153.9	108.86	-1587.9	-783.25	12.52
25	103.68	317.3	108.86	-1505.8	-621.90	48.15
26	103.68	317.3	108.86	-1474.3	-568.57	64.28
27	180.17	317.3	108.86	-2553.5	-973.74	116.00
28	180.17	397.6	108.86	-2323.3	-589.94	235.58
30	177.99	144.5	4.94	-2734.3	-1359.46	17.47
31	177.99	98.8	4.94	-2768.8	-1447.03	8.17
32	180.17	317.3	108.86	-2388.7	-694.53	200.40
N1	874.36	636.6	1.10	61.4	1158.62	289.98
N3	388.33	405.7	1.08	-75.0	386.48	63.47
N5	415.80	1716.6	1.08	-139.1	977.96	642.73

$No.$	$\dot{m}$ $[kg/s]$	T $[°C]$	p $[bar]$	$\dot{H}$ $[MW]$	$\dot{S}$ $[kW/K]$	$\dot{E}$ $[MW]$
N10	415.80	1525.1	1.08	-248.7	920.08	549.87
N12	415.80	413.5	1.04	-839.8	419.62	102.94
N13	866.91	15.0	1.01	-132.5	77.66	-0.81
N14	415.80	347.3	1.00	-871.5	375.93	83.87
N15	415.80	217.2	1.00	-932.0	266.42	54.84
N16	413.75	226.6	1.06	-926.5	265.73	55.53
N17	413.75	150.0	1.01	-961.1	196.21	41.03
N18	98.51	306.7	11.14	15.5	13.98	29.01
N22	486.04	405.7	1.08	-93.8	483.73	79.44
N23	486.04	347.3	1.04	-125.3	440.58	60.39
N24	486.04	191.2	1.04	-207.4	288.24	22.16
N25	486.04	95.6	1.01	-256.3	174.77	5.99
N26	412.81	174.4	1.01	-956.0	217.52	34.90
N27	898.85	132.4	1.01	-1212.3	411.55	35.21
N28	866.91	306.7	11.14	136.7	123.04	255.31
N29	768.41	982.2	10.81	712.3	787.21	622.03
N30	7.45	15.0	20.00	-35.1	-49.97	386.09
N31	775.86	1333.8	10.48	673.4	1055.57	914.21
N33	768.41	306.7	11.14	121.2	109.05	226.30
N34	0.49	1721.6	1.08	0.7	1.39	0.75
N35	413.75	217.2	1.00	-930.8	264.19	51.70
N36	415.80	1721.6	1.08	-136.2	979.41	645.19
N37	27.96	15.0	1.08	-56.8	-105.51	782.94
N38	2.05	217.2	1.00	-1.2	2.23	3.14
N40	6.75	174.4	1.01	-75.1	-15.55	0.53
N41	5.81	15.0	1.01	-70.1	-15.37	0.27
N42	874.36	572.0	1.10	-3.9	1084.15	246.12

Table C.4 (Cont'd)

C.5 PFBC power plant

Table C.5: Mass flows, temperatures, pressures and flow rates of enthalpy, entropy and exergy for the PFBC base case.

$No.$	$\dot{m}$ $[kg/s]$	T $[°C]$	p $[bar]$	$\dot{H}$ $[MW]$	$\dot{S}$ $[kW/K]$	$\dot{E}$ $[MW]$
2	8.22	46.5	0.10	-111.3	-14.52	1.89
10	152.40	324.1	38.27	-1971.5	-444.52	177.37
13	154.89	145.6	4.23	-2378.7	-1181.26	15.42
14	21.70	42.9	15.86	-342.6	-191.23	0.20
15	152.37	149.0	220.63	-2335.7	-1160.33	18.98
17	128.49	42.9	15.86	-2028.8	-1132.36	1.20
18	2.52	149.0	220.63	-38.6	-19.19	0.31
19	141.27	42.2	0.08	-1923.7	-270.88	27.55
20	150.19	42.2	0.08	-2372.1	-1324.97	1.11
21	8.22	264.8	4.59	-106.7	-16.87	7.18
23	154.23	537.9	166.49	-1938.3	-462.52	239.99
26	62.39	340.8	206.51	-898.0	-362.27	33.66
27	62.39	364.5	201.68	-884.0	-339.93	41.17
28	62.39	364.5	196.86	-844.1	-277.17	63.04
29	62.39	405.0	196.86	-817.6	-236.66	77.81
30	62.39	540.8	173.75	-784.1	-188.18	97.39
34	92.50	340.8	206.51	-1331.4	-537.13	49.91
38	4.70	264.8	4.59	-61.0	-9.64	4.10
40	21.70	128.9	15.38	-334.8	-169.29	1.72
41	152.37	244.7	220.63	-2271.5	-1023.45	43.75
42	128.49	128.6	15.86	-1982.6	-1002.91	10.16
43	2.52	244.5	220.63	-37.6	-16.93	0.72
44	154.89	341.0	211.32	-2229.4	-899.59	83.62
48	154.89	540.8	173.75	-1946.6	-467.20	241.79
51	152.75	537.8	33.76	-1898.4	-325.57	220.84
54	150.19	42.3	15.86	-2371.9	-1324.87	1.37
59	13575.53	23.9	1.10	-215447.7	-123153.29	41.69
60	13575.53	29.7	1.01	-215120.0	-122060.15	54.42
61	92.50	540.8	173.75	-1162.5	-279.02	144.40
N1	104.00	15.0	1.01	-9.9	13.13	-0.06
N6	5.72	150.0	16.24	0.2	-1.64	1.46
N10	103.41	643.1	16.24	-173.9	182.42	568.92
N12	543.72	1266.4	13.93	-212.5	700.74	636.88
N13	552.87	151.0	1.05	-937.5	282.41	33.57

$No.$	$\dot{m}$ $[kg/s]$	T $[°C]$	p $[bar]$	$\dot{H}$ $[MW]$	$\dot{S}$ $[kW/K]$	$\dot{E}$ $[MW]$
N14	552.87	259.6	1.05	-873.3	417.11	58.96
N15	552.87	390.2	1.05	-793.6	550.85	100.14
N16	552.87	656.3	1.05	-619.3	769.35	211.46
N17	552.87	412.6	1.05	-779.7	571.53	108.13
N18	552.87	137.5	1.05	-945.4	263.63	31.14
N19	552.87	476.3	1.05	-739.7	627.24	132.03
N20	552.87	637.9	1.05	-635.8	752.77	199.80
N21	552.87	517.9	1.05	-713.3	661.58	148.58
N22	550.67	137.5	1.05	-920.3	267.44	26.96
N23	103.42	643.1	16.24	-173.9	182.44	569.12
N24	519.57	166.3	3.82	30.6	89.82	72.74
N25	103.42	860.2	16.24	-140.3	215.32	593.20
N26	82.09	342.8	16.24	20.1	9.05	28.28
N27	5.72	153.6	16.64	0.3	-1.63	1.48
N28	5.72	342.8	16.24	1.4	0.63	1.97
N31	73.35	15.0	1.01	-7.0	9.26	-0.04
N32	73.35	302.2	16.64	14.8	2.21	23.77
N33	73.35	508.0	16.64	31.2	26.61	33.17
N34	73.35	300.1	16.44	14.6	2.17	23.61
N35	345.76	15.0	1.01	-32.9	43.66	-0.19
N36	345.76	300.1	16.44	69.0	10.23	111.31
N37	5.61	300.1	16.44	1.1	0.17	1.80
N38	3.91	300.1	16.44	0.8	0.12	1.26
N39	3.54	166.3	3.82	0.2	0.61	0.50
N41	0.01	643.1	16.24	0.0	0.01	0.19
N43	3.42	176.7	15.48	-22.9	-3.81	0.21
N44	4.62	318.3	15.48	-27.1	-3.31	0.71
N45	95.27	860.0	15.48	-131.4	80.60	72.06
N46	90.64	860.0	15.48	-107.1	80.56	69.49
N47	5.72	562.0	16.64	2.8	2.50	2.81
N48	10.88	860.2	16.24	-5.6	20.43	225.55
N49	32.60	15.0	1.01	-66.2	-123.00	912.70
N51	2.20	137.5	1.05	-25.1	-3.81	4.18
N52	87.81	342.8	16.24	21.5	9.68	30.25
N54	90.64	849.0	15.48	-108.3	79.51	68.60
N55	87.81	312.8	16.24	18.7	4.98	28.77
N56	87.81	300.1	16.44	17.5	2.60	28.27
N57	519.57	79.4	3.56	-15.7	-16.77	57.20
N58	549.33	781.5	1.93	-539.0	753.08	296.03

Table C.5 (Cont'd)

C.6 IGCC power plant

Table C.6: Mass flow rate, temperature, pressure and flow rates of enthalpy, entropy and exergy for each stream of the IGCC power plant.

$No.$	$\dot{m}$ $[kg/s]$	T $[^\circ C]$	p $[bar]$	$\dot{H}$ $[MW]$	$\dot{S}$ $[kW/K]$	$\dot{E}$ $[MW]$
1	100.82	271.7	22.1	-340.79	68.64	447.90
6	7.75	328.9	126.8	-105.33	-34.44	7.41
8	0.62	328.9	126.8	-8.41	-2.75	0.59
10	8.37	330.1	128.8	-111.39	-33.31	9.24
12	0.08	330.1	128.8	-1.09	-0.44	0.04
13	6.36	317.8	7.9	-81.91	-13.48	6.32
15	309.53	15.0	1.0	-29.46	39.14	-0.19
16	67.94	33.3	0.1	-930.50	-133.85	8.96
17	92.20	28.4	0.1	-1461.49	-830.52	0.33
18	4.19	129.3	2.6	-55.57	-10.03	2.92
19	60.18	537.8	104.6	-752.60	-164.39	92.67
20	243.02	15.0	1.0	-23.13	30.73	-0.15
23	15.48	92.2	34.0	0.87	-10.49	5.85
26	0.51	176.8	9.3	-6.86	-1.70	0.41
27	7.08	176.8	9.3	-95.09	-23.53	5.61
28	0.43	325.9	122.0	-6.18	-2.53	0.21
34	165.89	615.6	1.0	-283.80	217.65	59.92
35	165.89	526.2	1.0	-301.80	196.31	48.07
36	177.94	533.1	1.0	-322.23	212.41	52.52
38	343.83	328.7	1.0	-705.02	292.77	53.01
39	343.83	253.7	1.0	-734.18	241.03	38.76
40	343.83	215.0	1.0	-748.99	211.83	32.36
41	343.83	193.3	1.0	-757.25	194.53	29.09
42	343.83	174.9	1.0	-764.24	179.26	26.51
43	343.83	163.5	1.0	-768.54	169.52	25.00
44	343.83	137.3	1.0	-778.39	146.25	21.86
45	46.59	235.7	36.9	-696.68	-315.15	11.85
46	4.53	129.3	2.6	-60.03	-10.84	3.15
47	72.74	248.2	36.9	-957.33	-240.57	76.48
48	72.74	432.2	36.2	-922.01	-181.32	94.72
49	177.94	615.6	1.0	-304.41	233.45	64.28
50	31.03	409.6	17.2	9.76	6.19	12.04
53	10.37	310.7	114.0	-151.13	-63.03	4.59

$No.$	$\dot{m}$ $[kg/s]$	T $[°C]$	p $[bar]$	$\dot{H}$ $[MW]$	$\dot{S}$ $[kW/K]$	$\dot{E}$ $[MW]$
54	45.67	310.7	114.0	-665.22	-277.43	20.22
55	10.37	320.7	114.0	-137.67	-40.36	11.52
60	1.87	154.8	4.1	-24.68	-4.64	1.44
62	309.53	409.6	17.2	97.37	61.72	120.14
63	243.02	409.6	17.2	76.45	48.45	94.33
64	16.04	311.5	129.3	-233.65	-97.46	7.14
66	8.45	311.5	129.3	-123.06	-51.33	3.76
69	8.45	318.0	129.3	-122.72	-50.76	3.93
70	16.32	311.7	129.3	-237.70	-99.12	7.27
71	16.32	327.9	125.3	-216.97	-64.58	18.05
72	16.04	327.9	125.3	-213.26	-63.48	17.74
74	0.28	322.9	125.3	-4.05	-1.66	0.14
75	0.28	323.4	129.3	-4.05	-1.66	0.14
76	27.66	238.5	129.3	-413.23	-186.92	7.39
78	43.70	327.9	125.3	-626.49	-248.66	24.63
79	27.66	129.3	2.6	-426.74	-215.69	2.17
81	17.15	238.5	129.3	-256.15	-115.87	4.58
82	17.15	129.3	2.6	-264.52	-133.70	1.35
84	10.80	311.5	129.3	-157.30	-65.61	4.81
87	10.80	178.0	129.3	-164.28	-79.07	1.71
89	15.39	131.0	129.3	-237.20	-119.93	1.43
90	10.00	28.6	22.5	-158.49	-90.07	0.06
91	29.00	116.1	22.5	-448.99	-230.30	1.89
92	19.00	116.1	22.5	-294.17	-150.88	1.24
94	19.00	28.6	22.5	-301.12	-171.13	0.12
95	0.72	124.9	22.4	-11.21	-5.82	0.11
98	1.84	145.6	21.2	-28.18	-14.00	0.19
100	66.52	392.5	16.9	19.70	11.80	25.01
101	66.52	178.0	16.9	4.64	-15.48	17.81
103	38.54	113.3	26.4	-120.91	78.25	453.55
104	66.52	35.0	16.9	-5.98	-44.13	15.45
105	55.65	169.5	22.3	-357.03	42.91	433.39
107	79.00	217.7	24.4	-1188.03	-547.45	17.21
112	79.00	123.0	25.9	-1220.77	-621.48	5.80
115	60.00	124.9	22.4	-932.91	-485.26	5.21
117	0.42	40.0	23.8	-6.58	-3.69	0.02
121	10.00	116.1	22.5	-154.82	-79.41	0.65
122	20.00	545.8	7.9	-247.82	-28.52	25.58
128	66.52	409.6	17.2	20.93	13.26	25.82

Table C.6 (Cont'd)

$No.$	$\dot{m}$ $[kg/s]$	T $[^\circ C]$	p $[bar]$	$\dot{H}$ $[MW]$	$\dot{S}$ $[kW/K]$	$\dot{E}$ $[MW]$
129	96.01	69.9	21.2	-1505.10	-813.40	2.30
130	96.01	99.9	20.1	-1493.03	-779.63	4.64
131	75.04	99.9	20.1	-1166.87	-609.32	3.63
132	20.98	99.9	20.1	-326.18	-170.33	1.01
134	20.98	99.9	22.5	-326.18	-170.32	1.02
138	79.00	162.9	25.4	-1207.29	-589.05	9.94
139	79.00	175.0	24.9	-1203.12	-579.62	11.38
140	20.00	229.7	7.9	-261.31	-49.31	18.09
142	0.51	176.8	9.3	-7.78	-3.74	0.07
143	7.08	176.8	9.3	-99.25	-32.79	4.11
148	37.38	222.4	22.4	-113.12	92.42	419.96
149	55.65	246.5	22.3	-350.05	57.45	436.18
150	38.54	215.6	26.9	-115.24	90.95	455.56
152	39.01	179.8	24.8	-123.55	87.48	454.39
153	312.81	1412.8	16.9	-274.10	418.74	443.60
155	37.38	40.0	23.3	-122.68	67.76	417.50
156	37.38	100.2	22.9	-119.53	77.27	417.92
159	211.99	409.6	17.2	66.69	42.27	82.28
160	66.52	15.0	1.0	-6.33	8.41	-0.04
162	63.20	50.2	21.2	-995.92	-550.96	0.82
163	5500.00	21.8	1.0	-88273.57	-52447.37	15.84
165	63.20	28.6	22.5	-1001.62	-569.21	0.38
166	67.94	33.2	0.1	-1075.65	-607.58	0.31
167	39.01	123.8	24.3	-126.70	80.36	453.28
170	0.04	40.0	23.3	-0.14	0.08	0.46
172	0.04	40.0	23.3	-0.14	0.08	0.46
173	92.20	28.6	22.5	-1461.23	-830.41	0.56
174	177.94	364.6	1.0	-357.55	163.31	31.35
175	165.89	361.1	1.0	-334.01	151.21	28.86
176	39.01	178.9	25.3	-123.55	87.06	454.53
180	5500.00	21.8	2.8	-88272.18	-52446.90	17.09
181	45.67	153.3	118.1	-699.50	-345.35	5.52
182	45.67	195.0	116.1	-691.24	-326.86	8.45
183	60.18	382.0	37.0	-769.83	-160.94	74.45
184	30.28	129.3	2.6	-467.08	-236.08	2.38
186	44.81	238.5	129.3	-669.38	-302.79	11.97
187	61.40	540.6	108.5	-767.78	-168.47	94.95
188	61.40	432.2	111.2	-785.78	-192.89	83.99
189	45.67	131.1	120.2	-703.80	-355.74	4.21

Table C.6 (Cont'd)

$No.$	$\dot{m}$ $[kg/s]$	T $[°C]$	p $[bar]$	$\dot{H}$ $[MW]$	$\dot{S}$ $[kW/K]$	$\dot{E}$ $[MW]$
191	343.83	261.9	1.0	-731.04	246.96	40.20
193	46.59	165.0	38.0	-711.49	-346.47	6.06
194	1.78	129.3	2.6	-27.48	-13.89	0.14
197	1.76	245.7	36.9	-23.23	-5.86	1.85
198	0.76	25.5	3.4	0.00	-0.14	0.08
199	0.34	129.3	2.6	-4.46	-0.81	0.24
200	24.25	15.0	1.0	-385.83	-223.10	0.06
201	45.17	294.9	22.5	8.03	-10.02	16.78
202	45.17	320.0	22.1	9.26	-7.63	17.32
206	67.61	192.4	2.6	-887.01	-141.10	50.08
208	15.48	25.5	3.4	-0.01	-3.99	3.10
210	72.74	540.6	36.2	-904.19	-157.81	105.77
211	1.11	40.0	2.5	-2.53	0.88	33.59
212	39.01	78.3	25.8	-129.22	72.56	453.04
213	43.28	324.0	119.0	-574.98	-170.09	47.83
215	1.28	40.0	23.8	-20.40	-11.82	0.03
216	38.57	40.0	23.8	-125.48	68.11	452.21
218	343.83	615.6	1.0	-588.21	451.10	124.20
220	343.83	105.0	1.0	-790.47	117.85	17.97
221	5500.00	27.3	1.0	-88127.02	-51955.20	20.56
222	38.59	40.0	23.8	-125.82	68.07	452.22
224	44.81	235.7	36.9	-670.05	-303.10	11.39
225	61.40	320.7	114.0	-817.99	-244.18	66.56
226	46.59	130.0	39.0	-718.48	-363.09	3.87
227	1.78	235.7	36.9	-26.63	-12.05	0.45
228	4.53	129.3	2.6	-69.89	-35.32	0.36
229	67.94	192.1	2.6	-891.48	-141.90	50.31
231	4.37	450.6	60.0	1.99	-1.20	2.44
232	1.23	537.8	104.6	-15.36	-3.35	1.89
N1	38.54	330.0	27.4	-108.83	102.41	458.66
N2	21.73	330.0	27.4	-61.37	57.75	258.65
N7	0.75	70.8	3.4	0.04	-0.16	0.10
N16	60.27	330.0	27.4	-170.20	160.16	717.31
N17	0.10	330.0	27.4	0.03	0.07	3.34
N19	20.01	121.6	1.0	-7.10	10.65	583.69
N21	21.73	353.9	30.4	-60.61	58.10	259.32
N23	38.64	1400.0	28.0	-43.00	164.12	510.03

Table C.6 (Cont'd)

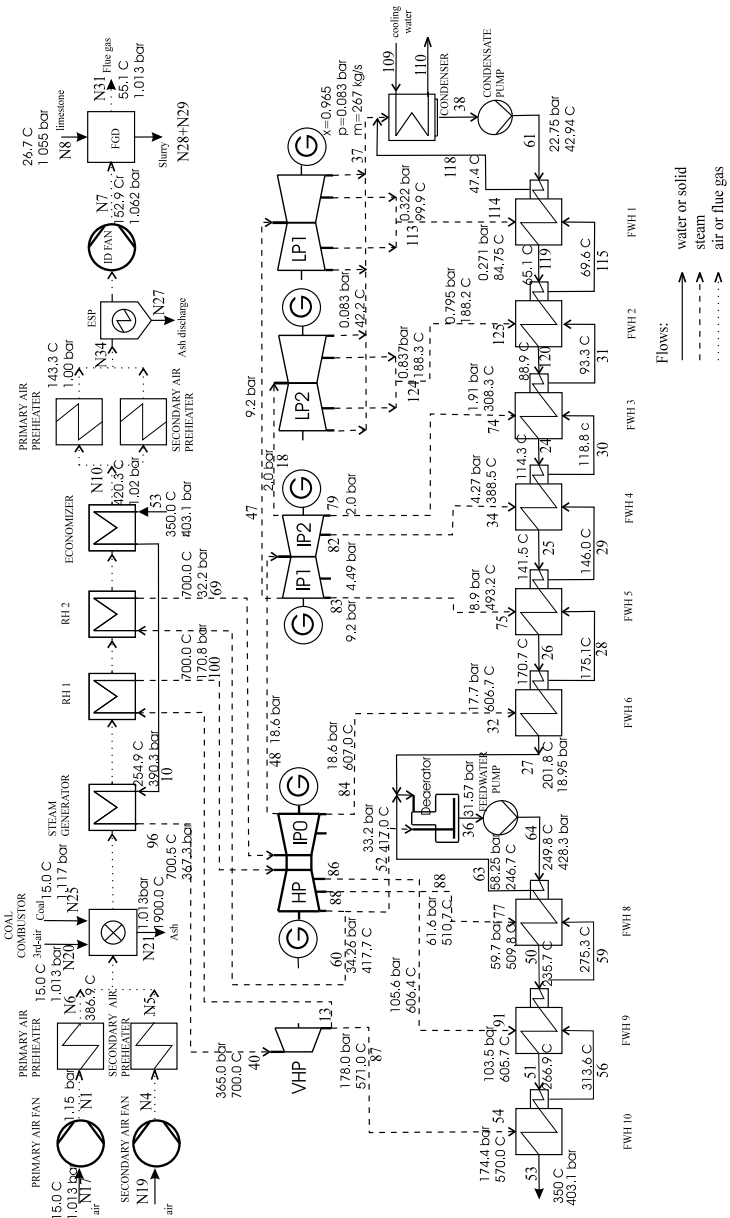

Figure C.1: Flowsheet for the supercritical steam power plant "700 °C".

D. Thermodynamic Analyses

D.1 Conventional steam power plant

Table D.1: Exergy destruction rate and exergy destruction ratio for the conventional steam power plant fired with Illinois No. 6 coal (net power output 507.6 MW).

Component	$\dot{E}_{D,k}$ or $\dot{E}_{L,k}$ (MW)	$\frac{\dot{E}_{D,k}}{\dot{E}_{F,tot}}$ or $\frac{\dot{E}_{L,k}}{\dot{E}_{F,tot}}$ (%)
Coal combustion	397.50	28.04
Steam generator	280.59	19.79
Flue gas	60.63	4.28
Condenser	58.01	4.09
Steam turbine	38.63	2.73
FWH system	18.69	1.32
Solid discharge	15.94	1.12
Remaining components	11.11	0.78
Blowdown	1.67	0.12
Sum of the above	882.76	62.27

D.2 Supercritical steam power plant "580°C"

Table D.2: Exergy destruction rate and exergy destruction ratio for the SC power plant with 290 bar/582°C/580°C/580°C (the values in parentheses are from the conventional steam power plant).

Component	$\dot{E}_{D,k}$ or $\dot{E}_{L,k}$ (MW)	$\frac{\dot{E}_{D,k}}{\dot{E}_{F,tot}}$ or $\frac{\dot{E}_{L,k}}{\dot{E}_{F,tot}}$ (%)
Coal combustion	354.18 (397.50)	27.33 (28.04)
Steam generator	225.32 (280.59)	17.39 (19.79)
Flue gas	59.55 (60.63)	4.60 (4.28)
Condenser	48.50 (58.01)	3.74 (4.09)
Steam turbine	26.83 (38.63)	2.07 (2.73)
FWH system	20.43 (18.69)	1.58 (1.32)
Solid discharge	14.62 (15.94)	1.13 (1.12)
Remaining components	10.61 (11.11)	0.82 (0.78)
Blowdown	1.18 (1.67)	0.09 (0.12)
Sum of the above	761.21 (882.76)	58.75 (62.27)

D.3 Supercritical steam power plant "700°C"

Table D.3: Exergy destruction rate and exergy destruction ratio for the supercritical steam power plant with 350 bar/700°C/700°C/700°C (the values in parentheses are for the supercritical steam power plant "580°C").

Component	$\dot{E}_{D,k}$ or $\dot{E}_{L,k}$ (MW)	$\frac{\dot{E}_{D,k}}{\dot{E}_{F,tot}}$ or $\frac{\dot{E}_{L,k}}{\dot{E}_{F,tot}}$ (%)
Coal combustion	329.45 (354.18)	27.33 (27.33)
Steam generator	169.39 (225.32)	14.05 (17.39)
Flue gas	55.36 (59.55)	4.59 (4.60)
Condenser	42.01 (48.50)	3.48 (3.74)
Steam turbine	24.09 (26.83)	2.00 (2.07)
FWH system	25.97 (20.43)	2.15 (1.58)
Solid discharge	13.60 (14.62)	1.13 (1.13)
Remaining components	9.8 (10.61)	0.81 (0.82)
Blowdown	1.37 (1.18)	0.11 (0.09)
Sum of the above	671.04 (761.21)	55.66 (58.75)

Table D.4: The key parameters and thermodynamic results for the SC "580 °C" and the SC "700 °C" power plants.

	SC "580 °C"	SC "700 °C"
POWER SUMMARY		
Net system power output, MW	507.6	507.8
Net system efficiency, % HHV	40.05	43.06
Net system efficiency, % LHV	41.88	45.03
Exergetic efficiency, % exergy input	39.17	42.12
Auxiliaries, % in generator output	6.94	7.37
STEAM CYCLE		
Throttle pressure, bar	290	365
Throttle temperature, °C	582	700
Reheat temperatures, °C	580	700
1st reheat pressure, bar	94	118
2nd reheat pressure, bar	19	34
Number of feedwater heating stages	10	10
Expansion end line pressure, bar	0.083	0.083
Exhaust steam quality, %	0.962	0.965
Feedwater temperature to SG, °C	300	350
Gas temperature at economizer exit,°C	420	420
SG economizer ΔT_{pinch}, °C	120	70
Flue gas temperature leaving SG, °C	143	143
Air preheating temperature, °C	386	386
Excess air for coal combustion, %	26.8	26.8
Main steam mass flow rate, kg/s	380	356
Boiler flue gas mass flow rate, kg/s	574	534

D.4 HIPPS

Table D.5: Exergy destruction rates and exergy destruction ratios for the HIPPS and the fully coal-fired HIPPS (in parentheses), respectively.

Component	$\dot{E}_{D,k}$ or $\dot{E}_{L,k}$ [MW]		$\frac{\dot{E}_{D,k}}{\dot{E}_{F,tot}}$ or $\frac{\dot{E}_{L,k}}{\dot{E}_{F,tot}}$ [%]	
Gas turbine	153.93	(59.45)	13.17	(4.89)
Coal combustion	202.93	(303.83)	17.37	(24.98)
High temperature furnace	94.84	(118.03)	8.12	(9.71)
HRSG	41.96	(42.77)	3.59	(3.52)
Flue gas	40.89	(49.75)	3.50	(4.09)
Condenser	22.16	(23.20)	1.90	(1.91)
Steam turbine	16.43	(17.12)	1.41	(1.41)
Solid discharge	4.43	(7.16)	0.38	(0.59)
Feedwater and Deaerator sys.	1.05	(0.83)	0.09	(0.07)
Sum of the above items	578.60	(622.15)	49.52	(51.16)
Destruction with combustion	294.38	(303.68)	25.19	(24.97)
Total system exergy input	1168.50	(1216.09)	100.00	(100.00)

D.5 PFBC power plant

Table D.6: Exergy destruction rate and exergy destruction ratio for the PFBC power plant.

Component	$\dot{E}_{D,k}$ or $\dot{E}_{L,k}$ [MW]	$\frac{\dot{E}_{D,k}}{\dot{E}_{F,tot}}$ or $\frac{\dot{E}_{L,k}}{\dot{E}_{F,tot}}$ [%]
Gas turbine	161.83	17.73
Carbonizer	134.34	14.72
PFBC	89.42	9.80
Flue gas	29.53	3.23
Condenser	28.81	3.16
Steam turbine	14.70	1.61
HRSG	14.48	1.59
Solid discharge	5.40	0.59
FW heating and deaerating	1.20	0.13
Sum of the above items	479.72	52.55
Destruction in carb./comb.	292.46	32.04

D.6 IGCC power plant

Table D.7: Exergy destruction rate and exergy destruction ratio for the IGCC power plant.

Component	$\dot{E}_{D,k}$ or $\dot{E}_{L,k}$ (MW)	$\frac{\dot{E}_{D,k}}{\dot{E}_{F,tot}}$ or $\frac{\dot{E}_{L,k}}{\dot{E}_{F,tot}}$ (%)
Coal preparation	1.77	0.30
Gasification process	76.39	12.96
High temperature syngas cooling	14.26	2.42
Solid removal	1.86	0.32
HCN conversion process	1.44	0.24
Acid gas removal	0.19	0.03
Air separation unit	4.24	0.72
Syngas saturation	7.51	1.27
Heat recovery in gasification island	0.86	0.15
Steam turbine	5.60	0.95
HRSG	11.28	1.91
Feedwater heating and deaerating	2.57	0.44
Gas turbine	130.07	22.06
Sour water stripping	0.01	0.00
Sulfur recovery plant	10.42	1.77
Steam headers	1.20	0.20
Condenser	10.04	1.70
Flue gas	17.97	3.05
Gas vented	5.73	0.97
Blowdown	22.52	3.82
Solid discharge	4.94	0.84
Sum of the above items	330.86	56.11
Destruction in gasif./comb.	168.57	28.59

E. Calculation of the total capital requirement

E.1 Component scaling exponents and corresponding capacity parameters

Table E.1: Scaling exponents for the purchased-equipment costs and the corresponding capacity parameters used in this study.

Equipment	Capacity parameter	Scaling exponent
Combustion gas turbine	Net output	0.89
Steam turbine (condensing)	Power	0.90
Feedwater heater	Surface	0.66
Heat exchanger	Surface	0.66
Ash handling	Ash mass flow rate	0.60
Coal and sorbent handling	Coal mass flow rate	0.60
Coal and sorbent preparation and feed	Coal mass flow rate	0.68
Flue gas cleanup	Flue gas mass flow rate	0.60
PFBC pressure vessel	Gas mass flow rate	0.55
Cooling tower	Cooling water flow rate	0.93

E.2 Total capital requirement

The total capital requirement takes into account the following items:

- Total cash expended (total plant cost),
- Allowance for funds used during construction,
- Cost of land,
- Organization and startup costs,
- Inventory capital.

E.2.1 Total plant cost

The total plant cost consists of Total Direct Costs (TDC) and Total Indirect Costs (TIC).

The TDC for the four types of power plants are made available from different sources. All these cost data are brought to a reference year (here middle 1998), with the aid of the Chemical Engineering (CE) Plant Cost Index. The TDC of the power plants under study are presented in Appendices F, G, H, and I.

The TIC consists of four cost items. The first two items are the construction costs & contractor's profit and the engineering & construction management service, estimated at 12% and 15% of the TDC, respectively. 15% of these two items plus 15% of the TDC results in the third item, the project contingency. The process contingency, the fourth item, is set equal to zero for all types of power plants considered excluding the HIPPS. Because of the high temperature furnace, 14.825 million dollars (end-1993 dollars) are included as the process contingency, which is 20% of the purchased-equipment cost of the HTF.

The total cash expended is the sum of the escalated fractions of total plant cost using the assumed costs of money. It is assumed that the 34%, 33%, and 33% of the TPC are expended in the first, the second, and the third year of design and construction period, when the construction lasts for 3 years. In case this period is 4 years, these percentages remain valid for the second, the third, and the fourth year, respectively, and no cash is expended in the first year of design and construction.

E.2.2 Allowance for funds used during construction

The allowance for funds used during construction (AFUDC) is calculated according to the method presented in Ramachandran (1993). Hence, the total plant cost is first divided among the construction years and then escalated accordingly. Note that the system-financing fractions, 50% for the common equity and and 50% for the debt, are valid and the AFUDC is calculated for the two types of financing separately. We assume that the AFUDC for the common equity is to be recovered at the end of the plant economic life.

E.2.3 Cost of land

For all the power plants this cost is assumed as 500,000 dollars (mid-1998 dollars), paid at the beginning of the design and construction period.

E.2.4 Organization and startup costs

The organization and startup costs include the following items and are due middle of the last year of design and construction period:

- One month of fixed operating and maintenance costs,
- One month of variable operating costs at full load,
- One week of fuel at full load,
- 2 % of the plant facilities investment.

E.2.5 Working capital

The working capital is assumed by adding up:

- 2 months of fuel costs at full load,
- 2 months of variable operating costs at full load,
- 3 months of labor costs, and
- 25 % of the sum of the above three items.

The working capital is due at the end of the last year of design and construction period.

F. Cost estimation for the steam power plants

The purchased-equipment costs for the conventional PCC power plant are derived based on the report by Becker et al. (1994). For the cost estimation of the SC power plants, the principles by Guthrie (1969) are referred to as well.

F.1 Conventional steam power plant

Table F.1: Breakdown of the total direct costs for the conventional steam power plant (in mid-1993 thousand-dollars).

Coal and sorbent handling system	13002
Coal and sorbent preparation and feed system	15693
Feedwater and miscellaneous system and equipment	19483
PC boiler and accessories	52110
Flue gas cleanup	48983
Combustion turbine and accessories	0
Waste heat boiler, ducting and stack	15095
Steam turbine generator and auxiliaries	54835
Cooling water system	8689
Ash/spent sorbent recovery and handling	6172
Accessory electric plant	14071
Purchased-equipment installation	182270
Instrumentation and control	9758
Improvements on site	3073
Buildings and structures	18692
Total Direct Costs	461926

Table F.2: Breakdown of the total capital investment (in mid-1998 thousand-dollars) for the conventional steam power plant.

Total plant cost	715737
Cost of land	480
Organization and startup costs	17947
Working capital	17012
AFUDC	79611
Total capital investment	830787
Total capital requirement (in mixed-dollars)	932304

Table F.3: Case specific economic parameters and costs for the conventional steam power plant.

Plant service date	Jan. 2003
Average plant-capacity factor	0.85
Labor positions per shift	30
Annual direct labor costs (in mid-1998 thousand-dollars)	7301
Monetary units in mid-2003 thousand-dollars	
Annual fixed operating and maintenance	16358
Annual variable operating and maintenance (85% of design capacity)	14333
Mass flow of coal (kg/s)	50.636
Cost of coal (in mid-2003 thousand-dollars)	64100

Table F.4: Calculated key economic parameters for the conventional steam power plant.

Net plant power output (MW)	508
Purchased-equipment costs (mid-1998, $/kW)	531
Total plant cost (mid-1998, $/kW)	1410
Total capital requirement (mixed-dollar, $/kW)	1837
20-year Levelized cost of electricity (cent/kWh)	6.81

F.2 SC steam power plant "580°C"

Table F.5: Breakdown of the total direct costs for the SC "580°C" base case (in mid-1993 thousand-dollars).

Coal and sorbent handling system	12320
Coal and sorbent preparation and feed system	14764
Feedwater and miscellaneous system and equipment	28494
PC boiler and accessories	95140
Flue gas cleanup	46412
Combustion turbine and accessories	0
Waste heat boiler, ducting and stack	15095
Steam turbine generator and auxiliaries	69113
Cooling water system	7371
Ash/spent sorbent recovery and handling	5846
Accessory electric plant	14071
Purchased-equipment installation	205629
Instrumentation and control	9758
Improvements on site	3073
Buildings and structures	18692
Total Direct Costs	545776

Table F.6: Case specific economic parameters and costs for the SC "580°C" base case.

Plant service date	Jan. 2004
Average plant-capacity factor	0.85
Labor positions per shift	30
Annual direct labor costs (in mid-1998 thousand-dollars)	7301
Monetary units in mid-2004 thousand-dollars	
Annual fixed operating and maintenance	18361
Annual variable operating and maintenance (85% of design capacity)	14048
Mass flow of coal (kg/s)	46.290
Cost of coal (in mid-2004 thousand-dollars)	60123

F.3 SC steam power plant "700°C"

Table F.7: Breakdown of the total direct costs for the SC steam power plant "700°C" (in mid-1993 thousand-dollars).

Coal and sorbent handling system	11797
Coal and sorbent preparation and feed system	14056
Feedwater and miscellaneous system and equipment	30131
PC boiler and accessories	109474
Flue gas cleanup	44452
Combustion turbine and accessories	0
Waste heat boiler, ducting and stack	15095
Steam turbine generator and auxiliaries	72898
Cooling water system	6410
Ash/spent sorbent recovery and handling	5601
Accessory electric plant	14071
Purchased-equipment installation	210407
Instrumentation and control	9758
Improvements on site	3073
Buildings and structures	18692
Total Direct Costs	565916

Table F.8: Case specific economic parameters and costs for the SC steam power plant "700°C".

Plant service date	Jan. 2004
Average plant-capacity factor	0.85
Labor positions per shift	30
Annual direct labor costs (in mid-1998 thousand-dollars)	7301
Monetary units in mid-2004 thousand-dollars	
Annual fixed operating and maintenance	18723
Annual variable operating and maintenance (85% of design capacity)	13668
Mass flow of coal (kg/s)	43.063
Cost of coal (in mid-2004 thousand-dollars)	55932

Table F.9: Levelized annual costs and TRR in current and constant dollars for levelization time period of 20 and 30 years for the SC steam power plant "700°C". All values are in million dollars.

	Current Dollars:	Constant Dollars:
20-year period		
Coal costs	66.7 (23.4%)	56.3 (27.2%)
O&M costs	38.4 (13.5%)	32.4 (15.6%)
Carrying Charges	180.0 (63.1%)	118.7 (57.2%)
TRR	285.0 (100.%)	207.4 (100.%)
30-year period		
Coal costs	70.3 (25.0%)	56.5 (29.0%)
O&M costs	40.3 (14.3%)	32.4 (16.6%)
Carrying Charges	170.5 (60.7%)	105.9 (54.4%)
TRR	281.1 (100.%)	194.8 (100.%)

G. Cost estimation for the HIPPS

For the HIPPS base case, the total direct costs are provided by Klara (1994a) and Klara (1994b). The breakdown of the total direct costs for this base case is given in Table G.1 (in end-1993 thousand-dollars).

Table G.1: Breakdown of the total direct costs for the HIPPS base case (in end-1992 thousand-dollars).

Coal handling system	13255
Coal train unloading system	8680
HTF material	74540
HTF erection	37060
Wet flue gas desulfurization	62612
Electrostatic precipitator	11111
Combustion turbine and accessories	72450
Waste heat boiler, ducting and stack	17100
Steam turbine generator and auxiliaries	33850
Cooling water system	9500
Accessory electric plant	31479
Mechanical installation	31070
Electrical/I&C installation	15985
Balance of mechanical equipment	22500
Instrumentation and control	7135
Improvements on site	0
Buildings and structures	36410
Total Direct Costs	484737

Table G.2 shows the breakdown of the total capital investment for the HIPPS base case.

The case specific economic parameters and costs for the HIPPS base case are presented in Table G.3.

Table G.2: Breakdown of the total capital investment (in mid-1998 thousand-dollars) for the HIPPS base case.

Total plant cost	776722
Cost of land	500
Organization and startup costs	19332
Working capital	17595
AFUDC	80534
Total capital investment	894683
Total capital requirement (in mixed-dollars)	1011232

Table G.3: Case specific economic parameters and costs for the HIPPS base case.

Plant service date	Jan. 2004
Average plant-capacity factor	0.80
Labor positions per shift	45
Annual direct labor costs (in mid-1998 thousand-dollars)	10951
Monetary units in mid-2004 thousand-dollars	
Annual fixed operating and maintenance	22564
Annual variable operating and maintenance (80% of design capacity)	10541
Mass flow of coal (kg/s)	27.965
Mass flow of natural gas (kg/s)	7.45
Cost of coal (in mid-2004 thousand-dollars)	34185
Cost of natural gas	33280

H. Cost estimation for the PFBC power plant

The case specific economic parameters and costs for the base case of the PFBC power plant are presented in Table H.1.

Table H.1: Case specific economic parameters and costs for the base case of the PFBC power plant.

Plant service date	Jan. 2003
Average plant-capacity factor	0.80
Labor positions per shift	30
Annual direct labor costs (in mid-1998 thousand-dollars)	7301
Monetary units in mid-2003 thousand-dollars	
Annual fixed operating and maintenance	15418
Annual variable operating and maintenance (80% of design capacity)	10772
Mass flow of coal (kg/s)	32.6
Cost of coal (mid-2003 thousand-dollars)	38840

The breakdown of the total direct costs for the base case of the PFBC power plant is given in Table H.2 (in mid-1993 thousand-dollars). These costs are based on cost information extracted from Buchanan et al. (1994), (Klara (1994a), Price (1992), and Bechtel (1995)).

Table H.3 shows the breakdown of the total capital investment for the base case of the PFBC power plant.

Table H.2: Breakdown of the total direct costs for the base case of the PFBC power plant (in mid-1993 thousand-dollars).

Coal and sorbent handling system	13325
Coal and sorbent preparation and feed system	22139
Feedwater and miscellaneous system and equipment	2143
PFBC pressure vessel	2500
PFBC boiler	7627
PFBC economizer	0
PFBC accessories	1700
Carbonizer and accessories	25373
Flue gas cleanup (ESP)	12321
Combustion turbine and accessories	44731
HRSG	23772
Ducting and stack	3564
Steam turbine generator and auxiliaries	28861
Cooling water system	4198
Ash/spent sorbent recovery and handling	7757
Accessory electric plant	11815
Purchased-equipment installation	129750
Instrumentation and control	18081
Improvements on site	7403
Buildings and structures	36397
Total Direct Costs	403457

Table H.3: Breakdown of the total capital investment (in mid-1998 thousand-dollars) for the base case of the PFBC power plant.

Total plant cost	625143
Cost of land	480
Organization and startup costs	15283
Working capital	11642
AFUDC	69534
Total capital investment	722082
Total capital requirement (in mixed-dollars)	810334

I. Cost estimation for the IGCC power plant

The breakdown of the total direct costs for the IGCC power plant is given in Table I.1 (in mid-1995 thousand-dollars).

Table I.1: Breakdown of the total direct costs for the IGCC power plant (in mid-1995 thousand-dollars).

Coal reclaiming and transfer	2718
Air separation unit	30686
Gasification	115191
GT, ST generator, HRSG and auxiliaries	142233
Stack, saturator, and support systems	10396
Relief & blowdown systems	178
Compressed air systems	232
Cooling water system	6025
Raw water supply and treatment	136
Fire protection	692
Sewers and effluent treating	3346
Purchased-equipment installation	20513
Interconnecting piping	9029
Electrical switchyard/distribution	11971
Instrumentation and control	6535
Improvements on site	1456
Buildings and structures	3388
Total Direct Costs	364725

Table I.2 shows the breakdown of the total capital investment (in mid-1998 thousand-dollars) for the IGCC power plant. The case specific economic parameters and costs for the IGCC power plant are presented in Table I.3.

Table I.2: Breakdown of the total capital investment (in mid-1998 thousand-dollars) for the IGCC power plant.

Total plant cost	532653
Cost of land	500
Organization and startup costs	13369
Working capital	10331
AFUDC	55277
Total capital investment	612130
Total capital requirement (in mixed-dollars)	708772

Table I.3: Case specific economic parameters and costs for the IGCC power plant.

Plant service date	Jan. 2004
Average plant-capacity factor	0.85
Labor positions per shift	45
Annual direct labor costs (in mid-1998 thousand-dollars)	10951
Monetary units in mid-2004 thousand-dollars	
Annual fixed operating and maintenance	18964
Annual variable operating and maintenance (85% of design capacity)	10006
Mass flow of coal (kg/s)	20.8
Cost of coal (in mid-2004 thousand-dollars)	27016

Bibliography

Ahrendts, J., 1977. Die Exergie chemisch reaktionsfähiger Systeme. Tech. Rep. VDI-Forschungsheft 579, Verein Deutscher Ingenieure.

Alderliesten, P. T., 1990. System Study - High Temperature Gas Cleaning at IGCC Systems. *Joint system study performed by ECN, KEMA, Stork Boilers and TNO.*

Ambrose, S., Green, C. L., Dryden, R. & Provol, S. J., 1993. The Midwest Power PCFB demonstration projects - AHLSTROM PYROFLOW first and second generation pressurized circulating fluidized bed (PCFB) technology. *Proceedings of the American Power Conference*, pp. 133–139.

American Wind Energy Association, 1999. Global Wind Energy Market Report.

Aspen Plus User Guide - Release 9.3-1. Aspen Technology, Inc.

Baehr, H. D., 1979. Die Exergie der Brennstoffe. *Brennstoff-Wärme-Kraft* **31**, pp. 292–297.

Bechtel, 1995. IGCC Process Evaluation for Korea Electric Power Corporation Research Center. Tech. Rep., Bechtel Corporation, Gaithersburg, Maryland.

Becker, D. F., Buchanan, T. L., Goldstein, H. N., Harvey, L. E. & Rubow, L. N., 1994. Clean Coal Reference Plants: Pulverized Coal Boiler with Flue Gas Desulfurization. Tech. Rep. 3008, Gilbert/Commonwealth, Inc.

Beer, J. M. & Garland, R. V., 1997. A coal-fueled combustion turbine cogeneration system with topping combustion. *J. of Eng. for Gas Turbine and Power* **119**, pp. 85–92.

Bejan, A., Tsatsaronis, G. & Moran, M., New York, 1996. Thermal Design & Optimization. John Wiley & Sons, Inc.

Birol, F. & Argiri, M., 1999. World energy prospects to 2020. *Energy* **24**, pp. 905–918.

Buchanan, T. L., Goldstein, H. N., Harvey, L. E., Rubow, L. N. & Zaharchuk, R., 1994. Clean Coal Reference Plants: Pressurized Fluid Bed Combustor. Tech. Rep. 3009, Gilbert/Commonwealth, Inc.

Campbell, W. M., Cho, J. C., Domahidy, H., Gbordzoe, E. A., Goebel, K. W., Lin, Y. Y. & O'Donnell, J. J., 1990. Pressurized Fluid-bed Combustion Alternate Advanced Concepts. Tech. Rep. DE-AC21-88MC25000, The M. W. Kellogg Company, Houston, Texas.

Cotton, K. C., 1998. Evaluating and Improving Steam Turbine Performance. Cotton Fact Inc., Rexford, New York.

Dodd, A. M., Dryden, R. J., Provol, S. J. & Morehead, H. T., 1997. Mcintosh Unit 4 PCFB (pressurized circulating fluidized bed) demonstration project. *Proceedings of American Power Conference,* Chicago, Illinois, April 1-3, pp. 562–567.

DOE, 1989. Conceptual Design and Optimization of a Second-generation Pressurized Fluidized Bed Combustion Plant. Tech. Rep. DOE/MC/21023-2825, Office of Fossil Energy, U. S. Department of Energy.

DOE, 1990. The Coal-fired Air Furnace Combined Cycle - Thermodynamic Analysis of an External-fired Gas Turbine Electric Generating Plant. Tech. Rep., Office of Fossil Energy, U. S. Department of Energy.

DOE, 1999a. Clean Coal Technology Demonstration Program. Tech. Rep. DOE/FE-0402, Office of Fossil Energy, U. S. Department of Energy.

DOE, 1999b. Coal & Power Systems. Tech. Rep., Office of Fossil Energy, U. S. Department of Energy.

DOE, 1999c. HIPPS Status. *Web-site, Office of Fossil Energy, U. S. Department of Energy.*

DOE, 1999d. LEBS Status. *Web-site, Office of Fossil Energy, U. S. Department of Energy.*

DOE, 1999e. Market-Based Advance Coal Power Systems. Tech. Rep., Office of Fossil Energy, U. S. Department of Energy.

DOE, 1999f. Nuclear Power. Tech. Rep. DOE/EIA-0848(99), Office of Fossil Energy, U. S. Department of Energy.

DOE, 2000a. 21st Century Technologies for the Era of Efficiency. *Web site, Office of Fossil Energy, U. S. Department of Energy.*

DOE, 2000b. Geothermal Energy. *Web-site, Office of Fossil Energy, U. S. Department of Energy.*

DOE, 2000c. Integrated Gasification Combined Cycle. *Web site, Office of Fossil Energy, U. S. Department of Energy.*

DOE, 2000d. Concentrating Solar Power. *Web site, Office of Fossil Energy, U. S. Department of Energy.*

Eisermann, W., Johnson, P. & Conger, W. L., 1980. Estimating thermodynamic properties of coal, char, tar and ash. *Fuel Proc. Tech.* **3**, pp. 39–53.

Engi, D. & Icerman, L., 1995. Impacts of energy R&D strategies of OECD members on the USA. *Energy* **20(12)**, pp. 1251–1264.

EU, 1999. The role of conventional coal-fired plant. *Newsletter, Directorate General for Energy, European Commission*, February.

Eurlings, J. T. G. M., 1999. Eine Zukunft für die IGCC-Technik. *VGB Kraftwerkstechnik* **4**, pp. 53–57.

Farmer, R. (Chief Editor), 1997. Gas Turbine World Handbook. Victor de Biasi.

Flavin, C., 2000. Coming of age – the energy revolution. *Renewable Energy World* **2**.

Horazak, D. A. & Brushwood, J. S., 2000. Renewables prospects in todays conventional power generation market. *Renewable Energy World* **2**.

Hartman, J. J., Matchak, T. A., Sipe, H. E. & Wu, M., 1983. Shell-Based Gasification-Combined-Cycle Power Plant Evaluations. Tech. Rep. EPRI AP-3129, Electric Power Research Institute, California.

Guthrie, K. M., 1969. Capital cost estimating. *Chemical Engineering* **76(6)**.

Johansson, T. B., Bodlund, B. & Willians, R. H., 1989. Electricity. Lund University Press, Lund, Sweden.

Kjær, S., 1990. Kohlenstaubbefeuerte Kraftwerksblöcke mit fortgeschrittenem Wasser-/Dampfprozess. *Proceedings of VGB Kraftwerkstechnik 70 (1990)* **Heft 3**, pp. 201–208.

Kjær, S., 1998. Status of USC power plants Skærbæk 3 / Aalborg 3 and the advanced (700 °C) joint European project (THERMIE project). *Proceedings of the EU Seminar '98*, Düsseldorf, Germany.

Klara, J. M., 1994a. Cost Data for the HIPPS. *Private communication, DOE, USA.*

Klara, J. M., 1994b. High-performance power system for the near-term and beyond. *ASME Turbo Expo*, The Hague, Netherlands, June 13-16.

Lazzaretto, A. & Tsatsaronis, G., 1996. A general process-based methodology for exergy costing. *Proceedings of the ASME Advanced Energy Systems Division* **AES-Vol.36**, pp. 413–428.

Lowe, A., 1998. Status of IGCC. *Carbon Copy* **1(6)**.

Maude, C., 1996. Modular Options for Coal-fired Power Stations. Tech. Rep. IEAPER/25, IEA Coal Research.

Overend, R. P., 1997. Production of Electricity from Biomass Crops – US Perspective. Industrial Technologies Division, NREL, USA.

PAUL, I., 2000. A Technology Successfully Deployed in Developing Countries. *World Bank Group's Web-site.*

PILLEUL, R., 1994. Integrating the VEGA 109FA combined cycle in gasification processes. *GEC Alsthom Technical Review, No.14.*

PRICE, D., 1992. Exergoeconomic Evaluation of Dow-Based IGCC Power Plants. Master's thesis, Tennessee Technological University.

PRUSCHEK, R., 1998. Improvements of economics and efficiency for IGCC (JOULE project). *Proceedings of the EU Seminar '98*, Düsseldorf, Germany.

RAMACHANDRAN, G., 1993. Technical Assessment Guide. Tech. Rep. RP1678, Electric Power Research Institute.

REHMAT, A. & GOYAL, A., 1993. Advanced pressurized fluidized-bed staged combustion. *Proceedings of the Joint ASME/IEEE Power Generation Conference,* Kansas City, Kansas, October 17-22.

RINEHART, B., 1999. Hydropower R&D. Tech. Rep. BP791-0699-IM-T, Idaho National Engineering and Environmental Laboratory.

ROBERTSON, A. & BONK, D., 1993. Effect of pressure on second-generation pressurized fluidized bed combustion plants. *Proceedings of the International Gas Turbine and Aeroengine Congress and Exposition,* Cincinnati, Ohio, May 24-17, 1993.

RUTH, L. A., 2001. Advanced coal-fired power plants. *Journal of Energy Resources Technology* **123**, pp. 4-9.

RUTH, L. A., 1999. Product Line: Pulverized Coal Combustion. *Website, Office of Fossil Energy, U. S. Department of Energy.*

SAHAN R. A., 1997. Use of an air fluidized-bed separator in a dry coal cleaning process. *Energy Conversion & Management* **38**, pp. 269–286.

SCARLIN, B., May 1997. Advanced high-efficiency turbines utilizing improved materials. *IMechE Conference Transactions, International Conference on Advanced Steam Plant*, pp. 49–63.

Scott, D. H., May 1997. Emerging coal-fired power generation technologies. *IMechE Conference Transactions, International Conference on Advanced Steam Plant*, pp. 213–221.

Sellakumar, K. M. & Lamar, T. W., 1995. Application of pressurized circulating fluidized bed technology for combined cycle power generation. *Heat Recovery Systems & CHP* **15**, pp. 163–179.

Spencer, R. C., Cotton, K. C. & Cannon, C. N., 1974. A Method for Predicting the Performance of Steam Turbine-Generators, 16,500 kW and Larger. Tech. Rep. 62 WA 209, ASME Report.

Stultz, S. C. & Kitto, J. B., 1992. Steam - Its Generation and Use. The Babcock & Wilcox Company, Barberton, Ohio, U.S.A.

Taud, R. & Karg, J. & OLeary D., 2000. Gas Turbine Power Plants. *World Bank Group's Web-site.*

THERMIE, 1996. Energy Technology Projects - Solid Fuels. Tech. Rep., European Commission.

Traupel, W., 1988. Thermische Turbomaschinen, Band I. Springer-Verlag, Berlin.

Tsatsaronis, G., 1999. Strengths and limitations of exergy analysis. *A. Bejan and E. Mamut (eds.), Thermodynamic Optimization of Complex Energy System,* Kluwer Academic Publishers, pp. 93-100.

Tsatsaronis, G. & Winhold, M., 1984. Thermoeconomic Analysis of Power Plant. Tech. Rep. EPRI AP-3651, Desert Research Institute, Reno, Nevada.

Tsatsaronis, G., Pisa, H. & Lin, L., 1990. The effect of assumptions on the detailed exergoeconomic analysis of a steam power plant design configuration - Part I: Theoretical development; Part II: Results and discussion. *A Future for Energy - Proceedings of the Florence World Energy Research Symposium,* Firenze, Italy, May 28 - June 1, 1990, pp. 771–792.

Tsatsaronis, G., 1993. Thermoeconomic analysis and optimization of energy systems. *Progress in Energy and Combustion Systems* **19**, pp. 227–257.

TSATSARONIS, G., 1995. On the efficiency of energy systems. *Proceedings of the International Conference on Efficiency, Costs, Optimization, Simulation and Environmental Impact of Energy Systems (ECOS'95)*, Istanbul, Turkey, July 11-15, pp. 53–60.

TSATSARONIS, G., 1998. Design optimization using exergoeconomics. *Presentation at the NATO Advance Study Institute Thermodynamics and Optimization of Complex Energy Systems.* Neptun, Constanza, Romania, July 13-24.

UNIVERSITY OF COTTBUS, 2000. Zirkulierende Druckaufgeladene Wirbelschichtfeuerung der 2. Generation. *Newsletter, March, Branderburgische Technische Universität Cottbus.*

UNIVERSITY OF ESSEN, 2000. The IGCC Plant. *University of Essen Web-site.*

VANSTONE, R. W., KLAUKE, F., KJÆR, S. & KRISTENSEN, P., 1998. Advanced ("700°C") PF Power Plant. Tech. Rep. SF/1001/97/DK, ELSAMPROJEKT.

VEAG, 1994. Kombikraftwerk mit Zirkulierender Druckwirbelschichtfeuerung . Tech. Rep. (Forschungsbericht), Vereinigte Energiewerke AG Berlin.

WESSELMANN, C. & UNGER, H., 2000. Kernenergieerzeugung. *BWK* **52(5)**.

WHITE, J. S., GETTY, R. T. & TORPEY, M. R., April, 1995. Commercial Second-Generation PFBC Plant Transient Model Task 15. Tech. Rep. DE96000570, Office of Fossil Energy, U. S. Department of Energy.

WILSON, D. G., 1984. The Design of High-Efficiency Turbomachinery and Gas Turbines. The MIT Press, Cambridge.

WORLD BANK, March 2000. Clean Coal Technologies in China. *Website.*

ZEHNER, P., 1998. Status of development and market penetration of clean coal technologies (CCT) for power generation. *Proceedings of the EU Seminar '98*, Düsseldorf, Germany.